APPLICATIONS OF THIN FILMS IN ELECTRONIC ENGINEERING

DEVELOPMENT, over the last few years, of integrated solid circuits for electronic applications has somewhat overshadowed the steady development that has been taking place in thin-film technology. The fact that this development has gone on—and continues—is sufficient evidence that thin-film components have an important place in electronic circuits.

For some time the rather naïve view was held that the trend to micro-miniaturization of electronic components meant that *either* the integrated solid circuit *or* the thin film circuit would be developed and that there was not room for both. The appearance of the hybrid 'flip-chip' circuit, which combines solid circuit and thin-film components in one unit, is a clear demonstration that the techniques are complementary, not competitive.

Individual thin-film resistors and capacitors have been on the market for some time and manufacturers are now able to offer complete circuit packages in which high-stability thin-film components are combined with solid-circuit devices to give precision performance. Alongside these developments the search for a fully-compatible thin-film device has continued. The thin-film field-effect transistor is emerging as a possibility and, when realized, will greatly extend the range of integrated thin-film circuits. In addition to the purely circuit applications, thin films are being used in magnetic computer stores, as transducers of different kinds and in a variety of other fields.

Whilst there has been a number of conferences on the physics of thin films, and on different specific applications of them, there has not yet been one which brought together those concerned with their application in the electronics industry generally. The Programme and Papers Committee of the I.E.R.E. therefore felt that the time is now ripe for those concerned to discuss the current state of the art and to consider the present and future place of the thin film technology in the electronics industry. In view of the wide ranging interest of these techniques, the Electronics Division of the Institution of Electrical Engineers was invited to collaborate in planning a Joint Conference, and an Organizing Committee of members from both Institutions has been set up.

The Conference will be held at the Imperial College of Science and Technology of the University of London and will last four days—Monday, 11th July to Thursday, 14th July, 1966. The subject is being dealt with in five sessions: Preparation of Thin Films; Thin Film Elements and Integrated Circuits; General Applications; Magnetic Films; and Cryoelectric Films. The final programme is now being drawn up and it is expected that there will be approximately forty papers presented. These will be preprinted for the Conference and subsequently brought up to date with the addition of late papers and discussion reports etc., for publication as 'I.E.R.E. Conference Proceedings No. 7'.

The interest which has so far been shown, both in this country and from overseas, leads the Organizing Committee confidently to state that any member of either Institution having an interest in the future of the industry will find this a most worthwhile Conference to attend.

J. C. ANDERSON

Joint I.E.R.E.–I.E.E. Conference on
"APPLICATIONS OF THIN FILMS IN ELECTRONIC ENGINEERING"

IMPERIAL COLLEGE OF SCIENCE AND TECHNOLOGY, LONDON, 11th to 14th JULY 1966

OUTLINE TIMETABLE

Final details, which may indicate further papers and/or alterations to the provisional timing shown, will be sent to those registering to attend the Conference.

Monday, 11th July

8.30—10.00 a.m.   REGISTRATION.

10.00—10.15 a.m.   Opening Address by Professor Sir Willis Jackson, F.R.S.

(10.15 a.m.—12.15 p.m.; 2.15—5.00 p.m.)

Session I—PREPARATION OF THIN FILMS
Chairman: Professor J. C. Anderson

Introductory paper: 'Preparation of Thin Films'—D. S. CAMPBELL.

'The Deposition of Oxide Films by Reactive Sputtering'—N. F. JACKSON, E. J. HOLLANDS and D. S. CAMPBELL.

'Low Pressure Sputtering'—D. W. GILES and R. J. BAKER.

'A Micro-engraving Technique for Thin Films'—T. M. JACKSON and P. G. ELDRIDGE.

'The Formation of High Resolution Silica Films by an Electron Beam Process'—A. F. BEER, J. KELLY, H. N. G. KING, E. D. ROBERTS and J. M. S. SCHOFIELD.

'Electron Beam Machining of Silicon Observed with the Scanning Electron Microscope'—T. H. P. CHANG and W. C. NIXON.

'Economic Methods of Pattern Production in Film Circuits'—W. L. CLOUGH.

'Preparation of Microcircuit Elements by the Selective Etching of Multi-layer Thin Films'—D. C. CORNISH.

'A Compatible Thin Film Cermet Resistor'—P. E. CASPAR.

6.00—7.30 p.m.—CONFERENCE RECEPTION

Tuesday, 12th July 9.15 a.m.—12.15 p.m.; 2.15—5.00 p.m.

Session II—THIN FILM ELEMENTS AND INTEGRATED CIRCUITS
Chairman: C. P. Sandbank

Introductory paper: 'Thin Film Elements and Circuits'—D. BOSWELL.

'The Preparation and Application of Tantalum Thin Film Passive Components'—R. NAYLOR and R. FAIRBANK.

'Factors Influencing the Humidity Sensitivity of Silicon Oxide Vacuum Deposited Capacitors'—L. R. CALLARD.

'The Effect of Hydrogen on the Dielectric Properties of Silicon Oxide Capacitors'—G. SIDDALL and C. S. GIDDENS.

'An Automatic Method for the Evaluation of Thin Film Capacitors'—V. J. HAMMOND.

'Electron Transfer Process through Tantalum-Tantalum Oxide Diodes'—W. E. FLANNERY and S. R. POLLACK.

'The Effect of Semiconductor Film Thickness on Thin-Film-Transistor Performance'—A. C. TICKLE, E. J. SWYSTUN and D. H. TRELEAVEN.

'Field Effect Studies in Indium Antimonide Thin Films'—C. JUHASZ and J. C. ANDERSON.

'Evaporated Thin Film Active Devices'—C. J. KENNEDY and M. A. REID.

'Low Pass Active Filters'—H. BLACKBURN, D. S. CAMPBELL and A. J. MUIR.

'Cadmium Sulphide Thin Film Devices'—D. J. PAGE.

'A Thin Film Resistive Memory Device'—J. G. SIMMONS and R. R. VERDERBER.

'A Hot Electron, Cold Cathode Emitter'—R. R. VERDERBER and J. G. SIMMONS.

Wednesday, 13th July 9.15—10.45 a.m.

'Why Thin Film Circuits ?' A Discussion on the relative merits of thin films and other techniques.

11.15 a.m.—12.15 p.m.; 2.15—5.00 p.m.

Session III—GENERAL APPLICATIONS
Chairman: F. M. Foley

'Thin Film Galvanomagnetic Devices'—K. G. GÜNTHER and H. FRELLER.

'The Fundamental Properties of Evaporated Thin Film Strain Gauges'—M. J. KNIGHT.

'Properties of Germanium Thin Film Strain Gauges'—G. BARALIS and MISS M. PLASSA.

'Vacuum-Deposited Thin Films as Ultrasonic Transducers'—N. F. FOSTER.

'Thin Film Components with Close Tolerances for use in Tuned Circuits'—H. G. MANFIELD and D. J. WINDLE.

'Thin Film Components in R.F. Power Measurements.—A. A. LUSKOW.

'Thin Films in Hybrid Radar Receivers'—W. S. WHITLOCK.

'The Design and Application of Thin Film Modules for Professional Television Equipment.—E. O. HOLLAND and MISS P. R. K. CHAPMAN.

Thursday, 14th July 9.15 a.m.—12.15 p.m.

Session IV—MAGNETIC FILMS
Chairman: Dr. K. Hoselitz

Introductory paper: 'Magnetic Films'—R. V. PEACOCK.

'Thin Films in Computers'—A. D. BOOTH.

'Domain Wall Storage and Logic Devices'—A. C. TICKLE.

'The Improvement of Magnetic Properties of Thin Ferromagnetic Films by Use of Ternary Alloys'—I. MELNICK and G. GRUNBERG.

'A $\frac{1}{4}$-microsecond 200 000-bit Magnetic Thin Film Store with Improved Transistor Address Matrix'—K. H. SINDEN.

'A Small Capacity High Speed Magnetic Film Memory'—J. L. MUDGE, D. C. BUCHANAN, R. M. PICKARD and G. R. HOFFMAN.

'High Density Recording Using High Coercivity Films'—B. K. MIDDLETON and P. A. WALKER.

2.15—5.00 p.m.

Session V—CRYOELECTRIC FILMS
Chairman: Professor A. D. Booth

Introductory paper: 'Cryoelectric Films'—H. FEISSEL.

'An Improved Cryotron Storage Cell for Non-destructive Read-out'—W. HELMBERGER.

'Cryotron Storage Cells for Random Access Memories'—V. L. NEWHOUSE and H. H. EDWARDS.

'Relations between Deposition Parameters and Operating Characteristics of Crossed Film Cryotron Structures'—R. JOYNSON.

'The Feasibility of the Superconducting Continuous Film Memory'—V. A. J. MALLER and P. A. WALKER.

'Radio Frequency Switching of Crossed Film Cryotrons.—G. F. JONES and G. R. HOFFMAN.

All Sessions will take place in the main lecture theatre of the Department of Mechanical Engineering at Imperial College of Science and Technology; other theatres will also be used if necessary, linked by closed-circuit television. There will be a supporting exhibition of demonstrations associated with the papers.

Synopses of Papers to be presented at the Conference

SESSION I—PREPARATION OF THIN FILMS

The Deposition of Oxide Films by Reactive Sputtering

N. F. JACKSON, E. J. HOLLANDS AND D. S. CAMPBELL. (*Allen Clark Research Centre, The Plessey Company Ltd., Caswell, Northamptonshire.*)

Both single and mixed oxide films have been prepared by the reactive sputtering of the appropriate metals in an oxygen or argon-oxygen mixture. Satisfactory single oxide films have been found using zirconium cathodes—these films have a permittivity of approximately 16 and exhibit high breakdown strength (4 mV/cm) at thickness of around 1000 Å. They are however humidity sensitive if prepared in a 80 : 20 argon : oxygen mixture. Using 100% oxygen the breakdown strength is considerably reduced ($\sim 10^5$ V/cm) but it can be increased by wet anodization.

Mixed oxide film using a lead/titanium cathode have been prepared. Various types of cathodes have been employed. The most satisfactory results have been obtained using a segment cathode and permittivity versus composition curves have been plotted. With a lead content of between 55–85%, the films are pinhole free and show a permittivity of about 20 with a loss of 0·4% (tan δ). The electron diffraction analysis of the structure is discussed.

Low-Pressure Sputtering

D. W. GILES AND R. J. BAKER. (*Standard Telephones and Cables Limited, Capacitor Division, Paignton, Devon.*)

Thin films of materials, used for example in microcircuitry, are vacuum deposited *either* by evaporation or sublimation—in which the source material is heated by various methods until its vapour pressure is of the order of microns, *or* by sputtering—in which case the source material is disintegrated by ion bombardment in a glow discharge.

By passing an electron beam, 2 to 10 amps, through the sputtering gas, and by concentrating the beam with a coaxial magnetic field, a highly conductive plasma can be supported down to gas pressures in the 10^{-4} torr range. By arranging for the plasma to be generated by electrodes other than the substrates and holder, the cooling systems used in conventional sputtering now become superfluous.

The mean energy of the bombarding ion is more closely related to the target voltage, since the probability of collision and energy loss in the dark space is lower. With suitable electrode design, the probability of the sputtered material reaching the substrate without collision is high, so that the material transfer is not diffusion limited. The increased sputtering rates thus achieved are for tantalum typically 600 Å/min with a target voltage of 600, whilst the two-electrode system gives 140 Å/min with 5000 volts applied. Properties of the films and devices have been examined in some detail.

The energy of particles sputtered under these conditions has been shown by Stuart and Wehner to extend to 48 eV (evaporated particles to 1·3 eV). The adhesion of the films is enhanced, so that a wider range of materials and substrates can be used than that possible with either of the previous methods. The uniformity of the deposited films is governed for example by plasma density, electrode configuration and target voltage.

A Microengraving Technique for Thin Films

T. M. JACKSON AND P. G. ELDRIDGE. (*Standard Telecommunications Laboratories, Harlow, Essex.*)

A spark microengraving technique for precise machining of deposited thin film on insulating substrate is described. The resolution of the process is compared with other means of precise delineation, such as, in-contact photolithography and electron and laser beam processes. The results of electrical and physical measurements on microengraved films are given. The application of microengraving to the fabrication of thin film circuits is discussed and a means of automatic control is described.

The Formation of High Resolution Silica Films by the Electron Beam Process

A. F. BEER, J. KELLY, H. N. G. KING, E. D. ROBERTS AND J. M. S. SCHOFIELD. (*Mullard Research Laboratories, Redhill, Surrey.*)

Electron beams can be used to stimulate chemical reactions at a surface in a partial vacuum. Vapours introduced into the system are absorbed on the target surface and the incident electrons make and break inter-atomic bonds by a collision process.

Since the reactions appear to occur only where the electrons strike the target, this provides a way of making high resolution patterns suitable for the construction of solid circuits.

Work on the production of siliceous films intended for use as boron diffusion barriers is described. A description of analytical work on the films produced and the electron beam equipment is given. Work directed towards the production of an m.o.s. transistor using this process is discussed.

Electron Beam Machining of Silicon Observed with the Scanning Electron Microscope

T. H. P. CHANG AND W. C. NIXON. (*Department of Engineering, University of Cambridge.*)

An electron optical column has been used for both machining thin films and observing the effect of this operation. For machining, two magnetic electron lenses are used to produce an electron probe size in the range $\frac{1}{2}$ μm to 10 μm diameter, current of 20 to 200 μA at 25 kV. A pattern generator is used to control the electron beam power with respect to the position of the electron probe within the scanned area of up to 1 mm square. In this way a predetermined pattern may be cut into the surface with pulse lengths of 5 μs and upwards in steps of 1 μs or greater.

After a pattern has been cut, a third magnetic electron lens is switched on and the electron probe size reduced to a few hundred angstroms and with much less beam current. This probe scans the specimen in a normal square raster and the secondary electrons produced give a signal that is used to modulate the brightness of a display cathode ray tube. In this way a scanning electron microscope image of the surface is obtained and recorded by photographing the screen of the c.r.t.

When machining silicon covered with a layer of silicon oxide 3500 Å thick the oxide layer cracks when short pulses are used, i.e. 5 to 10 μs. For longer pulses, from 10 μs to 5 ms, molten material from below the surface emerges through the cracks and forms a distinctive 'egg'-shaped projection. For still longer pulses, 10 ms to 100 ms, a crater is formed and the molten material remains in the interior of this depression. When silicon without an oxide layer is machined there is no 'egg' formation and the crater form appears at 5 to 10 μs instead of 10 to 100 ms when an oxide layer is present. Representative photographs demonstrate these two effects.

Economic Methods of Pattern Production in Film Circuits

W. L. CLOUGH. (*Welwyn Electric Limited, Bedlington, Northumberland.*)

Many techniques exist for the delineation of two-dimensional patterns in microminiature circuits including some whereby very high resolution of line can be achieved. Where large volume production is envisaged it is essential to adopt the simplest and most economic process consistent with the required degree of resolution and accuracy.

In one particular process involving the chemical deposition of resistive films, in-contact masking techniques are used, and with line resolutions of down to 0·010 in photolithographic and stencil screen techniques have been studied and compared. The relative merits and limitations of these techniques using both additive and subtractive processes are discussed. Comparative costs and prospects of further development of these methods for higher resolution work are given.

Increasing interest in the use of 'thick film' materials for micro-miniature circuitry has given added impetus to the work on stencil screen methods. In this case the need to control the thickness of deposit is an additional critical parameter.

To provide versatility of service and to offer either thin film or thick film circuits as required there is considerable advantage in developing similar pattern production processes for both techniques. A summary of the desirable features of printing equipment having the required degree of versatility is outlined and discussed.

Preparation of Microcircuit Elements by the Selective Etching of Multi-layer Thin Films

D. C. CORNISH. (*British Scientific Instrument Research Association, South Hill, Chislehurst, Kent.*)

Present-day techniques for the preparation of thin film microcircuits are limited mainly to the evaporation of films through out-of-contact masks and to the individual photomechanical processing of resistor and conductor layers. The technique described in this paper enables all the constituent films, including dielectric material, to be deposited during one pump-down. The multi-layers so formed are then photomechanically etched, one film at a time, to produce the desired components. The problem of connections to capacitor top plates can be overcome by simple masking during the deposition stage. As the preparation of the multi-layers is completely divorced from the photomechanical processing, they could be deposited by a jobbing evaporation contractor, enabling the subsequent manufacture of the microcircuits to be carried out with the minimum of capital equipment and labour.

A Compatible Thin Film Cermet Resistor

P. E. CASPAR. (*Great Baddow Laboratories, The Marconi Company Limited, Great Baddow, Essex.*)

A process for the manufacture of micro-sized high tolerance resistors is discussed with particular reference to full compatibility with active devices. Problems of patterning the cermet resistors by various methods are examined in detail and a possible process is outlined. Attention is given to the design of the evaporant source for the production of pinhole-free film and finally specimen results are presented for some pre-production runs.

SESSION II—THIN FILM ELEMENTS AND INTEGRATED CIRCUITS

The Preparation and Application of Tantalum Thin Film Passive Components

R. NAYLOR AND R. FAIRBANK. (*Ferranti Limited, Wythenshawe, Manchester.*)

The paper describes the techniques used in the fabrication of passive components using tantalum as the starting material. The tantalum is deposited by sputtering and the required patterns are determined by photo-etching techniques. These techniques have been studied in some detail such that resistors less than 0·001 in. wide can be made with reasonable tolerances.

The paper then continues to give characteristics and performance of the components and to conclude, examples are given of circuits using thin film components on both glass and oxidized silicon substrates. Since the latter form of substrate can contain diffused active components, this provides a small-scale economic method of fabricating thin film circuits.

Factors Influencing the Humidity Sensitivity of Silicon-Oxide Vacuum Deposited Capacitors

L. R. CALLARD. (*British Aircraft Corporation (Operating) Limited, Bristol.*)

Various methods of manufacture of silicon-oxide capacitors and the resultant electrical characteristics are described. Particular reference is made to the relationship between certain manufacturing parameters and the effect of moisture on the electrical characteristics.

All the results quoted are obtained from measurements on 120 groups of capacitors deposited on a 4 in × 4 in Corning 0211 microsheet substrate, giving 960 capacitors on each substrate as each group consists of 8 binarily related capacitors. The largest capacitor has an area of 12·8 mm² giving a capacitance of 1950 pF.

The principal manufacturing conditions that have been studied are the silicon-oxide deposition rate, substrate temperature, ambient pressure and the method of base electrode manufacture. A number of the results quoted are from capacitors whose base electrode geometry has been defined by an etching process.

The electrical characteristics reported are the capacitance, loss tangent and its variation with frequency, d.c. conductivity, breakdown stress and dielectric constant.

All the capacitors described have been made in a conventional evaporation system. A few mass spectrometer measurements of the residual atmosphere have been made.

The Effect of Hydrogen on the Dielectric Properties of Silicon Oxide Capacitors

G. SIDDALL AND C. S. GIDDENS. (*The Electrical Research Association, Leatherhead, Surrey.*)

Vacuum deposited silicon oxide capacitors are used extensively in thin film integrated circuits, but show unexplained variation of dielectric properties with deposition parameters. Experiments have been carried out under carefully controlled conditions in very clean vacuum systems in order to determine the reasons for these variations.

It has been established that hydrogen can be absorbed by the oxide film giving rise to much higher values of dielectric loss. The capacitors also exhibit a voltage dependent capacitance which can be partly explained in terms of space charge effects.

An Automatic Method for the Evaluation of Thin-Film Capacitors

V. J. HAMMOND. (*G. V. Planer Ltd., Sunbury-on-Thames, Middlesex.*)

The positions and distribution of electrically weak points in a thin-film capacitor may be recorded by exposing a fine grain photographic emulsion to the scintillations which occur when the dielectric is subjected to large electric fields. Successive autophotographs of the dielectric corresponding with increasing electrical stress enables the sequence in which different areas break down to be determined. Automatic equipment is described which employs such an autophotographic method for recording breakdown events in vacuum-deposited, thin-film capacitors as a function of applied stress (increased in steps) and of time.

The Effect of Semiconductor Film Thickness on Thin-Film Transistor Performance

A. C. TICKLE, E. J. SWYSTUN AND D. H. TRELEAVEN. (*Department of Electrical Engineering, University of Saskatchewan.*)

In this paper the characteristics of thin film transistors are shown experimentally to be strongly dependent on the thickness of the semiconductor film. In order to eliminate the effect of random variations in the deposition conditions a method of batch fabrication was used. The conductance of CdSe films was found to be a non-linear function of film thickness, and increased rapidly after a certain critical thickness was reached. As the film thickness was reduced the Fermi level was found to fall deeper below the conduction band. The gate to source voltage required for the on-set of drain conduction was found to increase rapidly with decreasing film thickness.

Electron Transfer Processes through Tantalum-Tantalum Oxide Diodes

W. E. FLANNERY (*Sperry Rand Corporation, Univac 'Division, Blue Bell, Pa.*) AND S. R. POLLACK (*Department of Metallurgical Engineering, University of Pennsylvania, Philadelphia.*)

The electron transfer processes in thin film diode structures of $Ta-Ta_2O_5-Au$ have been studied by Cubert, Murphy, Pollack *et al.* with a view to their application in diode-transistor logic circuitry and possible use as tunnel cathode emitters. The structures were prepared by electron beam evaporation of tantalum at 10^{-6} torr followed by plasma oxidation of the tantalum film to the desired thickness. The counter-electrode metal was then evaporated without breaking the vacuum. Current-voltage-temperature characteristics of these structures were studied. Tunnel emission was observed when the tantalum electrode was biased positively and Schottky emission was observed for the tantalum electrode biased negatively. Trapezoidal energy barrier models have been used by many authors to explain electron injection and transfer through extremely thin insulating films.

Such a model is proposed in this paper for the tantalum-tantalum oxide system, and it is shown that it provides a self-consistent framework for describing both Schottky and tunnel emission electron transfer processes in these structures. Using this model, it was found that the barrier height at the parent tantalum-oxide interface is 1.0 eV and the built-in voltage with a gold counterelectrode is 0.5 eV. The model does fail, however, to provide a description of capacitance data. This failure has been previously noted in aluminium-aluminium oxide structures.

The results of these studies indicate that the tantalum-tantalum oxide system does not provide any distinct advantages for use in d.t.l. circuitry over the aluminium-aluminium oxide system previously studied. The high gold-vacuum work function precludes the use of these structures as tunnel cathode emitters. The results of capacitance measurements on thicker (> 100 Å) tantalum oxide films prepared by plasma oxidation indicates that this process is amenable to fabrication of thin film capacitors.

Low Pass Active Filters

H. BLACKBURN, D. S. CAMPBELL (*Allen Clark Research Centre, The Plessey Company Ltd., Caswell, Northamptonshire*) AND A. J. MUIR (*British Telecommunications Research Ltd., Taplow, Berkshire.*)

Microminiature low pass active filters have been constructed using a combination of thin film and silicon integrated circuit techniques. The advantages of such an approach are discussed.

The filters requirements could be met by fifth order Chebychev functions and the method of realization was to split the transfer function into quadratic and linear factors. Each factor could then be realized separately. The tolerances required have been examined using a Monte Carlo computer program and the results are discussed.

Two different filters for use in p.c.m. systems have been constructed and are illustrated in detail.

Field Effect Studies in Indium-Antimonide Thin Films

C. JUHASZ AND J. C. ANDERSON. (*Department of Electrical Engineering, Imperial College of Science and Technology.*)

Field effect studies have been carried out on thin-film indium antimonide–inert insulator solid–solid interfaces. The films were prepared by the protected recrystallization method, namely vacuum evaporation and subsequent annealing of the resulting insulator–semiconductor–insulator sandwiches. The high annealing temperatures permissible without danger of re-evaporation of the more volatile component gave films with high mobility, 10^3–10^4 cm²/V s and relatively low carrier concentrations, 10^{15}–10^{17}/cm³. The good bonding of the insulator to an inherently clean semiconductor surface resulted in a low fast surface state density $\sim 10^{11}$/cm², which would permit the use of these films for field effect transistor applications. Thin films are very well suited for field effect investigations. Surface Hall effect and surface conductivity against surface potential gave the trapped and mobile charge density with the relevant Hall and field effect mobility directly. A model of fast surface states based on these results is proposed.

Cadmium Sulphide Thin Film Devices

D. J. PAGE. (*Westinghouse Electric Corporation, Research and Development Center, Pittsburgh, Pennsylvania, U.S.A.*)

A new method of preparing thin films of CdS, and the use of such films in the construction of dielectric diodes and triodes is described.

The films are produced by indirect co-evaporation of the elements and result in a material having useful optical, acoustical and electrical properties. By adjusting the growth parameters, the density and depth of the trapping centres in the CdS films may be varied over a wide range. This, in turn, results in a wide variety of electrical characteristics.

Dielectric diodes constructed from this material are described. These devices have a very high reverse resistance, greater than 10^{10} ohms, and rectification ratios of the order of 10^9 are common.

Dielectric triodes, produced by the evaporation of this material through appropriate masks on to planar p-n junctions in silicon, are also described.

Evaporated Thin Film Active Devices

C. J. KENNEDY AND M. A. REID. (*Department of Electrical Engineering, University of Edinburgh.*)

The Weimer-type thin film triode has attractive possibilities for integrated circuit systems, but will not be a realizable proposition until erratic variations in the device characteristics can be overcome. There appear to be three main areas where uncertainties exist: the conducting channel, the contacts and the thin dielectric layer. Experiments are reported on the first two of these areas.

Semi-insulators with a high resistivity and mobility are required for the formation of space charge limited currents. A large band gap semiconductor, e.g. cadmium sulphide, is thus essential, preferably in the form of a single crystal. Evaporated films of cadmium sulphide have been prepared by different methods, including co-evaporation, on different substrate materials, some with a similar crystalline structure to cadmium sulphide. The effects of these preparation methods on the film properties, e.g. resistivity and mobility, are described.

Attempts have been made to fabricate evaporated thin film diodes and triodes and, in particular, some factors influencing the metal to semiconductor contact are discussed.

A Hot Electron, Cold Cathode Emitter

R. R. VERDERBER AND J. G. SIMMONS. (*Standard Telecommunication Laboratories Ltd., Harlow, Essex.*)

A conduction mechanism has been observed in thin film metal–insulator–metal sandwiches which results in a $V–I$ characteristic with a pronounced d.c. voltage-controlled negative resistance region. In addition, the cold emission of electrons from the device has been observed and is of practical interest because the emitted electron can be used to excite a phosphor quite intensely; this property makes the device attractive as a display element. The density of the emitted current depends exponentially upon the biasing voltage across the sandwich and is not thermal in nature.

A Thin Film Resistive Memory Device

J. G. SIMMONS AND R. R. VERDERBER. (*Standard Telecommunication Laboratories Ltd., Harlow, Essex.*)

Two-terminal, thin-film diodes have been fabricated which exhibit resistive memory characteristics. The device can be used either as a binary or analogue memory, and all memory states are non-volatile and also provide non-destructive read-out access. The various memory states are set by voltage pulses ranging between 4 and 8 V, reading voltages up to about 2·5 V can be used, and switching from the higher impedance memory states to the lowest impedance memory state is accomplished by applying a voltage to the device in excess of about 3 V. Devices have been stored, without power, for several weeks and interrogated several million times without degradation of the original memory state. The device can be switched from the high to the low impedance state and back again in about 1 μs, but the repetition time at present is slow, approximately 10–100 ms but is suitable for use as a semi-permanent, low power store. The device is very simple and cheap to fabricate and its structure permits very high packing densities.

SESSION III—GENERAL APPLICATIONS

Thin Film Galvanomagnetic Devices

K. G. GÜNTHER AND H. FRELLER. (*Siemens-Schuckertwerke A.G., Nuremberg.*)

The extreme high mobility of III-V semiconducting compounds like indium arsenide and indium antimonide enables the development of galvanomagnetic devices like Hall-probes or magneto-resistors.

The following properties of thin film galvanomagnetic devices are discussed: Conductivity and Hall coefficient versus temperature; conductivity and Hall coefficient versus magnetic-induction; Hall-voltage versus control current. Further some typical data about misalignment voltage, long time stability and the dimensions of thin film Hall-effect devices are given. Some applications of Hall probes are described.

The Fundamental Properties of Evaporated Thin Film Strain Gauges

M. J. KNIGHT. (*Electronics Department, The Electrical Research Association, Leatherhead, Surrey.*)

The idea of using evaporated metal films for strain gauges was first patented in 1951, but it is only during the past year that they have started to become commercially available.

This paper discusses various mechanisms responsible for changes in electrical conductivity when thin evaporated metal films are mechanically strained. A brief review of recent work in this field is given and this is followed by an experimental investigation over a range of temperatures of the strain sensitivity of metal films deposited on amorphous substrates. The results obtained are related to the film structures observed by electron microscopy.

Properties of Germanium Thin Film Strain Gauges

G. BARALIS. (*Centro Ricerche Metallurgiche, Turin*) AND MISS M. PLASSA (*Istituto Dinamometrico Italiano, Turin.*)

The possibility of using thin vacuum deposited germanium films as strain gauges has been studied. A relationship between strain sensitivity and occurrence of preferred orientations was to be established as well as comparison between the experimental and theoretical values.

Films were evaporated on muscovite and phlogophite mica substrates, in a vacuum of about 10^{-5} torr, with a deposition rate of 2000 or 3300 Å/min, and a film thickness of 2000 or 3300 Å.

In general, gauge factor was found to be about 34, with a slight or nearly nill effect form preparation methods or texture. The calculated values ranged from 65 to 72. The discrepancy between experimental and theoretical data is probably due to the fact that the properties of germanium thin layers are strongly affected by surface states.

Practical application appears to be possible since scattering of gauge factors of films obtained under similar conditions is generally restricted to the reasonable limit of $\pm 5\%$.

Thin Film Components with Close Tolerances for use in Tuned Circuits

H. G. MANFIELD AND D. J. WINDLE. (*Royal Radar Establishment, Malvern, Worcestershire.*)

It is known that accurate resistors and inductors can be made from thin film circuits. To date capacitors have been trimmed to set a circuit on the desired frequency.

Improvements in dielectric consistency and control of evaporation processes is making it possible to design a 'non-trimmed' tuned circuit using inductive and capacitive components with associated resistors on an inorganic substrate.

Thin Film Components in R.F. Power Measurements

A. A. LUSKOW. (*Marconi Instruments Limited, St. Albans, Hertfordshire.*)

The application of thin film components to the design of radio frequency power meters is discussed.

The design is based on the simple principle of sampling incident power in a through-line a.c.-d.c. converter and absorbing the remainder in a terminating load. By applying thin film techniques a frequency range from d.c. into the microwave region has been achieved and true mean power, independent of waveform, from 100 mW to 1 kW can be measured. The use of several novel substrate materials and configurations is explained.

The Design and Application of Thin Film Modules for Professional Television Equipment

E. O. HOLLAND AND MISS P. R. K. CHAPMAN. (*The Marconi Company Ltd., Broadcasting Division, Chelmsford, Essex.*)

The paper describes the method of making closely controlled thin film circuits. The precautions taken to obtain the maximum reliability are listed. Further, the reasons why these modules have been chosen for use in the Marconi colour television camera are discussed.

Thin Films in Hybrid Radar Receivers

W. S. WHITLOCK. (*Admiralty Surface Weapons Establishment, Portsdown, Cosham, Hampshire.*)

Hybrid radar receivers have been constructed using silicon integrated circuits, in both chip and flat-pack form, which are mounted on glass substrates carrying thin film passive components. The work has highlighted limitations and deficiencies, particularly at high frequencies, of the thin film components as made using current production techniques.

For example, SiO/Al thin film capacitors can have inadequate Q value, range and tolerance for certain applications. Special design and trimming techniques are used to minimize this limitation. Good plated-up thin film inductors can be made with values between $0 \cdot 1$–10 μH. Problems associated with their inclusion in thin film tuned circuits and subsequent problems of encapsulation are discussed.

Vacuum Deposited Thin Films as Ultrasonic Transducers

N. F. FOSTER. (*Bell Telephone Laboratories, Murray Hill, New Jersey.*)

Vacuum deposited films of CdS have been shown to act as efficient high frequency ultrasonic transducers in the frequency range from 14 Mc/s to 70 Gc/s. These transducers have been fabricated for the generation of longitudinal or shear waves with losses as low as 4 dB per transducer at 200 Mc/s and 12·5 dB per transducer at 1500 Mc/s. The transducer films have been deposited on the desired ultrasonic medium without requiring bonding agents or bonding operations. Zinc-oxide films have been deposited by d.c. sputtering and these have also shown very high transducer efficiencies. The superior material parameters of ZnO compared with CdS could make the ZnO sputtered films most attractive for high frequency transducers if the deposition can be controlled to the same extent as has been possible in CdS evaporation.

SESSION IV—MAGNETIC FILMS

Thin Films in Computers

A. D. BOOTH. (*College of Engineering, University of Saskatchewan.*)

The M.4 computing machine in the Department of Electrical Engineering, University of Saskatchewan, is at present in course of construction. It has been designed in the light of experiments and experiences with high speed discrete circuit elements such as the tunnel diode, and with thin film magnetic devices. In its initial concept the M.4 was to work almost entirely with magnetic elements, these being used for storage, auxiliary data processing, such as that involved in shift registers, and logical operations using in-domain logic.

As a result of experimental work on thin film magnetics, the notion of using the films for shift registers and logic has now been abandoned. Reasons for this are discussed and the final design in which thin films are used for a part of the ultra-high-speed storage unit whereas other thin film active elements are proposed for the arithmetic and control sections of the machine are described in detail.

High Density Recording Using High Coercivity Films

B. K. MIDDLETON AND P. A. WALKER. (*International Computers and Tabulators (Engineering) Ltd., Stevenage, Herts.*)

Theoretical analysis has shown the dependence of packing density upon recording medium, head gap and head to coating separation. The implications of this theory are discussed, particular attention being given to the relative importance of these factors.

The magnetic and recording characteristics of high coercivity metal films prepared by a variety of techniques are compared with those obtainable with thin oxide coatings and an attempt is made to assess the relative merits of the two types of recording media.

The full potentialities of high coercivity metallic coatings can only be realized by the use of narrow gap heads and small head to coating separations. These requirements are discussed and attention is drawn to the importance of the wear characteristics of the coating and the flatness and surface finish of the substrate material.

Domain Wall Storage and Logic Devices

A. C. TICKLE. (*Department of Electrical Engineering, University of Saskatchewan.*)

Storage devices are described in which magnetic domains, representing binary information, are propagated through a uniaxial magnetic film by means of controlled domain boundary movement. The operating tolerances, bit rate, and error rate are related to the design of the devices and the magnetic film properties. The nucleation and subsequent morphology of domains has been studied with particular emphasis on the spurious modes of generation and destruction of data-representing magnetic states. A number of these modes have been classified, and they may be avoided by a suitable choice of operating conditions. Devices storing 45 bits per linear inch have been operated at 1 Mc/s. A new mode of interaction between moving domains has been observed, which permits the exclusive OR function. This introduces the possibility of data storage and processing entirely within the storage medium.

The Improvement of Magnetic Properties of Thin Ferromagnetic Films by Use of Ternary Alloys

I. MELNICK AND G. GRUNBERG. (*Centre d'Etudes Nucleaires de Grenoble.*)

Desirable properties in magnetic films for computer applications are low anisotropy field H_k, low dispersion α_{90}, no skew and a high degree of inversion.

The paper first shows how skew (in practice the most difficult parameter to control over a large area), is related to the magnetostriction, and how it can be kept under $\pm 1°$ by adjusting the rate of evaporation from run to run. The paper then briefly describes several experiments with NiFe plus variable percentage ($> 5\%$ in the deposit) of Ta, Ti, Cr, Si, Pd or Au. It then shows that some of these ternary alloys (especially NiFe Ta and NiFe Pd) have a very low dispersion ($\alpha_{90} < 0.5$), a low H_k and a controllable degree of inversion. At the same time the zero magnetostriction seems easier to maintain than in binary NiFe.

A ¼-microsecond 200 000-bit Magnetic Thin Film Store with Improved Transistor Address Matrix

K. H. SINDEN. (*E.M.I. Electronics Limited, Hayes, Middlesex.*)

Starting from the design of a proven store, the design philosophy of a modified version is described having a greater capacity, faster cycle time, improved reliability and reduced production cost. The actual store module consists of 8 large planes comprising 256 words of 100 bits each, multi-word operation being employed as far as external use is concerned.

A transistor matrix is used for word selection, which has one set of co-ordinates arranged as a series of transmission lines running throughout the store in the same direction as the digit-sense lines. These lines are such that a constant time relationship is maintained between address and digit-sense lines, resulting in faster operation of the store. The cycle time in production will be 250 ns.

A Small Capacity High Speed Magnetic Film Memory

J. L. MUDGE, D. G. BUCHANAN, R. M. PICKARD AND G. R. HOFFMAN. (*Electrical Engineering Laboratories, University of Manchester.*)

The paper describes the design and construction of a 128-word, 48 bit 100 ns cycle time magnetic film store. Discrete planar elements are used and have been deposited in a high vacuum on a clean glass substrate under precisely controlled conditions. The shape and size of the elements have been chosen to optimize the magnetic properties and minimize the drive requirements. A geometrical arrangement of the storage plane has been used which is determined by the degree of interference that can be tolerated on the sense lines. The logical design of the system includes the operational facilities: (read and re-write), (read, hold address, write), (write) and (read and destroy). Facilities are also available to test the operating margins (under worst case conditions) of the system.

SESSION V—CRYOELECTRIC FILMS

Radio Frequency Switching of Crossed Film Cryotrons

G. F. JONES AND G. R. HOFFMAN. (*Electrical Engineering Laboratories, University of Manchester.*)

The switching behaviour of crossed film cryotrons under radio frequency control and gate currents is considered. The mutual characteristic for threshold switching, which is analogous to the d.c. mutual characteristic, is found to be frequency dependent. An explanation is suggested in terms of the ratio of the time constant for thermal decay and the time period of the switching waveform. A proposed non-destructive read-out system using radio frequencies and their difference frequency as a sensing technique at a selected storage location is described.

Cryotron Storage Cells for Random Access Memories

V. L. NEWHOUSE AND H. H. EDWARDS. (*Research and Development Center, General Electric Company, New York.*)

Cryotron storage cells are attractive for random access memory because of their broad tolerances. In the past, their lower size limit has been set by the fact that their read-out signal becomes too small and short to be sensed by conventional amplifiers. A new sensing method has been developed which removes this limitation, so that the lower limit of cell size is now determined by fabrication technology only.

The paper describes this technique as well as a number of old and new cryotron cells compatible with it. Cell dimensions are calculated in terms of fabrication parameters and a comparison of the densities of various bit and word organized designs is made.

Relations between Deposition Parameters and Operating Characteristics of Crossed Film Cryotron Structures

R. JOYNSON. (*Research and Development Center, General Electric Co., New York.*)

The operating characteristics of crossed film cryotron structures are strongly dependent upon the deposition parameters of fabrication. Electrically, the stabile material presents no major problem since the main requirement is that it always remains superconducting at the operating temperature. For example, lead, the usual control and circuit material, has a high critical temperature ($7 \cdot 2°$K), a sufficiently high critical field (600 Oe) in the operating range $3 \cdot 2°$K to $3 \cdot 6°$K, and can be deposited readily without serious contamination. Problems of adhesion, recrystallization and corrosion do arise, however. Partial solutions of these problems are described.

The labile gate materials, tin or indium, require much more detailed consideration to achieve proper and uniform characteristics. Tin is highly anisotropic exhibiting a large change of critical temperature with strain. The critical temperature of tin is thus a function of the coefficient of expansion of the substrate, the orientation of film grains, the presence of a penumbra, and film thickness. Indium, however, having a low yield stress, relaxes by plastic flow giving films (not too thin) having transition temperatures close to its bulk value.

An example of differences of cryotron characteristics produced by various fabrication techniques is given by a comparison of the $I_g–I_c$ curves for tin gates produced by deposition through stencils and by the photomask-photoresist process.

The role of fabrication studies in the successful developments of an operating cryogenic computer and a multi-plate content addressed memory are described.

The Feasibility of the Superconducting Continuous Film Memory

V. A. J. MALLER AND P. A. WALKER. (*International Computers and Tabulators (Engineering) Ltd., Stevenage, Herts.*)

A specification is derived for a cryogenic computer store taking into account the economics and performance of competitive room-temperature stores. The extent to which the superconducting continuous film memory can meet this specification is investigated. The operating tolerances of the continuous film memory cell are derived and compared with experimental values. The tolerances of an array of such cells are considered and the parameters affecting this tolerance are discussed. The problem of obtaining an adequate yield of working batch fabricated planes is considered and it is concluded that the continuous film memory can only become a viable proposition if significant improvements are made to the fabrication technology, and a suitable redundancy scheme is designed.

An Improved Cryotron Storage-Cell for Non-Destructive Read-Out

W. HELMBERGER. (*Siemens Halske AG, Zentral-Laboratorium, Munich.*)

The paper describes essential improvements that can be achieved by using a three-cryotron cell consisting of two circuits, i.e. a storing circuit and a sensing circuit. The two circuits are superposed and inductively coupled. The storing circuit contains—comparable to the one-cryotron cell—only one write-in cryotron, while the sense circuit comprises a read-out cryotron and a sense cryotron. Employing two circuits per element permits non-destructive read-out. The sense signal is undisturbed. Starting from known characteristic data of cryotrons the following properties of the three-cryotron storage cell are derived: The maximum sense voltages at smallest cell size are obtained with in-line cryotrons. The minimum cell dimensions depend on the efficiencies of the cryotrons. The time constant of the storing circuit may be small at will. The drive current margins are wide enough to tolerate deviations in, for instance, film thickness or operating temperature. The paper brings out two important features of the three-cryotron cell compared to the one-cryotron cell which are, firstly, that for equal sense voltage the former—properly designed—occupies less area on the store plane and, secondly, that in spite of its more complicated structure, only a slightly greater masking effort is necessary during manufacture.

INSTITUTION NOTICES

Conference on Thin Films

Details of the programme together with synopses of most of the papers to be given at the Joint I.E.R.E.-I.E.E. Conference on 'Applications of Thin Films in Electronic Engineering', are published elsewhere in this issue of the *Journal*.

Registration forms and further information may be obtained from the Institution on request. Early application is advisable if residential accommodation in a college hall is required.

Conference on Electronic Engineering in Oceanography

The Institution's Conference on Electronic Engineering in Oceanography will be held at the University of Southampton from 12th to 16th September 1966. The outline programme is as follows:

Monday, 12th September (afternoon):

Opening of the Conference by Dr. G. E. R. Deacon, F.R.S. (Director of the National Institute of Oceanography).

Session I: Measurements concerned with the Body of the Sea (physical, chemical and biological aspects as well as movement therein).

Conference Reception (evening).

Tuesday, 13th September (morning and afternoon):

Session I continued.

Wednesday, 14th September (morning and afternoon):

Session II: Measurements concerned with the Sea Surface and Sea Bed.

Conference Dinner (evening).

Thursday, 15th September (morning and afternoon):

Session III: Ships, Buoys and Submerged Vehicles (including telemetry, data handling and navigation).

Friday, 16th September:

Visit to National Institute of Oceanography, Wormley, near Godalming, Surrey. (Numbers will be limited.)

The Organizing Committee are now making a selection from the large number of papers which have been offered and it is expected that the final programme will include over 30 papers and short contributions; more than a third of these will be by authors from countries outside Great Britain, e.g. from the United States of America, Canada, France, Germany and Norway. Working and static demonstrations in the laboratory and at sea will support the papers.

The sessions will take place in the Lanchester Building of the University and the Conference Reception will be in the Senior Common Room.

There will be residential accommodation for those attending the Conference in the University's Connaught Hall of residence, where the Conference Dinner will also be held.

The registration charge, which will cover the cost of preprints, and lunch and other refreshments for the three-and-a-half days of the Conference will be £10.

Further details and an outline programme of the Conference will be published in the next issue of *The Radio and Electronic Engineer*, but members and others are invited to apply now for registration forms which will be ready shortly.

Conference on Electrical Networks

The Conference on Electrical Network Theory and Design which is being organized jointly by the University of Newcastle and the Ministry of Technology (Northern Region) and the I.E.E. and I.E.R.E., will take place in the Electrical Engineering Department of the University of Newcastle upon Tyne from Tuesday, 13th September to Thursday 15th September.

Further information and registration forms may be obtained by application to the Conference Office, Ministry of Technology, Northern Regional Office, Wellbar House, Gallowgate, Newcastle upon Tyne 1. The registration fee for the Conference is £7 7s. and there will be residential accommodation at the Henderson Hall of Residence. Return of registration forms by 26th August is requested.

Conference on Automatic Operation and Control of Broadcasting Equipment

An International Conference on the Automatic Operation and Control of Broadcasting Equipment will be held at the Institution of Electrical Engineers, London, from 9th to 11th November 1966. The meeting is sponsored jointly by the Television Groups of the I.E.E. Electronics Division and of the Institution of Electronic and Radio Engineers, with the support of the Television Society and the Institute of Electrical and Electronics Engineers (European Region).

The conference will cover the following aspects:

Programme distribution systems;

Picture and sound generation equipment (including automatic lighting control);

Switching and distribution equipment;

Communication equipment;

Primary and relay transmitting equipment;

Monitoring equipment.

Requests for further information and registration forms when available may be sent to I.E.R.E., 8–9 Bedford Square, London, W.C.1.

A Transfluxor Program Store
for an Airborne Digital Computer

By

B. W. RICKARD, M.A.†

Summary: Non-destructive read-out devices for digital computer storage can have two advantages over volatile storage. Program information may not be lost in the event of computer or power supply malfunction, and economy can often be achieved in drive circuitry and power consumption. The transfluxor can be used for a store which has both these advantages, and is, moreover, electrically alterable at microsecond speeds.

This paper discusses the design of a 2048-word 20-bit word-organized store, with particular reference to the severe requirements of an airborne environment. The wiring pattern is examined and economies peculiar to this type of store are explained. Brief details are given of the read amplifier, in which a novel method of sense-line switching gives rise to further economies in circuitry.

1. Introduction

The transfluxor store is an immediate access non-volatile ferrite store. Its contents are electrically alterable by equipment which may be disconnected when filling is complete.

Its application is to cases where program or data information is required to be kept on a semi-permanent basis, but is, nevertheless, required to be quickly and easily altered on occasion. In such cases it is tedious to fill a complete volatile store from tape every time the computer is used. Examples of this sort of application arise in the whole field of computer usage—in the telephone exchange, where subscriber information is normally unaltered from day to day but may be changed occasionally; in the scientific computer, where constants and subroutines may be fixed for the duration of a series of experiments; and in commercial applications where item lists have to be associated with price and similar data, which is substantially constant over a considerable period of time.

A further application of a transfluxor store is in computers designed for a severe environment, for instance military and airborne computers. Here, a digital computer may be subjected to power supply interruption or lightning or nuclear radiation flashes. In these circumstances, temporary circuit malfunctions may be expected. If the program were held in a ferrite store using the normal read–restore cycle of operation, transient errors would be perpetuated, and the program would be lost unless extensive precautions were taken.

A transfluxor store would retain its information in such circumstances, thus enabling the program to continue when normal electronic operation was restored.

Economy of size, weight, and power consumption is essential in the design of airborne equipment. The non-destructive property of transfluxor storage affords a unique way of achieving such economies.

2. The Transfluxor

2.1. Fundamentals

The transfluxor is a two-aperture ferrite core as shown in Figs. 1 and 2. Basically, the information state is written into the core by means of the write-aperture and is non-destructively read out of the read-aperture.

Figure 1 shows the flux patterns during writing and reading of transfluxors. During the writing operation, a block current is passed through the write-aperture and sets the device to the zero state as shown in Fig. 1(a). Where necessary, the device is then set to the 'one' state by passing a set current in the reverse direction (Fig. 1(b)).

During the reading operation, a read current is passed through the read-aperture. The device is then re-set by means of a re-set current passed in the reverse direction before the next read-out cycle. In the blocked state, the read-out cycle, is unable to switch any flux because, for both read and re-set currents, one of the narrow legs is already saturated in the direction in which it is being driven (Fig. 1(c)). In the set state, the read and re-set currents successively reverse the flux in the two narrow legs, pro-

† Formerly with G.E.C. (Electronics) Ltd., Stanmore, Middx.; now with Electronic Memories Inc., California, U.S.A.
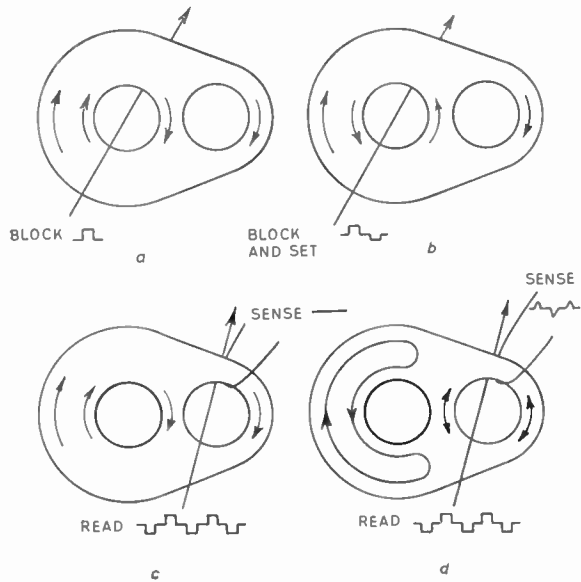
Fig. 1. The basic operation of the transfluxor. (a) the blocked state (0), (b) the set state (1), (c) the blocked state being interrogated, and (d) the set state being interrogated.

Fig. 2. Details of the transfluxor used by the author.

ducing voltage pulses on a sense winding (Fig. 1(d)). In either case, the state at the end of the cycle is left identical to that at the beginning.

Figure 2 shows the transfluxor used by the author. The following sections discuss the characteristics of transfluxors in general, but where specific values of drive currents and other parameters are quoted, they refer to the transfluxor of Fig. 2.

For this transfluxor, none of the operating conditions are unduly critical. The read-out cycle, which typically takes place during operational use, is particularly tolerant of drive current and environmental excursions.

2.2. Details

The 'write 0', or 'block', current when passed through the write-aperture, must switch all the flux in the core. Its minimum value is therefore determined by the outer circumference of the transfluxor, which is the longest flux path (Fig. 1(a)). A current of about 600 mA is sufficient, and there is no upper limit. To ensure that sufficient flux is available to saturate the centre and right-hand legs, the left-hand leg is made larger than the sum of the other two.

The 'write 1', or 'set', current, passes through the write aperture in the opposite direction to the block current (Fig. 1(b)). The transfluxor must be initially in the blocked state. The set current reverses most or

all of the flux in the centre leg but must not affect the flux in the right-hand leg. This imposes upper and lower limits on its amplitude, but for a large enough read aperture (e.g. that of Fig. 2) the tolerance is not tight. A further requirement of the 'set' current arises because it is necessary to 'set' particular elements in a rectangular matrix of transfluxors. The principle of coincident-current selection is used to achieve this, half-set currents being passed simultaneously along two orthogonal wires in the matrix. Half-set currents must therefore be insufficient to switch any flux around the write aperture. This is achieved by dimensioning the element so that the circumference of the hole is greater than half the circumference of the toroidal region in which flux switches in a fully selected element. A suitable value for the half-set currents is 170 mA $\pm 10\%$.

The read-out cycle comprises currents of alternate polarity through the read-out aperture, which switch any available flux backwards and forwards in the two legs adjacent to that aperture. The first effective pulse through the read-out aperture after 'setting' the element is one in the same direction as the 'set' current (i.e. a normal 're-set' pulse). This 'conditioning' pulse alters the flux pattern from that shown in Fig. 1(b) to that shown in Fig. 1(d). This is followed by a pulse of opposite polarity, i.e. in the same direction as the 'block' current. This is the 'interrogate' pulse. It is the response due to this pulse which is observed on the sense winding to determine whether any flux is being switched on read-out. Sense winding outputs from a transfluxor in both states are shown superimposed in Fig. 3.
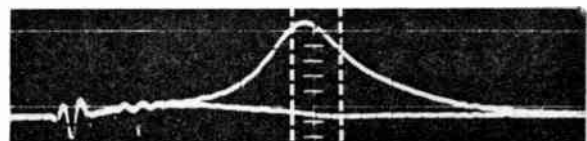

Fig. 3. Sense winding signals from a transfluxor in the blocked and the set states. Scales: vertical 50 mV per major division; horizontal 0·2 μs per major division. The dotted lines indicate the strobe period.

The re-set current as just described must be limited in amplitude, as the 'blocked' state would be disturbed by a re-set current large enough to switch flux round a loop enclosing both apertures. Subsequent read-out cycles would observe any flux thus switched as flux reversals around the read-out aperture, and the element would appear to be in a 'set' state.

This drawback does not apply to the interrogate pulse, which would only tend to reinforce the blocked state. There is no question of the interrogate pulse disturbing the 'set' state, because all the flux that could possibly pass through the right-hand leg can be accommodated in the centre leg. A 350 mA interrogate is sufficient to switch all the flux 'set' around the read aperture. There is no upper limit to this current, but little point in going higher.

The deleterious effect of too large a re-set current is averted to a large extent by adopting a more complicated path for this current (Fig. 4).
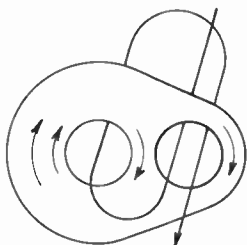
Fig. 4. An improved 're-set' winding. The transfluxor is shown in the blocked state.

The purpose of the re-set pulse is to switch flux (in the 'set' state) around the read-out aperture, and the winding now threads this flux path twice. However, the flux loop encircling both apertures, in which spurious switching would cause deterioration of the 'blocked' state, is threaded by only one turn of the re-set winding.

The re-set current can therefore be kept small and given wide tolerances without risk of altering the blocked state of any transfluxor. A typical figure for re-set current is 200 mA $\pm$ 25%. At nominal drive currents no switching process takes more than 1·5 μs.

3. Organization of the Store Matrices

A word-organized store was considered necessary because of the severe environmental conditions to be encountered in the airborne applications envisaged for this store. However, the non-destructive read-out property of the transfluxor affords the opportunity for considerable economy in drive circuitry, compared with a word-organized volatile store.

There are two reasons for this. Firstly, the interrogate current can be passed through more than one word. The sense lines can then be switched to select the required word. This is made possible because the interrogate current does not destroy the information state, therefore it is not necessary to detect the output from all interrogated elements. Secondly, the re-set current can be passed through more words than those which have been interrogated. This allows for economy in re-set driving circuits, and moreover, if no location is required to be read out more than once in a given period (as, for instance, in a sequentially accessed store), a saving of time results, since all interrogated words can be re-set simultaneously by a common re-set pulse at the end of the period.

Against these advantages must be set the drawbacks of extra windings and driving circuits for filling the store, although the filling equipment is typically a separate unit that plugs into the computer when a program is required to be written into the store.
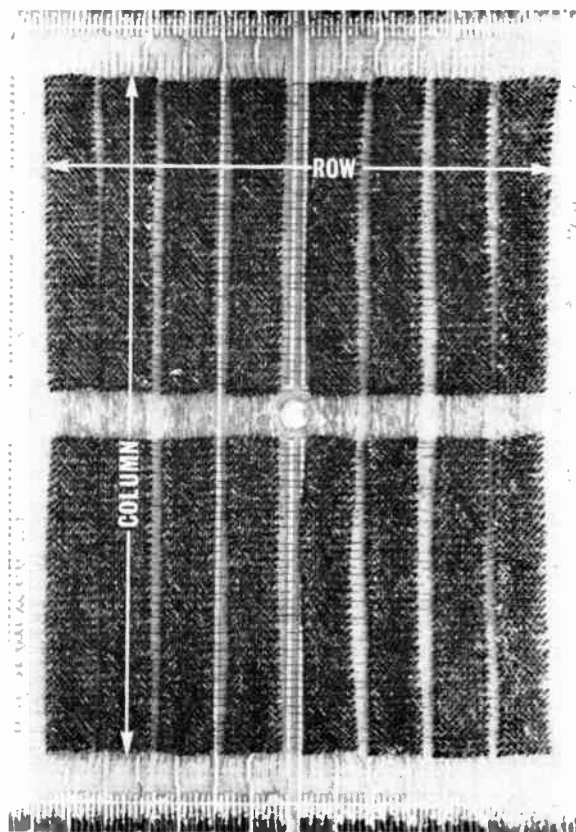

Fig. 5. A single transfluxor plane showing the layout of the windings. The whole of the core area in this photograph is encapsulated in a clear silicone jelly. An area of about 6 in × 4½ in is shown. The 2048 word store is made up of eight such planes each containing 256 words in a 64 × 80 bit array.

Also, in general, manufacturing and wiring costs for transfluxors are somewhat greater than for toroidal cores.

A photograph of one plane of the 2048-word 20-bit store with which the author has been concerned is shown in Fig. 5. There are eight such planes, and each plane has 64 columns and 80 rows of transfluxors. The following sections explain how the various current routing requirements discussed in Section 2.2 are met by the windings on this plane.

3.1. Interrogate Winding

This is a single pass of wire through the read aperture of all the transfluxors in one column. These 80 transfluxors comprise 4 words of 20 bits each. They are all interrogated whenever any one of the four words is addressed.

3.2. 'Vertical Half-set' Winding

This is a single pass of wire through the write aperture of all the 80 transfluxors in one column.

3.3. Re-set Winding

Each re-set winding threads every transfluxor in eight adjacent columns. Each element is threaded three times, as in Fig. 4, but wiring difficulties are eased by the diagonal layout of the wire which ensures that the wire always passes parallel to the axes of the apertures. These wires are most prominent in Fig. 5, and the eight blocks of 8 columns can be easily identified.

3.4. Block Windings

These thread the same groups of eight columns as the re-set windings, but consist of only one pass of wire, through the write aperture. These columns comprise 32 words, which are arranged to have consecutive addresses. There is no facility for blocking (i.e. writing a '0' into) individual locations, but if a word in the stored program is required to be altered, only the group of 32 words with the block winding common to that word need be blocked and refilled.

3.5. Horizontal Half-set/Sense Winding

The horizontal half-set winding passes through the write aperture of one *row* of transfluxors, so that when one horizontal and one vertical half-set winding are energized simultaneously, the transfluxor at their intersection is uniquely selected and switches to the 'set' state. The 'row' of elements is to be interpreted as the 512 transfluxors occupying the same position in the columns on all eight planes. Each horizontal half-set winding is therefore required to jump from one plane to the next. The same applies to the sense winding which threads the read aperture of all 512 transfluxors in a row.

It would therefore appear necessary to provide a total of 160 jumper wires between adjacent planes for these two windings. This undesirable proliferation of wiring is avoided by making use of the property that both functions (half-setting and sensing) are unimpaired when the respective wire is passed through the other aperture in the opposite direction. A single length of wire with only two ends instead of four, can therefore be used for both functions, by passing it through both apertures in this way.
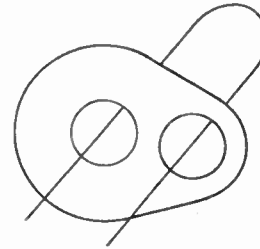

Fig. 6. Common sense/half-set winding.

Reference to Fig. 1 will show why this is possible. The dual-purpose winding can be regarded as passing round the middle leg only (Fig. 6). A pulse of current (in the same direction in the write aperture as the set current would pass in a single winding) tends to reverse the blocked flux in the middle leg (Fig. 1(a)). This flux cannot switch the right-hand leg which is already saturated, and therefore encourages a 'set' state in just the same way as a 'set' pulse passing through the write aperture only. Tests confirm that there is no difference in the effect of partial or full set currents between the two alternative windings.

The sense function of the dual-purpose winding is simple. On interrogation (and re-setting), flux switching is around the read aperture only, and it may therefore be sensed by a wire linking either the right-hand or the middle leg.

Figure 7 shows the configuration of the combined sense and horizontal half-set windings, and indicates how it passes from plane to plane with only 80 con-
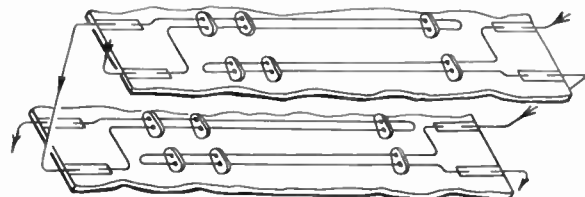

Fig. 7. Sense/half-set winding configuration. Only one connection at each side of the plane per row of transfluxors is needed. Both partial write and sense functions are performed by a single wire passing through both apertures.

nections at each edge for the 80 rows of transfluxors. An additional advantage of this scheme is that the wires are constrained to lie closely parallel and therefore pick up the minimum of stray e.m.f.

4. Operating Sequence

4.1. *Filling*

An automatic filling equipment reading from punched paper tape has been developed. The tape specifies the starting address and the data to be filled into that location and the successive following locations. The filling equipment adds one to the address after each location is filled. If the first or any subsequent address is divisible by 32, a block pulse is passed, which writes all zeros into each of the next 32 locations. For the next four addresses, current is supplied to a single vertical half-set bus-bar, and four successive groups of 20 horizontal half-set generators are energized. These are only allowed to pass current if the corresponding digit is required to be set. For the next four addresses the next vertical half-set bus-bar is energized while the required horizontal half-set pulses are again passed. The sequence is contained until the end of the tape is reached.

4.2. *Reading*

The timing sequence is shown in Fig. 8. The 5 µs access period contains two pulses of current, one interrogate and one re-set. The circuits referred to are described in Section 5.

5. Circuits

5.1. *Driving Circuits*

The pulse routing circuits are standard in design and will not be discussed in detail. In order to minimize connections to the store planes, a diode selection matrix system is used for all drive lines, reading and writing. Each drive line is connected to one of 16 'grounding bars' (transistor switches to a power rail), at one end, and, through a diode, to a 'bus bar' appropriate to the type of winding at the other end.

The selected bus-bar is connected to a source of current of the appropriate amplitude, for the required period of time, by a further transistor switch. The 32 interrogate and 32 vertical half-set bus-bars, combined with the 1-of-16 grounding bar selection, afford random access for reading or writing to any of 512 columns. Only four re-set and four block bus-bars are needed since each such winding threads eight columns.

5.2. *Sense Circuits*

Twenty sense amplifiers are used to achieve parallel read-out. They have to detect whether a transfluxor switching in the store is in the blocked or set state.

They have also to perform a one-of-four selection since four words are interrogated at once. In accordance with design requirements for an airborne computer, circuit complexity and interconnections are required to be reduced to the minimum.

Typical transfluxor outputs were shown in Fig. 3. The sense amplifier is designed to sample the output over a period of 0·15 µs when the difference between the blocked and set output is greatest. The amplified output is integrated over this period to give a direct indication of the amount of flux switched in this time.
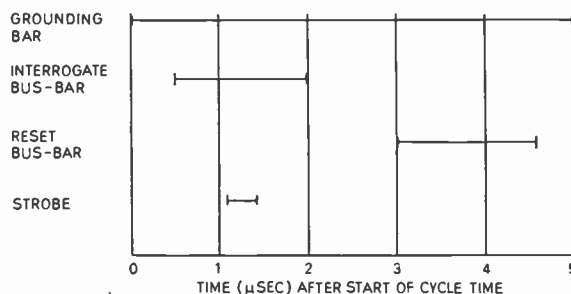

Fig. 8. Timing sequence for the read-out cycle. The horizontal bars indicate the 'on' periods of the circuits indicated at the left. Total duration = 5 µs.

The circuit used to achieve this is shown in Fig. 9. The outgoing waveforms from this circuit are passed into a further differential amplifier and pulse shaping circuitry which are quite standard and will not be discussed here.

The circuit is thus d.c. coupled throughout, which enables a complete absence of pattern sensitivity to be achieved. Moreover, the differential input stages give excellent common-mode rejection.

When no strobe pulse is applied, the transistors do not conduct and the outputs stand at equal quiescent levels of about +7 V, determined by the network of resistors and diodes. All read-out operations start from this quiescent state. The amplifier is therefore completely insensitive to time-dependent patterns of digits.

The initial stage of amplification and discrimination is performed by a pair of transistors, mounted in one case and matched for V_{be}. Such pairs are made by several manufacturers in Great Britain specifically for use in differential amplifier circuits such as this. Matching to 10 mV is achieved over a wide temperature range.

Four of the 80 sense lines represent the same digit in different words. One end of these four lines enters the read amplifier appropriate to that digit and is connected to the base of one transistor of a differential pair.
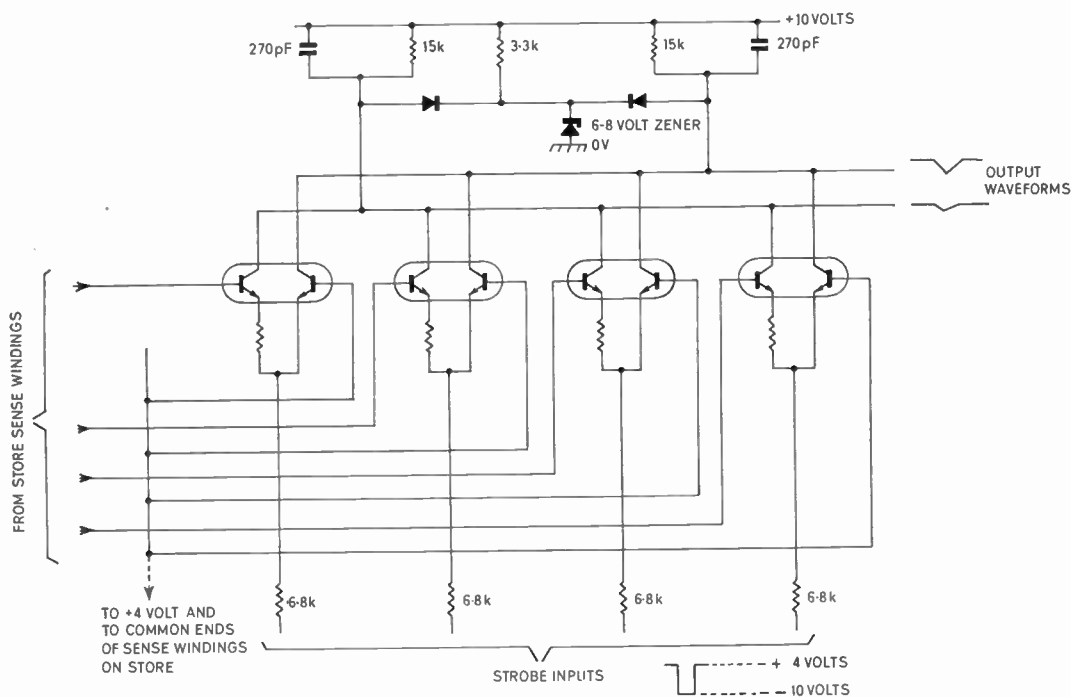
Fig. 9. The first stage of the transfluxor sense amplifier. This part of the circuit performs a one-of-four selection from four sense windings and integrates the signal on the selected line over a period determined by the strobe input. The dual transistors are matched for V_{be}.

The other ends of the four sense lines are connected together on the store stack, and, moreover, they are also connected to the other ends of all the other 76 sense lines, thus reducing the number of sense-line connections between the stack and the read amplifiers from 160 to 81. The common return line is connected to the base of the other transistor in all 80 pairs, and also to a power supply rail, at $+4$ V. All inputs to the amplifiers are terminated by 47 Ω resistors. No observable deterioration in the performance of the store is apparent as a result of this drastic simplification of the sense winding connections.

This mode of connection also suits the filling equipment, which uses the sense windings in their alternative role as half-set conductors. Current generators are applied to the 80 separate ends as required, and the common ends are left connected to the power supply. It is not found necessary to disconnect either the sense amplifiers or the current generators when they are not in use, although in service the filling equipment would normally be disconnected after use.

At the appropriate time (determined by a sample ferrite core energized by the actual driving currents) one of the four differential amplifiers is energized by connecting its strobe input to -10 V for a period

of $0.15 \, \mu$s. This causes a total current of about 2 mA to flow in the transistors (the bases are at or about $+4$ V). This current divides between the two transistors in a proportion depending on the two base-emitter voltages. Since the emitters are virtually connected together the ratio of the collector currents reflects the difference between the base voltages, in other words, the signal observed on the sense line during the strobe period.

The strobe is applied to a particular strobe input of all 20 read amplifiers in parallel, thus performing the 20-of-80 selection required to choose one word from the four interrogated.

The resistor in one emitter of the differential pair is typically 10 Ω, and serves to bias the amplifier so that the region of uncertainty between detecting the blocked and the set states lies midway between the actual observed limits of the transfluxor output.

Whichever of the four pairs of transistors is energized, the 2 mA of current flows principally from the two capacitors, causing them to discharge in the same ratio that the current divides between the two transistors. This results in the downward slope in the output waveforms shown. At the end of the $0.15 \, \mu$s the relative voltages at the two output points (regarding the quiescent level as datum) represent the integrated

values of the currents flowing in the transistors during this period, and therefore directly indicate the flux switching in the selected transfluxor.

At this time the relative voltages are further amplified and triggered into the output register, thus completing the read-out. With the strobe now off, the capacitors charge up to the quiescent state by means of the resistors of $+10$ V as shown by the upward slope on the output waveforms.

6. Computer Store

The store described in this paper now forms the program store for an advanced airborne digital computer. A scratch-pad store of 256 words using a 2-core-per-bit word organized toroidal core system is used in conjunction with the transfluxor store to provide storage which the computer can write into. Economy is achieved by using the same 16 grounding bar circuits as the transfluxor store, much of the same decoding, similar current steering and current defining circuits, and by using a fifth differential pair of transistors to route the sense signals into the transfluxor read amplifiers.

7. Conclusions

The transfluxor has been established as a viable means of achieving non-destructive read-out. A store of useful size has been built and is proving its value. Appreciable economies are achieved in driving circuitry and interconnections, and this reduces the size and weight of a computer designed for airborne use. The advantages of a random-access, word-organized store are retained, and stored information is rapidly alterable by means of an auxiliary electronic equipment.

8. References

1. J. A. Rajchman and A. W. Lo, 'The transfluxor', *Proc. Inst. Radio Engrs*, **44**, No. 3, pp. 321–32, March 1956.

2. A. W. Vinal, 'The development of a multi-aperture reluctance switch'. Read at the Western Joint Computer Conference, 1961.

Evaluation of High Quality Varactor Diodes

By

D. A. E. ROBERTS, B.Sc.†

AND

K. WILSON, B.Sc.(Eng.)‡

Summary: Recent measurement procedures used between 1 Mc/s and 40 Gc/s in evaluating very high cut-off frequency varactor diodes are discussed. The types of measurement are: bridge measurements at low frequencies, microwave coaxial line measurements, a transmission method near the diode series-resonant frequency, and a transmission method at diode parallel resonance.

Typical results from each type of measurement are given. The effect of bias on the parameters of the simple equivalent circuit is described.

Correlation of data from the four types of measurement has shown that the simple equivalent circuit does not describe the diode completely. Modification is necessary to take into account the effect at the junction of stray capacitance.

Some attempt is made to relate parametric amplifier performance to the results of diode measurements.

1. Introduction

The quality of varactor diodes used for parametric amplification has been steadily rising over recent years. Examples of modern GaAs varactor diodes are discussed in a companion paper[1] and these include diodes such as

CAY 10 (VX 3368) $f_c \simeq$ 150 Gc/s at zero bias
$\simeq$ 240 Gc/s at −6 V
VX 6508 $f_c \simeq$ 250 Gc/s at zero bias
$\simeq$ 350 Gc/s at − 6 V

Measurements of such diodes by the conventional techniques of Houlding,[2] Harrison[3] and Mavaddat[4] is made uncertain by losses in the measuring system. This problem has been discussed extensively by Hyde and Smith.[5] Furthermore, these measurements do not yield values of the equivalent circuit components, only of Q, whereas microwave engineers need to know values for these components in order that their circuits may make fullest use of the diodes. Semiconductor device manufacturers also require this information in order to determine the limitations on diode performance imposed by the encapsulation. With such information at hand, diodes and their encapsulations can be designed in such a manner as to minimize these limitations, making available the most useful diodes which the present state of the technology permits.

The four measurement techniques described in this paper were aimed at the direct evaluation of some or all of the components of the diode equivalent circuit. The results of these measurements have been consistent when considered on the basis of an equivalent circuit that includes the effect of stray capacitance at the junction.

Some attempt is made to relate parametric amplifier performance to the results of diode measurements.

2. Characterization of Variable Capacitance Diodes

A simple equivalent circuit that has frequently been used for the varactor diode is shown in Fig. 1(a). The circuit of Fig. 1(b)[5,6] has been suggested as a more accurate representation. Clearly the simpler circuit is to be preferred if it can be regarded as valid:
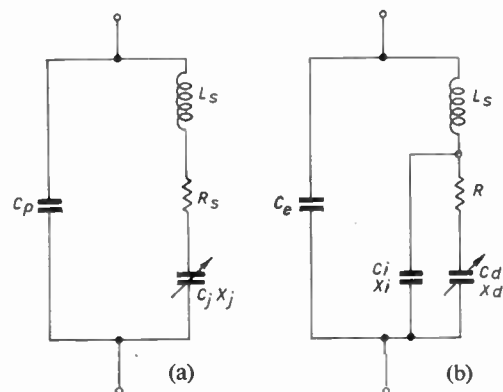

Fig. 1. (a) Simple equivalent circuit.
(b) Modified equivalent circuit.

† Mullard Research Laboratories, Redhill, Surrey; now with Philips Industries Limited, Netherlands.

‡ Associated Semiconductor Manufacturers Ltd., Wembley Laboratories, Middlesex.

in the present paper we discuss the discrepancies that arise when it is applied to high quality (low capacitance) varactors.

A cross-section through a typical high-quality varactor diode such as the VX3368 is shown in Fig. 2, together with the simple equivalent circuit. The components of the equivalent circuit are intended to have a physical significance:

R_S = series resistance. This is mainly due to the resistive losses in the mesa.

L_S = series inductance. The lead wires to the mesa and the pillar on which the semiconductor wafer is mounted form the series inductance.

C_j = capacitance of the p−n junction.

C_p = package capacitance. This is mainly due to the capacitance of the ceramic ring in the case.

The junction capacitance C_j is a function of bias; the function is theoretically

$$C_{j(V)} = \frac{C_{j(0)}}{\left(1 - \frac{V}{\phi}\right)^{1/n}} \qquad \ldots\ldots(1)$$

where $C_{j(V)}$ = junction capacitance with a bias of V volts.

$C_{j(0)}$ = junction capacitance at zero bias.

n = a constant dependent on the type of junction.

= 3 theoretically for a graded junction.

= 2 theoretically for an abrupt junction.

ϕ = contact potential of the diode.

$\simeq 1{\cdot}0$ V for GaAs diodes.

$\simeq 0{\cdot}7$ V for Si diodes.

A commonly-accepted figure to describe the quality of a diode is the Q factor of the junction capacitance when considered as a lossy capacitor.

$$Q = \frac{1}{2\pi f C_j R_S}$$
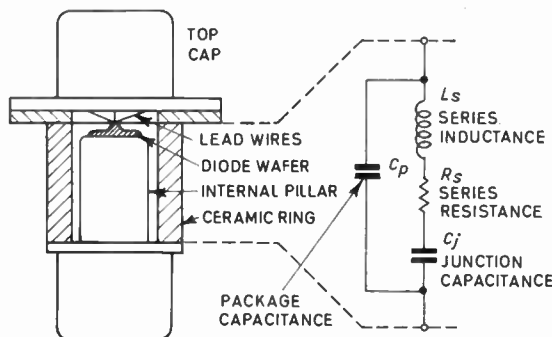
Fig. 2. Cross-section of the VX3368 varactor diode and the conventional equivalent circuit.
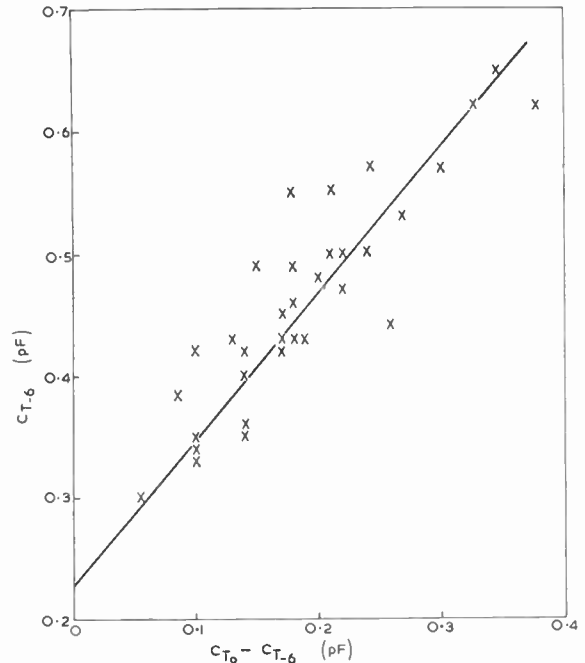

Fig. 3. Total capacitance at − 6 V vs. increase in capacitance between − 6 V and zero bias.

The frequency f and the bias corresponding to the above value of C_j need to be specified when quoting a value for Q.

The cut-off frequency f_c is defined as

$$f_c = \frac{1}{2\pi R_S C_j}$$

Again the bias needs to be specified when quoting a value for f_c.

The capacitance variation obtainable from a diode is a very important property and may be specified by the capacitance variation coefficient γ,

$$\gamma = \frac{C_{j(\max)} - C_{j(\min)}}{2(C_{j(\max)} + C_{j(\min)})}$$

For parametric amplifier work it is convenient to define γ between the typical limits of C_j encountered in such applications and to define

$C_{j(\max)} = C_j$ at 1 μA forward bias.

$C_{j(\min)} = C_j$ at 1 V reverse bias.

3. Measurement Techniques

The measurement techniques were all aimed at determining the components of the equivalent circuits of Fig. 1. From these it is then possible to determine the cut-off frequency and the capacitance variation coefficient.

3.1. *Bridge Measurements of Capacitance*

The total capacitance of the diodes (i.e. $C_j + C_p$) can conveniently be measured on a transformer ratio

arm bridge at 1 Mc/s where the series inductance and series resistance will be negligible.

C_j and C_p can be separated if the capacitance—voltage law can be determined from measurements on a large number of diodes. Each diode can be measured at two bias values such as zero bias and say -6 V. If $C_{T(-6)}$ is plotted against $C_{T(0)} - C_{T(-6)}$

where $C_{T(0)}$ = total capacitance at zero bias

$C_{T(-6)}$ = total capacitance at -6 V bias

for a large number of diodes, the result is a straight line, the slope of which enables the capacitance law to be determined. (See Appendix and Fig. 3). Knowing the capacitance law, measurements at two different biases on any diode of that type enable C_p and C_j for that diode to be found.

3.2. Coaxial Slotted Line Measurements

A method has previously been described[7] for the measurement of varactor diodes by a slotted-line technique. In this method the diode is mounted at the end of a 50-ohm slotted line and its impedance can be determined by means of standard microwave measuring techniques. Precautions have to be taken to keep the power level at the diode below that which will affect its impedance, and as the v.s.w.r. values obtained are high, the double minimum method of measurement is most suitable.

From the results of measurement at a number of frequencies typically between 3 and 18 Gc/s, a plot of the diode impedance against frequency can be obtained. A study of the results showed that the diodes could be represented at zero bias by the simple circuit of Fig. 1(a). The constants of this simple circuit can easily be obtained if we know the series resonant frequency, f_s, and the v.s.w.r. at this frequency, the parallel resonant frequency, f_p, and the reactance at one other frequency, typically $f_s/2$.

The foregoing assumes that it is possible to measure the parallel resonant frequency; however with present-day diodes this may be at too high a frequency to permit the use of a slotted line. In such a case a knowledge of the reactance value at the highest frequency of measurement, instead of f_p, enables the diode circuit constants and f_p to be calculated.

If bias is applied to the diode on the line, we may study for example the variation of f_s with bias. This is quite a simple measurement, and the variation of r.f. capacitance with bias, and hence γ, may readily be derived from it.

3.3. Transmission Measurements Near Series Resonance

A transmission measurement technique was first proposed by DeLoach[8] for measurement of un-encapsulated diodes. This technique is applicable to encapsulated diodes if the package capacitance has a

reactance which is large compared to the diode resistance at the series resonant frequency

$$f_s = \frac{1}{2\pi\sqrt{L_s C_j}}$$

The method as described here differs from that described by DeLoach in that a swept-frequency source is not required.

The diode is mounted between the broad faces of the reduced-height waveguide with well-matched tapers to full-height guide on either side as shown in Fig. 4. Means are provided for applying bias. The band chosen should be that which contains the diode series resonant frequency f_s. The presentation given here is based on the simple equivalent circuit for the diode.
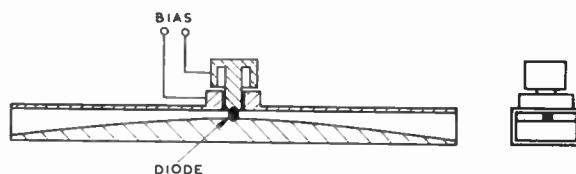

Fig. 4. Waveguide holder used for transmission measurements near the series resonant frequency.
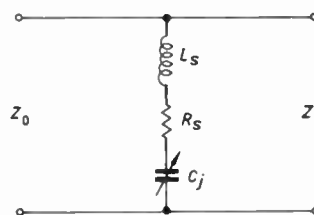

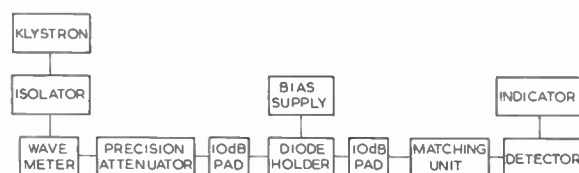Fig. 5. Equivalent circuit of a diode in the holder of Fig. 4.

Fig. 6. Apparatus for transmission measurements near the series resonant frequency.

The equivalent circuit of the system thus becomes the diode equivalent circuit shunting a transmission line. When the diode is near series resonance in most cases it will be found that the reactance of the package capacitance and the detector impedance are high enough to have negligible shunting effect. The equivalent circuit then reduces to a series LCR circuit shunting the transmission line (Fig. 5). Measurements of transmission loss past the diode can be made with the arrangement of Fig. 6. The following procedure can then be adopted.

(a) The frequency is found at which the transmission loss T is a maximum with zero bias on the diode. This corresponds to the series resonant condition when the diode behaves as a resistance R_S. The transmission loss is measured and the series resistance R_S can be determined since

$$T = \left(\frac{Z_0}{2R_S} + 1\right)^2$$

where Z_0 = characteristic impedance of the reduced height waveguide. The power-voltage definition of impedance is required.

(b) The variation of the series resonant frequency f_s with bias enables the capacitance variation to be found since

$$C_j = \frac{1}{4\pi^2 L_S f_s^2}$$

Thus plotting $\frac{1}{f_s^2}$ versus bias gives a plot of KC_j versus bias where k is an unknown constant, (Fig. 7).

(c) The frequency is reset to that required for series resonance at zero bias. The forward bias V_1 and the reverse bias V_2 required to double the transmitted power are measured. From the plot of KC_j versus bias corresponding values of KC_{j1} and KC_{j2} can be found. The Q of the diode is then given by

$$Q = \frac{KC_{j1} + KC_{j2}}{KC_{j1} - KC_{j2}}$$

(d) The cut-off frequency of the diode at zero bias is thus

$$f_{c(0v)} = Qf_{s(0v)}$$

(e) The junction capacitance at zero bias is

$$C_{j(0v)} = \frac{1}{2\pi R_S f_{c(0v)}}$$

This then enables the plot of KC_j versus bias to be calibrated.

(f) The series inductance L_S can be found since

$$f_{s(0v)} = \frac{1}{2\pi\sqrt{L_S C_{j(0v)}}}$$

(g) If the applied bias voltage for a forward current of 1 µA is V_F then values for $KC_{j(V_F)}$ and $KC_{j(-1)}$ can be read off the curve of KC_j versus bias. The capacitance variation coefficient can then be determined from the relation

$$\gamma = \frac{KC_{j(V_F)} - KC_{j(-1)}}{2(KC_{j(V_F)} + KC_{j(-1)})}$$

3.4. Transmission Measurements at Parallel Resonance

Measurements at the diode series-resonance give much useful information, but they do not include the effect of the package capacitance C_p. The diode parallel self-resonance involving C_p has significance in recent
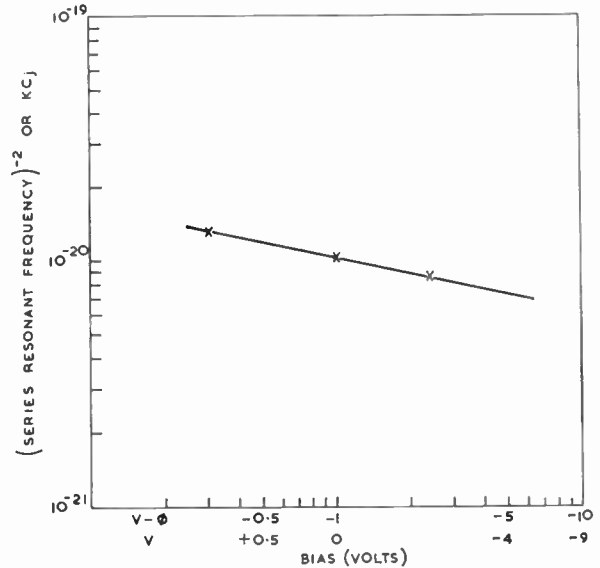
Fig. 7. (Series resonant frequency)$^{-2}$ vs. bias.

parametric amplifier design as it can be used as an idling resonance. Idling current can then be confined entirely to the diode capsule. Because of this possibility it is desirable to have a quicker method of finding the frequency and bandwidth of this resonance than that using the slotted line. By the extension of the slotted line technique mentioned in Section 3.2 it has been possible to predict that the parallel resonance frequency f_p for the VX3368 diodes may be expected to be in the region 27 Gc/s to 30 Gc/s.

An approach to a sweep type of measurement is now described. As the diode impedance is high at the parallel-resonant frequency, a method that is in some ways the dual of the one we use at the series-resonant frequency appears attractive. This requires the diode to be mounted in series with the source and the load: there should then be a minimum of transmission at f_p. A convenient way of doing this would be to mount the diode in the inner conductor of a coaxial line. However, as coaxial connectors are not (as yet) widely used at Q-band frequencies, the approach adopted here has been to mount the diode in the inner of a very short piece of coaxial line connecting two waveguide-to-coaxial transitions. The scheme is shown diagrammatically in Fig. 8. The diode can be removed and replaced by a brass dummy so that there is a direct coaxial line connection between the two waveguides.

Bias may be applied to the diode via the inner conductor of a choke system consisting of high and low impedance quarter-wave sections. The choke system is designed to present a very low impedance in series with the diode line.
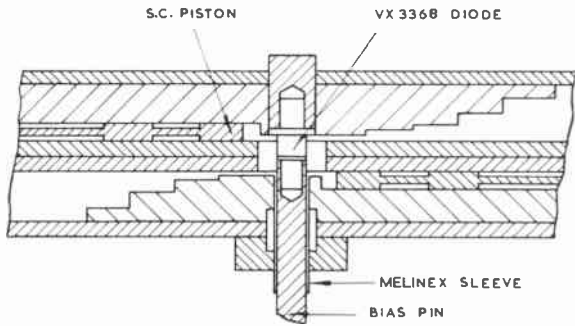
Fig. 8. Linked waveguide test circuit.

Experiments are carried out with the mount connected between a Q-band swept source and a well-padded crystal detector. Figure 9(a) shows a photograph of the oscilloscope trace when the waveguides were directly linked, and Figure 9(b) shows the corresponding trace when a diode was connected between the waveguides. In these and the other traces of Figure 9 the sweep range was 26·5 Gc/s to 30 Gc/s. Trace 9(b) taken alone gives no obvious indication of resonance, due to the variation with frequency of the source power and the insertion loss of the test device. However, if the ratio of the trace heights 9(a) and 9(b) is taken at corresponding frequencies, the results of curve (1), Fig. 10 may be obtained. This shows a resonance peak at about 27 Gc/s. This particular diode had also been measured by the coaxial line method at frequencies up to 15·5 Gc/s and from these measurements f_p had been predicted at 26 Gc/s. This seems to give a reasonable agreement.
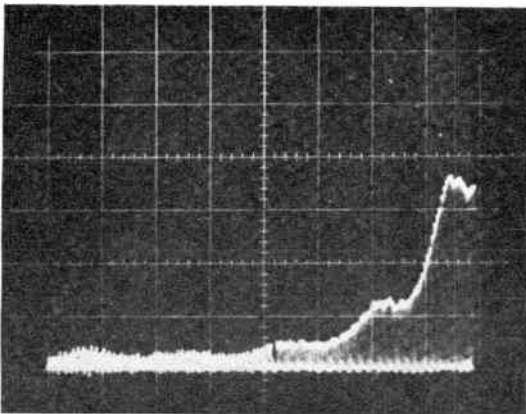
Trace 9(c) was taken with $-0·77$ V bias applied to the diode to reduce the junction capacitance C_j, and similar comparison of 9(a) and 9(c) gives the curve (2) in Fig. 10 showing an increase in f_p.
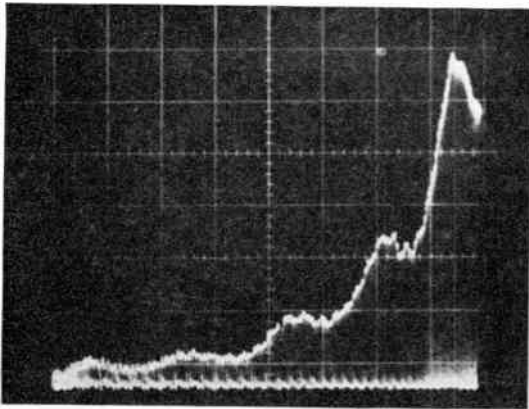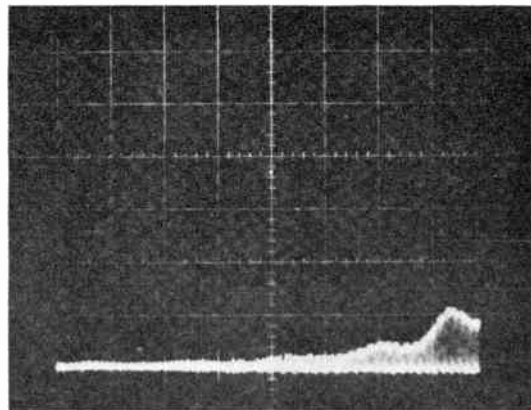

(a) Waveguides linked by brass inner.
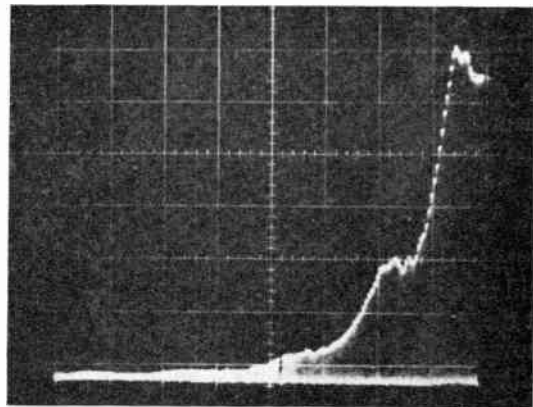
(b) Diode *in situ*, zero bias.

(c) Diode *in situ* $-0·77$ V bias.

(d) Residual coupling with diode removed.

Fig. 9. Oscilloscope traces from 'linked waveguide' measurement with VX3368 diode. Range of sweep 26·5 — 30 Gc/s.
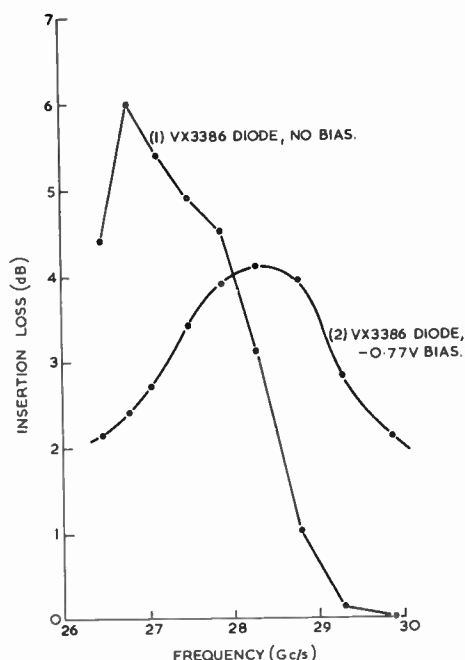
Fig. 10. Diode parallel resonance in linked waveguide mount.

If f_s and C_j are known (for example from the measurements of Sections 3.2 or 3.3) then C_p can be found from the relationship

$$\frac{C_j}{C_p} = \left(\frac{f_p}{f_s}\right)^2 - 1$$

Some perfection of the linked-waveguide technique is still required. For example, trace (d) of Fig. 9 shows that there is residual coupling even when the diode is removed. There is also scope for a more effective levelling scheme to flatten the response of the system.

4. Results of Measurements

Some inconsistencies between the results of the various measurements were noted on the basis of the simple equivalent circuit. As an example, the results obtained on a typical VX3368 diode are shown in Table 1.

It can be seen that fairly good agreement is obtained between the microwave measurements but the junction capacitance measured at microwave frequencies is of the order of 0·1 pF greater than that measured at 1 Mc/s. Figure 11 shows that this is the case over the range of bias values. Also the junction capacitance variation with bias (given as $C_{j(0V)}/C_{j(-6V)}$ in Table 1) is less at microwave frequencies, as can be seen from Fig. 11.
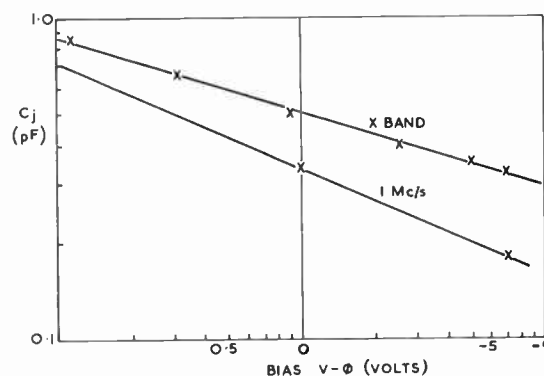

Fig. 11. Variation of C_j with bias.

Coaxial line measurements and transmission measurements at series resonance also showed that the measured value of series resistance appeared to vary with the bias level, at which the measurement was made, in the manner shown in Fig. 12.

5. A Modified Equivalent Circuit

The above effects indicate that the simple equivalent circuit assumed for the diode was not completely adequate and should be modified. Figure 1 compares the simple and modified equivalent circuits.

At microwave frequencies the effective stray capacitance directly across the diode terminals will be the same for both the conventional and the modified equivalent circuits, i.e. at microwave frequencies

Table 1

Measurement Technique	R_s (ohms) at 0 V	C_j (pF) at 0 V	C_j (pF) at − 6 V	$\dfrac{C_{j\,(0V)}}{C_{j\,(-6\,V)}}$	L_s (pH)	C_p (pF)	f_c (Gc/s) at 0 V
Bridge measurement 1 Mc/s	—	0·34	0·18	2·05	—	0·24	—
Coaxial line measurement (4 to 15·5 Gc/s)	2·2	0·50	—	—	580	0·07	142
Transmission measurement at series resonance	2·2	0·42	0·28	1·5	620	—	172
Transmission measurement at parallel resonance	—	—	—	—	—	0·08	—
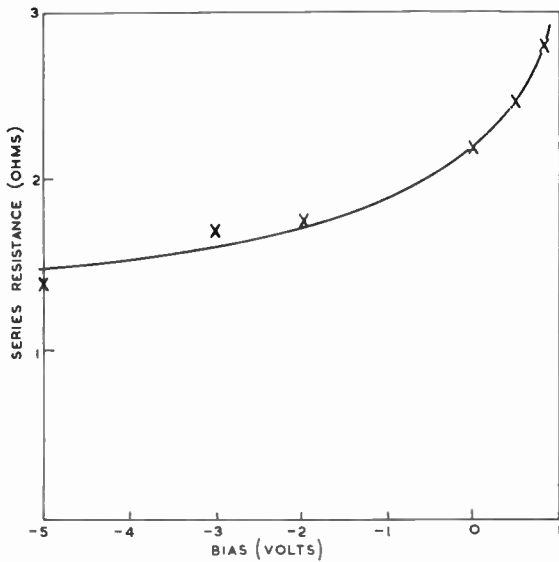
Fig. 12. Apparent series resistance variation with bias.

Table 2

	Junction Capacitance (C_j)	Package Capacitance (C_p)
1-Mc/s bridge measurement	C_d	$C_i + C_e$
Coaxial line measurement	$C_d + C_i$	C_e
Transmission measurement at series resonance	$C_d + C_i$	—
Transmission measurement at parallel resonance	$C_d + C_i$ (value assumed)	C_e

$C_p = C_e$. Hence by equating the impedances of the series branches of the two circuits it can be shown that

$$R_s = \frac{R X_i^2}{R^2 + (X_d + X_i)^2}$$

and

$$X_j = \frac{R^2 X_i + X_d X_i (X_d + X_i)}{R^2 + (X_d + X_i)^2}$$

which, if $R \ll X_i$, can be reduced to

$$R_s \simeq \frac{R}{\left(\dfrac{C_i}{C_d} + 1\right)^2} \qquad \ldots\ldots(2)$$

and

$$C_j \simeq C_d + C_i \qquad \ldots\ldots(3)$$

Equation (2) shows that R_s will vary with bias since C_d will vary with bias. By inserting typical values in (2) it has also been found that the variation of R_s with bias predicted by (2) is similar to that found in practice.

Equation (3) shows that the measured value of junction capacitance at microwave frequencies will be higher than the actual junction capacitance by an amount C_i which is about 0·15 pF for the VX3368.

The junction and package capacitances measured by the various methods will thus be as shown in Table 2.

If the modified equivalent circuit is assumed then the results of all measurements show fairly good correlation.

6. The Physical Basis of the Modified Equivalent Circuit

The diode package used for the VX3368 diode is shown in section in Fig. 2. Measurements on cases containing dummy short-circuit diodes have been made in the holder used for the transmission measurement described in Section 3.3. These measurements were compared with measurements on brass posts, of the same diameter as the package internal pillar, which were made to mount in the same holder. The results showed that the package inductance was due mainly to the internal pillar and was not greatly affected by the wire connections to the diode mesa.

Physically the internal stray capacitance $C_i \simeq 0·15$ pF cannot all be explained in terms of the capacitance existing between the top cap of the package and the diode wafer. However, capacitance measurements of empty diode cases on a 1-Mc/s bridge have shown that if the internal pillar is removed the case capacitance decreases by about 0·09 pF. This can only be explained in terms of the capacitance from the sides of the pillar to the top cap via the ceramic ring.
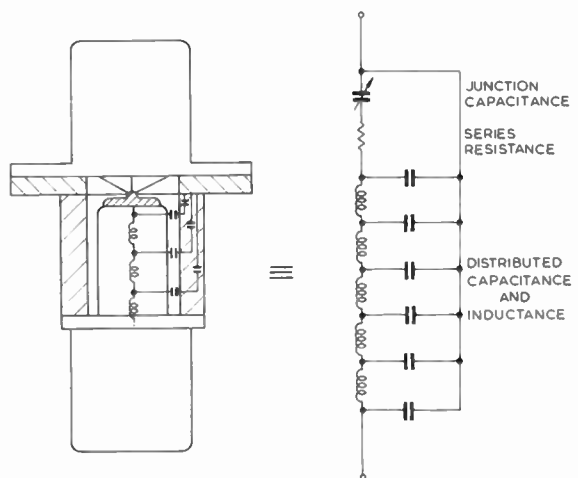

Fig. 13. The distributed nature of the stray capacitance and series inductance.

Since it has been established that most of the inductance occurs in the internal pillar, the true equivalent circuit thus has distributed stray capacitance and inductance as shown in Fig. 13. This can be approximated to the modified equivalent circuit used to analyse the microwave measurements.

7. Diode Measurements and Amplifier Performance

A diode that had been measured in terms of the simple equivalent circuit by the transmission technique of Section 3.3 was operated in a C-band parametric amplifier of a type described in a companion paper.[9] The signal frequency was 5·9 Gc/s and the idler frequency was 32 Gc/s. Measurements were made of the noise temperature of the amplifier at 20 dB gain (by measuring overall noise temperature and subtracting contributions from circulator and following receiver).

Also, when the amplifier was unpumped, v.s.w.r. measurements were made at the signal input.

The theoretical noise temperature contribution T from the amplifier is given by

$$T = T_0\left[\frac{R'_s}{R_g} + A\frac{f_1}{f_2}\left(1 + \frac{R'_s}{R_g}\right)\right] \quad \ldots\ldots(4)$$

where T_0 = temperature of diode (taken as 290°K)

R'_s = effective series resistance of diode as seen by the signal circuit.

R_g = signal circuit impedance presented to the diode.

A = constant; at 20 dB gain $A = 0·82$

f_1 = signal frequency

f_2 = idling frequency

R'_s differs from R_s because of the effect of the external stray capacitance C_e. While this may be neglected at the series resonance f_s in X-band, this is no longer the case away from the resonance, and we have

$$R'_s = \frac{R_s}{\left[\omega_1 C_e\left(\omega_1 L_s - \frac{1}{\omega_1 C_j}\right) - 1\right]^2} \quad \ldots\ldots(5)$$

where $\omega_1 = 2\pi f_1$

From the unpumped v.s.w.r. measurements we can derive the value of R_g/R'_s that applies in the amplifier.

This is given by

$$S_0 = \frac{R_g}{R'_s} \quad \ldots\ldots(6)$$

where S_0 = input v.s.w.r. at resonant frequency of the signal circuit.

Thus when R_g is known, the value of the effective diode resistance R'_s in the amplifier can be derived and compared with the value of R'_s obtained from the transmission measurements.

The v.s.w.r. S_0 may also be used to derive the operating value for the product $\gamma_0 f_{c0}$ where γ_0 is the capacitance variation coefficient that gives 20 dB gain. We have

$$\gamma_0 f_{c0} = \sqrt{A f_1 f_2\left(1 + \frac{R_g}{R'_s}\right)}$$
$$\simeq \sqrt{A f_1 f_2(1 + S_0)} \quad \ldots\ldots(7)$$

This may be compared with the product γf_{c0} derived from the transmission measurements where γ is defined by the capacitance values at 1 μA forward current and at -1 V bias.

Some values obtained are given in Table 3. The value of R_g for this amplifier was 6 ohms: C_e for the diode was taken as 0·07 pF.

Table 3

Diode resistance:	From X-band transmission measurements	1·60 ohms
	With correction for effect of C_e (eqn. (5))	1·30 ohms
	From v.s.w.r. in unpumped amplifier	1·56 ohms
Amplifier noise temperature:	Calculated from eqn (4)	119°K
	Measured	139°K
γf_{c0} (from diode measurements)		30·1 Gc/s
$\gamma_0 f_{c0}$ (from amplifier operation for 20 dB gain)		27·4 Gc/s

It can be seen that the diode resistance in the amplifier was measured as 20% above that of the corrected value derived from diode transmission measurements. The amplifier noise temperature was 17% greater than that predicted from the diode measurements. As the values of γf_{c0} (derived from measurement of the diode in the amplifier) are close it may be assumed that the definition of γ in Section 2 has practical significance. Diodes for which the transmission measurements showed γf_{c0} values less than about 27 Gc/s could only be made to give 20 dB gain in the amplifier when pumped into forward current, which degraded the noise performance.

8. Conclusions

Measurements have been made on high quality varactor diodes by four different techniques. These were bridge measurements at 1 Mc/s, coaxial line measurements from 4 Gc/s to 18 Gc/s, a transmission method in the region of the diode series resonance (about 10 Gc/s), and a transmission method at the diode parallel resonance (about 30 Gc/s).

When the results of the different methods were expressed in terms of the simple equivalent circuit there appeared to be discrepancies in capacitance,

and a variation in resistance with bias. The use of the full equivalent circuit has explained these effects and shown good agreement between the methods of measurement.

Although the modified equivalent circuit gives a better description of the diode, its application in circuit design is sometimes a little cumbersome. Here there is little to gain in the use of the full equivalent circuit, especially where, as in some parametric amplifier work, series circuit assumptions are already made.

The noise performance of a parametric amplifier (at 5·9 Gc/s) has been compared with that predicted from the diode measurements based on the simple equivalent circuit and the 'γf_c' product derived from the measurements has been shown to be of practical significance.

9. References

1. C. A. P. Foxell and K. Wilson, 'Gallium arsenide varactor diodes', *Proceedings of the Symposium on Microwave Applications of Semiconductors, London 1965, Paper No. 31. The Radio and Electronic Engineer*, **31**, No. 4, p. 245, April 1966.

2. N. Houlding, 'Measurement of varactor quality', *Microwave J.*, **3**, p. 40, 1960.

3. R. I. Harrison, 'Parametric diode Q measurements', *Microwave J.*, **3**, p. 43, 1960.

4. R. Mavaddat, 'Varactor diode Q factor measurements', *J. Electronics and Control*, **15**, p. 51, July 1963.

5. F. J. Hyde and R. B. Smith, 'Effect of losses in varactor diode impedance measurements', *Proc. Instn Elect. Engrs*, **111**, No. 3, p. 471 I.E.E. Paper No. 4440E, March 1964.

6. J. D. Pearson and K. S. Lunt, 'A broadband balanced idler circuit for parametric amplifiers', *The Radio and Electronic Engineer*, **27**, p. 331, May 1964.

7. D. A. E. Roberts, 'Measurements of varactor diode impedance', *Trans. I.E.E.E. on Microwave Theory and Techniques*, MTT-12, p. 471 July 1964. (Letter).

8. B. C. DeLoach, 'A new microwave measurement technique to characterize diodes and an 800 Gc/s cut-off frequency varactor at zero volts bias', *Trans. I.E.E.E.*, MTT-12, p. 15, January 1964.

9. C. S. Aitchison, R. Davies and P. J. Gibson, 'A simple diode parametric amplifier design for use at S-, C-, and X-band', *Proceedings of the Symposium on Microwave Applications of Semiconductors, London*, 1965. Paper No. 26. (I.E.R.E. Conference Proceedings, No. 5.)

10. Appendix

Low Frequency Capacitance Measurements

If $\quad C_{j(0)}$ = junction capacitance at zero bias

$C_{j(-6)}$ = junction capacitance at -6 V bias

C_p = package capacitance

$C_{T(0)}$ = total capacitance at zero bias
$$= C_{j(0)} + C_p$$

$C_{T(-6)}$ = total capacitance at -6 V bias
$$= C_{j(-6)} + C_p$$

Then from eqn. (1)

$$C_{j(-6)} = \frac{C_{j(0)}}{\left(1 + \dfrac{6}{\phi}\right)^{1/n}}$$

hence

$$C_{j(0)} - C_{j(-6)} = C_{j(-6)}\left[\left(1 + \frac{6}{\phi}\right)^{1/n} - 1\right]$$

Now

$$C_{T(0)} - C_{T(-6)} = (C_{j(0)} + C_p) - (C_{j(-6)} + C_p)$$
$$= C_{j(0)} - C_{j(-6)}$$

Therefore

$$C_{T(0)} - C_{T(-6)} = C_{j(-6)}\left[\left(1 + \frac{6}{\phi}\right)^{1/n} - 1\right]$$

If we assume n and ϕ are constant for all diodes of a given type the above can be rewritten as

$$C_{j(-6)} = A(C_{T(0)} - C_{T(-6)}) \qquad \ldots\ldots(8)$$

where

$$A = \left[\left(1 + \frac{6}{\phi}\right)^{1/n} - 1\right]^{-1}$$
$$= \text{a constant}$$

Now

$$C_{T(-6)} = C_{j(-6)} + C_p$$

Therefore

$$C_{T(-6)} = A(C_{T(0)} - C_{T(-6)}) + C_p$$

If C_p is constant for all diodes then plotting $C_{T(-6)}$ against $(C_{T(0)} - C_{T(-6)})$ for a large number of diodes should give a straight line cutting the $C_{T(-6)}$ axis at C_p (giving the average package capacitance of the diodes) and having a slope of A which is a measure of the capacitance law. Such a plot is shown in Fig. 3 for thirty-four VX3368 diodes.

The value of A from Fig. 3 is 1·19

Therefore

$$A = \frac{1}{\left(1 + \dfrac{6}{\phi}\right)^{1/n} - 1} = 1\cdot19$$

For GaAs diodes $\phi = 1$ V

hence $n = 2\cdot48$ or $1/n = 0\cdot404$.

The capacitance law has now been established i.e.

$$C_{j(v)} = \frac{C_{j(0)}}{(1-v)^{0\cdot404}}$$

Also, since we have established a value for A, then by measuring $C_{T(0)}$ and $C_{T(-6)}$ for any diode of this type the value of $C_{j(-6)}$ can be found from eqn. 8).

Performance and Realization of Broad-band Semiconductor Diode Frequency Triplers

By

W. HEINLEIN, Dr.-Ing.†

AND

A. KÜRZL, Dipl.-Ing.†

Summary: The paper deals with the mechanism of frequency multiplication by means of charge-storage diodes, discusses the theory of the noise of such multipliers, and shows the technical realization of a broad-band frequency tripler with lumped-element circuitry.

1. Multiplier Action of Semiconductor Diodes

Semiconductor diodes have proved to be useful frequency multipliers. Figure 1(a) shows the simplest circuit for producing harmonics with the aid of a back biased diode. This circuit is outstanding by the fact that it is terminated into a resistive impedance R for all harmonics. The fundamental-frequency generator produces the voltage $U_m \cos \omega t$. Normally the bias voltage U_0 is automatically produced by the rectified current of the diode. In this circuit the characteristic parameters of various diodes can be measured in a particularly simple manner.

Figures 1(b), (c) and (d) show how three typical diodes perform in the circuit of Fig. 1(a), namely a variable-resistance diode, a variable-capacitance diode, and a charge-storage diode. The figures show the dynamic characteristics of current i and charge $q = \int i \, dt$ vs voltage u of the series-connection of the diode with the load resistance R. The variable-resistance diode having approximately zero forward resistance and zero reverse conductance exhibits a current vs. voltage characteristic consisting of a broken line (Fig. 1(b)). This diode produces a high rectified current which feeds into the biasing source most of the fundamental-frequency power. Frequency multiplication by means of the variable-capacitance diode is based on the voltage-dependent barrier capacitance. The associated dynamic characteristics (Fig. 1(c)) still show great resemblance to the elliptical ones resulting from a constant capacitor in place of the diode. The charge-vs.-voltage characteristic of the barrier capacitance is shown in dashed line in Fig. 1(c). Unlike the variable-resistance diode, the charge-storage diode returns most of the charge injected by the forward current; ideally, almost no rectified current appears and the fundamental-frequency power is fully converted into harmonic power. The reverse current is clearly shown by the current-vs.-voltage characteristic (Fig. 1(d)). Fre-

quency multiplication with variable-resistance diodes has been studied by Page,[1] that with variable-capacitance diodes by Penfield and Rafuse[2] and that with charge-storage diodes by Leenov and Uhlir[3] and Krakauer.[4]

The areas A_1 and A_2, respectively, bounded by the characteristics in Fig. 1, are directly related to the reactive and the active power supplied by the fundamental-frequency source. From these areas the fundamental-frequency equivalent circuit of the driving point impedance can thus be derived. It consists of a conductance G and shunt capacitance C. The following relationships, which will not be proved here, hold for these values,
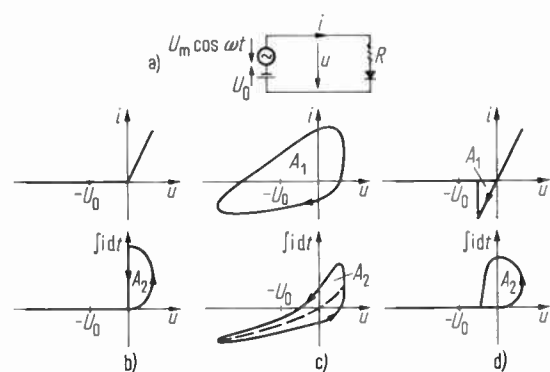
$$G = \frac{2fA_2}{U_m^2}$$

$$C = \frac{A_1}{\pi U_m^2}$$

Fig. 1. (a) Equivalent circuit of the simplest harmonic generator with a reverse biased semiconductor diode.

Dynamic current and charge characteristic vs. voltage of the harmonic generator using

(b) a variable resistance diode,

(c) a variable capacitance diode,

(d) an ideal step recovery diode.

---

† Central Laboratories, Siemens and Halske AG, Munich.

The elements G and C of the fundamental-frequency equivalent circuit of the diode in a special multiplier circuit must usually be determined empirically. In the present state of the art they cannot be calculated accurately enough from static diode data.

For frequency multipliers of high output power charge-storage diodes have given the best efficiencies. Usually all variable-capacitance diodes exhibit the charge-storage effect at sufficiently high frequencies. When variable-capacitance diodes are used for frequency multiplication, the best efficiency is only attained when the diode is driven with such a voltage swing that charge storage becomes fully effective. This is obvious from the relations measured between efficiency, input power, bias voltage, and rectified current, as will be shown.

Figure 2 shows an example for these relations in the form of a conversion chart,[5] the conversion loss K of a tripler being shown as a function of the input power P_i and the bias U_0 in the same way as the height contours of a mountain range on a map. Also shown in Fig. 2 are some lines of constant rectified current I_0. The dashed heavy line corresponds to zero rectified current. With sufficiently low input power and suitable bias voltages the diode is driven only in the reverse direction so that no rectified current flows. In this region the diode acts as a variable-capacitance diode, and the efficiency attainable is considerably below the possible maximum. The region between breakthrough voltage and forward voltage is fully used, if input power and bias voltage correspond to the branching point of the heavy dashed lines $I_0 = 0$ in Fig. 2. The maximum efficiency appears at an optimum bias $U_{0(opt)}$ and an optimum input power $P_{i(opt)}$. This optimum input power drives the diode already far into the forward direction. The improvement of the efficiency as compared to operation in the reverse direction only is due to the charge-storage effect.

If high efficiency is to be attained, care must be taken that, with the aid of suitable filter networks, the incoming fundamental-frequency power is converted as exclusively as possible into the desired harmonic alone. According to our experience, in this case the diode current, as well as the diode voltage, contains not only waves of the input and output frequency, but an optimum combination of all other harmonics. In practice neither current control, nor voltage control of the diode is thus realized. With current control the diode current contains only components of the input and the output frequency; with voltage control the same holds for the voltage.

The oscillographs of Fig. 3(a) and 3(b) show typical diode current waveforms in a frequency tripler with 230 Mc/s input frequency under optimum conditions.
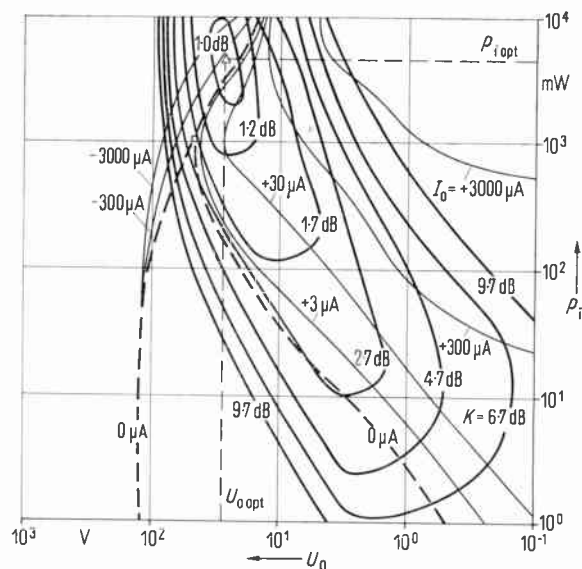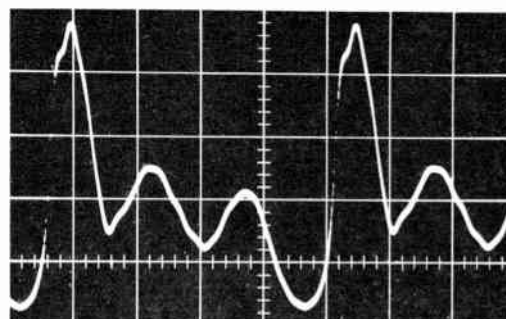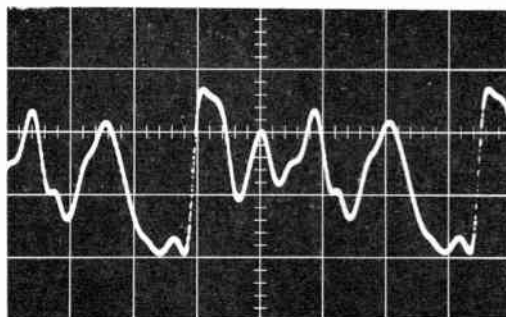

Fig. 2. Experimental conversion chart of a tripler with 230 Mc/s input frequency. Diode MA4060C. $K =$ conversion loss; $P_i =$ input power; $U_0 =$ bias voltage; $I_0 =$ rectified current.

(a) Diode MA4060C.

(b) Diode SV12/4.

Fig. 3. Optimum diode current waveform in an experimental test tripler with 230 Mc/s input frequency and a given input power (cf. Table 1).

Horizontal scale: 1 ns per large division.

Vertical scale: 220 mA per large division.

Table 1

Diode data and relative amplitudes and phases of optimum diode current harmonics

Tripler	Diode	Step recovery time	Input power	Conversion loss†		$|I_2/I_1|$	$\varphi_2 - \varphi_1$	$|I_3/I_1|$	$\varphi_3 - \varphi_1$	$|I_4/I_1|$
Fig. 3(a)	MA4060C	~ 0·5 ns	1650 mW	2·5 dB	..	0·90	− 25°	1·35	− 49°	
Fig. 3(b)	SV12/4	~ 0·2 ns	500 mW	2·0 dB	..	0·71	− 40°	1·40	− 70°	0·27

† Losses due to the 0·9-ohms series resistance of the current probe and to the circuit are included.

Table 1 shows the relative amplitudes and phases of the harmonics contained in the two current curves as well as the diode and multiplier data. According to the data of Table 1, the relative amplitudes of the optimum diode current harmonics are approximately the same for the two diodes; but the relative phases (expressed in degrees of the fundamental period) of these harmonics show larger differences.

The optimum driving conditions resulting in maximum efficiency of the diode are a complicated function of the diode data and have only been determined experimentally so far. To realize optimum driving conditions in the case of a tripler, the circuit must offer to the diode a predetermined impedance for all harmonics at least up to the fifth. Further demands must be satisfied by the circuit, however, if maximum efficiency is to be attained within a wider bandwidth without filter retuning, and if the output frequency has to be of the highest spectral purity possible.

2. Noise Performance of Frequency Multipliers†

Experience has shown that the output power of frequency multipliers with semiconductor diodes contains more or less noise power consisting in a random amplitude and phase fluctuation. This noise power normally considerably exceeds that due to processing of the input noise power. The thermal noise of the loss resistances and the shot noise of the diode current are also usually considerably less than the noise power measured at the output.

Experience further shows that the output noise power depends strongly on the tuning condition of the multiplier circuit. Even small variations in the tuning condition which hardly change the efficiency, may greatly affect the output noise power. This is due to the possible instability of tuned circuits containing a non-linear capacitance. Such instability makes itself felt by relaxation oscillations described in a number of papers.[6] By suitable tuning such relaxation oscillations can be positively suppressed, however. The

† The ideas outlined here briefly are discussed in more detail in Reference 7.

relaxation oscillations, like any other oscillations, are excited by smallest amounts of noise power that are present, e.g. by thermal noise power. Below the excitation threshold of the relaxation oscillations, however, the existing noise power is already more or less amplified by kind of positive feedback. This mechanism explains the actually measured high noise levels as will be outlined in the following paragraphs.

Figure 4(a) shows the equivalent circuit of the fundamental-frequency circuit of a frequency multiplier as a simple resonant circuit containing the fundamental-frequency generator of the amplitude E, the effective resistance R (including generator source
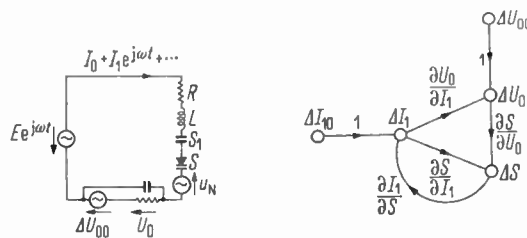
(a) Equivalent circuit. (b) Noise signal flow graph.

Fig. 4. Fundamental-frequency resonant circuit of a multiplier.

resistance and load resistance), the circuit inductance L, the circuit elastance S_1 (short-circuited for the d.c. diode current I_0), the mean diode elastance S, and an R-C network for generating the automatic bias U_0. The current consists of the rectified diode current I_0, the fundamental-frequency current of the complex amplitude I_1 and harmonic currents. The high frequency circuit also includes a noise voltage source u_N containing all thermal noise sources, the shot noise and the breakdown noise of the diode current. The low-frequency components of the mentioned noise sources are represented by a noise voltage source ΔI_{00} connected in series to the d.c. resistor R.

The mean diode elastance S depends on the generated bias U_0, and the current amplitude I_1. On the other hand, the current amplitude I_1 depends on the diode elastance S, since the latter affects the tuning condition of the circuit.

Assuming constant circuit components a noise current ΔI_{10} flows in the high frequency circuit which results from the noise voltage u_N and the driving point impedance of the circuit. Because of non-linearity of the diode elastance S a noise current ΔI_1 results, however, which can be calculated with the aid of the noise-signal flow graph of the fundamental-frequency circuit.

This noise-signal flow graph (Fig. 4(b)) shows the following relations: The noise current ΔI_1 gives rise to a bias variation ΔU_0, since the rectified current I_0 varies with the fundamental-frequency current amplitude I_1. The bias variation ΔU_0 in turn gives rise to a variation ΔS in the diode elastance. At the same time, however, the current variation ΔI_1 also furnishes a direct contribution to the elastance variation ΔS, since, even with constant bias, the mean diode elastance S depends on the current amplitude I_1. The elastance variation ΔS now causes in turn detuning of the circuit which in turn changes the current amplitude I_1. The resultant current variation ΔI_1, i.e. the resultant noise current, is further proportional to the original noise current ΔI_{10}. The resultant bias variation ΔU_0 is proportional to the original variation ΔU_{00}.

Since the noise components ΔI_1, ΔU_0, and ΔS are sufficiently small, the mutual relationships are governed by the corresponding first partial derivatives alone which are entered in Fig. 4(b). For the resultant noise current ΔI_1 the noise-signal flow graph yields the simple relation

$$\Delta I_1 = \frac{1}{1 - \beta\mu}(\Delta I_{10} + y\Delta U_{00})$$

where, much as in the theory of feedback amplifiers,

$$\mu = \frac{\partial S}{\partial U_0} \cdot \frac{\partial U_0}{\partial I_1} + \frac{\partial S}{\partial I_1}$$

is the 'amplification factor', and

$$\beta = \frac{\partial I_1}{\partial S}$$

the 'feedback factor'.

$$y = \frac{\partial I_1}{\partial S} \cdot \frac{\partial S}{\partial U_0}$$

represents a transfer admittance. Obviously the resultant noise current ΔI_1 can assume any desired value, depending on the denominator $1 - \beta\mu$. As soon as the latter vanishes or becomes less than zero, the circuit configuration is no longer stable and relaxation oscillations build up. When the denominator is less than unity and positive, kind of positive feedback exists so that the resultant noise current ΔI_1 always exceeds the exciting noise current ΔI_{10}. When the denominator exceeds unity, the feedback is negative so that the original noise current ΔI_{10} is more or less compensated for. Normally the quantities μ and β may also be complex. Suitable tuning of the resonant circuit can strongly affect the quantities μ, β and y. Consideration must be given to the fact that the noise current ΔI_{10} and $y\Delta U_{00}$ are partially or not correlated.

The actual processes in a multiplier are far more complex. The described variation ΔS of the mean diode elastance S also causes detuning of all harmonic circuits so that all harmonic currents likewise undergo a variation. On the other hand, the harmonic currents also affect the rectified current I_0 of the diode and thus the bias U_0. Besides, a variation of any harmonic current also causes a change of the fundamental-frequency current since the load resistance R of the fundamental-frequency circuit and the mean diode elastance in this circuit are also made to vary. It must further be considered that the thermal noise sources of the loss resistances and the shot noise of the diode current include spectral components at all harmonics of the input frequency so that even all harmonic current circuits contain a corresponding noise-voltage source.

As an example, Fig. 5(a) shows the equivalent circuit of a frequency tripler containing the fundamental-frequency circuit, the idler circuit for the frequency $2f$, the output circuit for the current of frequency $3f$ as well as circuits for the further harmonics shown by dots in Fig. 5(a). In the fundamental-frequency circuit the diode acts as a passive impedance; in the harmonic circuits, however, it acts as a generator.

The noise-signal flow graph of the frequency tripler is shown in Fig. 5(b), with consideration, however, only of the noise currents of the three first harmonics. The partial flow graph shown in heavy lines in Fig. 5(b) corresponds to the noise-signal flow graph of the fundamental-frequency circuit Fig. 4(b). Similar partial flow graphs hold for the circuits of the frequencies $2f$ and $3f$. These partial flow graphs are coupled by the resultant variations ΔU_0 and ΔS of the bias and diode elastance respectively. Direct coupling exists additionally in either direction between the noise currents of each of the three frequencies considered. The proportionality factors describing the interdependence of two variations are not explicitly shown in Fig. 5(b). They must be theoretically or experimentally determined. The resultant noise current ΔI_3 in the output circuit can then be calculated from the flow graph. It is obvious that the resultant noise current in the output circuit depends on a very large number of parameters.

Relations become even more complex when a number of cascaded frequency multiplier stages is considered. In this case the load impedance of an individual stage and the source impedance of the following stage are likewise non-linear. This gives rise to further reaction on the respective multiplier stage so that an accurate alignment of the circuit for minimum noise becomes more and more cumbersome. To avoid the reaction between cascaded multiplier stages, it proved advisable to use an isolator for decoupling two consecutive multiplier stages.
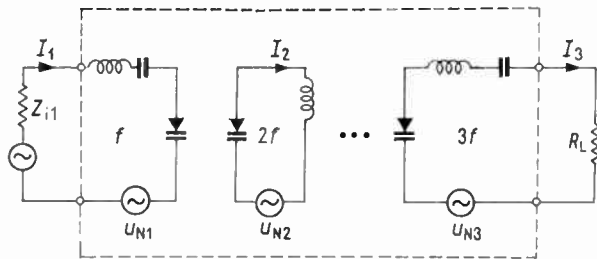
(a) Equivalent circuit.
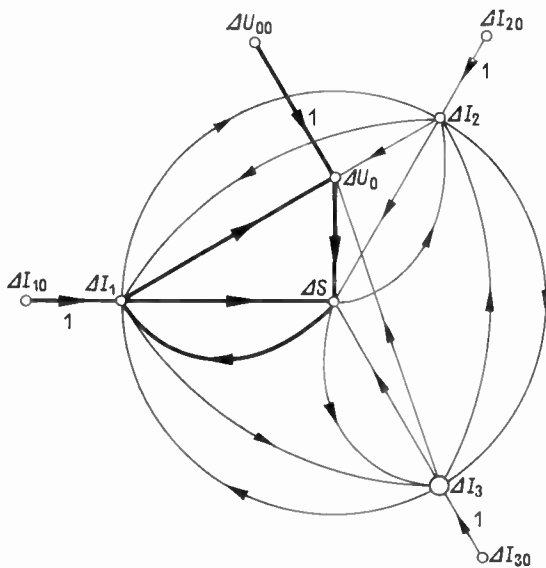
(b) Noise signal flow graph.

Fig. 5. Frequency tripler.

Figure 6 shows as an example the noise-signal flow graph of a multiplier cascade consisting of three tripler stages with interconnected isolators. Here, the noise-signal flow graphs of the individual tripler stages are already reduced to such an extent that they contain only two nodal points corresponding to the noise currents in the input and the output circuit.
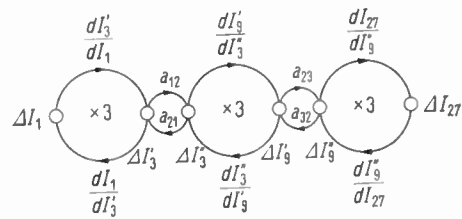

Fig. 6. Noise signal flow graph of a multiplier chain consisting of three triplers cascaded via isolators ($a_{12} = a_{23} \simeq 1$; $a_{21} = a_{32} \simeq 0$).

In practice the circuits of the multipliers are so tuned that the output noise power becomes a minimum with maximum efficiency. Optimum tuning for minimum noise is attained when as many feedback paths as possible in the noise-signal flow graph disappear or become minimum. This condition is more quickly reached according to the extent of the damping of the individual circuits and the wider the bandwidth of the filters used. Whether and how far the conditions for maximum efficiency and minimum noise are compatible is still a subject of further investigation.

With broad-band circuits minor variations in the component values, e.g. due to temperature changes, are least effective. Broad-band multiplier cascades offer in addition the practical advantage that no retuning or exchanging is needed with a frequency change.

3. Realization of Broad-band Triplers

The bandwidth of frequency multipliers can be considerably increased, if the input and the output filters consist of a number of tuned circuits. As an example, Fig. 7 shows the equivalent circuit of a broad-band tripler stage. The input and output filters consist each of double-tuned band-pass filters with capacitive coupling. The fundamental-frequency generator and the load impedance are inductively coupled to the filters. The band-pass filters are tuned by means of the circuit and coupling capacitances. A sufficiently high d.c. resistance is connected across the diode to produce the automatic bias. This resistance does not, in practice, consume any useful power. Also connected across the diode is a series-resonant circuit tuned to the frequency $2f$. This idler circuit is a simple single-tuned circuit. It does not restrict
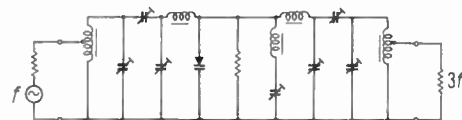

Fig. 7. Equivalent circuit of a broad-band tripler stage.

the bandwidth of the multiplier to any greater extent since the load impedance as well as the source impedance of the fundamental-frequency generator are transformed into the idler circuit as a damping load; the circuit-Q is thus sufficiently reduced. The circuit components are so proportioned that the diode sees favourable reactances also at the frequencies $4f$ and $5f$.

It has turned out advisable to realize the equivalent circuit of Fig. 7 with lumped components even at microwave frequencies. This offers the following advantages: The input filter stops positively even the fifth harmonic, the idler circuit has a non-ambiguous resonant frequency within the frequency range of interest and the output filter also stops sufficiently well all harmonics, except the wanted one. Because of their multiple resonances line-type resonators are not suitable for broad-band multiplier stages.

Fig. 9. Plot of the circuit impedance presented to the diode by the tripler 230 Mc/s/690 Mc/s.

impedances below the input frequency are also important for a perfect performance of the tripler. These impedances must not resonate in conjunction with the diode or else parametric oscillations might be excited.

Figure 10 shows the conversion loss of this tripler as a function of the output frequency and the input power in the form of contour lines. The minimum conversion loss is 1 dB. The relative bandwidth within which the conversion loss varies by less than
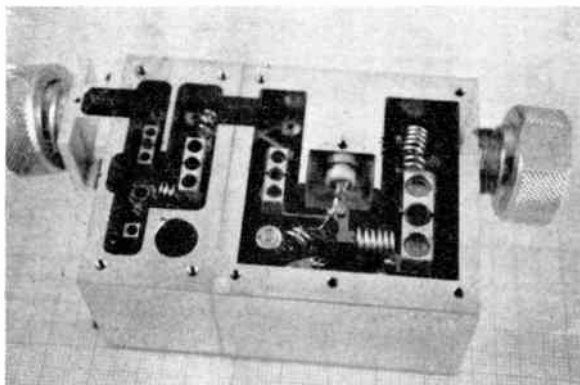

Fig. 8. Photograph of a broad-band multiplier chain for 230 Mc/s input frequency and 2070 Mc/s output frequency, consisting of two tripler stages coupled directly.

Figure 8 shows a tandem connection of two triplers designed according to Fig. 7 for a mean input frequency of 230 Mc/s. All components are obviously of the lumped type. The tuning capacitors are of the cylinder type, with their stators soldered to a metal-coated insulating board. Part of the inductors are self-supported wire-wound air-core coils, part are printed-conductor paths.

The circuit of the tripler for 230 Mc/s to 690 Mc/s offers to the diode an impedance whose plot between $0.5f$ and $5f$ is shown in Fig. 9 (f being the fundamental frequency). This impedance plot was measured with a measuring adapter which can be inserted into the circuit instead of the diode. The plot shows in heavy lines the frequency ranges corresponding to the operating frequencies. The impedances of the circuit vary slightly but obviously within the useful frequency range at the fundamental and its harmonics. The
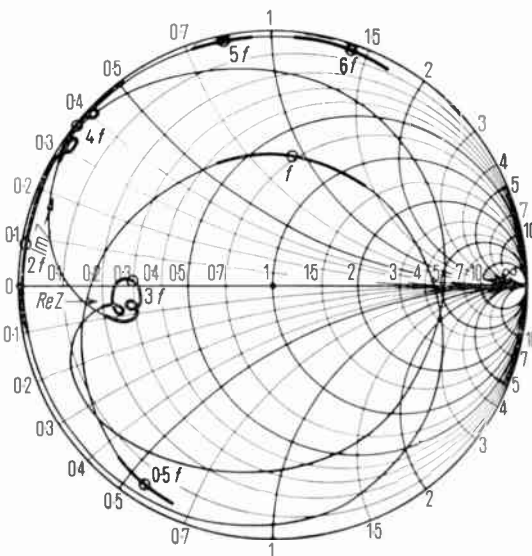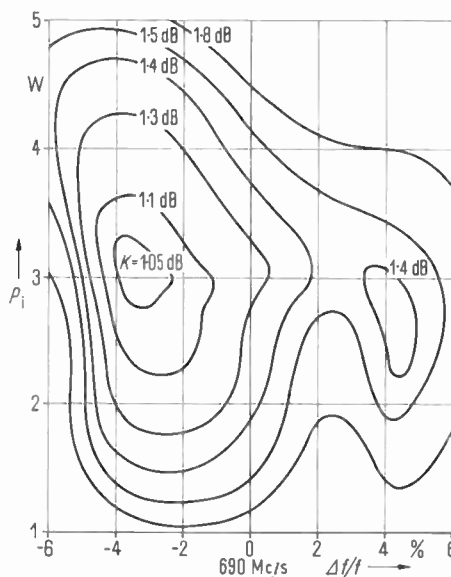

Fig. 10. Conversion loss K of the tripler 230 Mc/s/690 Mc/s. P_i input power; f_o output frequency.

0·5 dB is ± 5%. The optimum input power is 3 W. The input power may vary by ± 10% without causing more than 0·5 dB of conversion loss variation within the frequency range stated.

The measured output phase noise of the multiplier chain shown in Fig. 8 is plotted in Fig. 11. The measurements were made in a 2 kc/s bandwidth centred at a frequency f_m away from the carrier. The peak noise phase deviation $\Delta\varphi$ measured at three different output frequencies f_0 is less than $3·5 \times 10^{-5}$ in the frequency range $f_m = 50$ kc/s . . . 10 Mc/s.
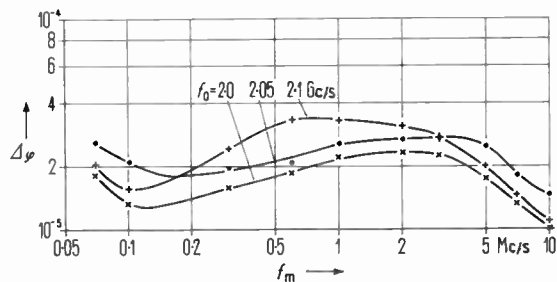

Fig. 11. Noise phase deviation $\Delta\varphi$ (peak value) of the output frequency f_0 of the multiplier chain shown in Fig. 8 in a 2 kc/s bandwidth at a frequency f_m from the carrier.

4. Acknowledgment

5. References

1. C. H. Page, 'Frequency conversion with positive non-linear resistors', *J. Res. Nat. Bur. Stand.* **56**, pp. 179–82, 1956.

2. P. Penfield, jr., and R. P. Rafuse, 'Varactor Applications', (M.I.T. Press, Cambridge, Mass., 1962).

3. D. Leenov and A. Uhlir, 'Generation of harmonics and subharmonics at microwave frequencies with p-n-junction diodes', *Proc. Inst. Radio Engrs*, 47, pp. 1724–29, 1959.

4. S. M. Krakauer, 'Harmonic generation, rectification and lifetime evaluation with the step recovery diode', *Proc. Inst. Radio Engrs*, **50**, pp. 1665–76, 1962.

5. A. Kürzl and W. Heinlein, 'Optimale Frequenzverdopplung mit Kapazitätsdioden', *Frequenz*, **17**, supplement edition, pp. 544–53, 1963.

6. A. A. Rabinovich and M. E. Gertsenshteyn, 'Relaxation oscillation in non-linear capacitance frequency multipliers', *Radio Engng Electronic Phys.* (U.S.A.), **8**, pp. 754–6, 1963 (from Russian).

7. W. Heinlein and J. Steinkamp, 'Rauschquellen und Rauschvorgänge in Frequenzvervielfachern mit Kapazitätsdioden', *Frequenz*, **20**, May, 1966.

A Real Time Seismic Array Data Analyser and its Associated Event Selector

By

W. H. HUTCHINS, C.Eng.

(Associate Member)†

Presented at a Symposium on 'Modern Techniques for Recording and Processing Seismic Signals' held in London on 13th May 1964.

Summary: A specialized data processing machine is being developed, which will be capable of using data from an array of seismometers to derive information on the direction of arrival, phase velocity and energy-time distribution of body waves from distant seismic events. The organization and method of operation of the machine are described and reasons for the choice of system are discussed. A simplified correlator which automatically selects events from the background noise has been in operation for some time. A description of this unit and some results obtained with it are presented.

1. Introduction

The main purpose of this paper is to describe a special purpose analyser which has been designed for processing seismic array data. The design and use of linear cross arrays, and the design of the associated recording systems have been described in complementary papers,[1, 2] whilst J. R. Truscott[3] has described general approaches to array processing. However, a brief outline of the scientific problems is given first in order to explain the requirements for the analyser, since these will be unfamiliar to the majority of readers.

The detection and identification of small underground nuclear explosions and earthquakes is difficult for three main reasons. Firstly, the amplitudes of the seismic signals are small at normal recording distances, and may be less than the level of the background seismic noise. Secondly, the signals are often complicated by the transmission path, and may contain many overlapping components. Thirdly, even when isolated signal components of adequate signal to noise ratio are received, there remains the problem of applying criteria to determine whether they were produced by an earthquake or by an explosion.

The signal to background seismic noise ratio can be improved by frequency filtering, and also by summing the signals recorded by an array of seismometers extending over an area at least several kilometres in diameter. If the dimensions of the array are comparable to the longest apparent wavelength of interest, and the array outputs are summed with appropriate phasing delays, then signals of a given apparent surface velocity and azimuth can be enhanced relative to other signals.[1] The azimuth and velocity of an unknown signal may be determined by applying a range of phasing conditions, and noting the values

which give maximum summed output. An improved estimate of azimuth and velocity can be obtained by use of correlation methods which are described below. These techniques are particularly valuable for signals recorded at distances of less than 2000 km, where many overlapping signal components of differing apparent velocity are received from the same event. The effect of the transmission path on signals recorded at distances of 3000–10 000 km is much less, and the primary (P) wave signal component is often separate in time from other components. The degree of complexity of the P wavetrain, propagated through the mantle to these distances, has received detailed investigation by U.K.A.E.A. workers in the search for criteria distinguishing between earthquakes and explosions.[4] Undesirable additional complexity may be caused by reflections and mode transformations of the P wave signal at rock boundaries within the earth's crust near the recording station. This complexity can be reduced by summation and correlation methods.

The summed signal for an array of n seismometers may be represented by

$$S_{\theta, V, t_1} = \sum_1^n a_i s_i(t_1 - \tau_{i(\theta, V)}) \qquad ......(1)$$

where a_i is the electronic gain of the channel corresponding to the ith seismometer within the selected frequency pass-band

     $s_i(t_1)$ is the output of the ith seismometer at time t_1

     $\tau_{i(\theta, V)}$ is the phasing delay inserted for azimuth θ and velocity V. For each summed output, θ and V is constant, and t_1 variable.

The correlation procedure preferred by U.K.A.E.A. workers is to sum the signals into two groups after applying phasing delays, multiply the two summed signals together and then integrate, allowing an exponential decay. This is done for each of a number

† United Kingdom Atomic Energy Authority, Atomic Weapons Research Establishment, Aldermaston, Berks.
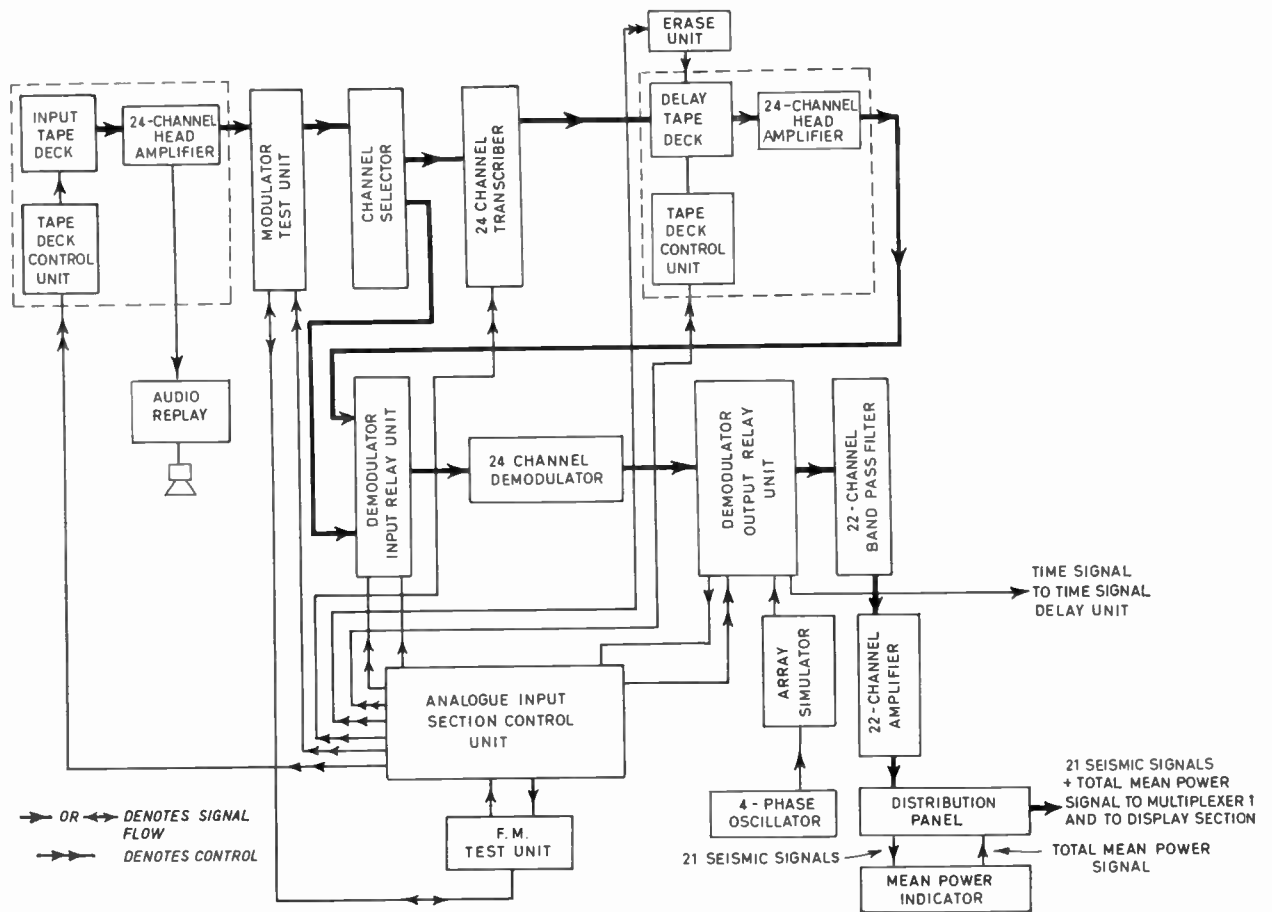
Fig. 2. Block diagram of the analogue input section.

from particular array elements to be routed to pre-determined machine channels. Outputs from the channel selector are taken either directly to the demodulators or through a tape loop deck which can insert any selected delay between limits 3 and 35 minutes. The loop recorder is mainly intended for use when input is from a continuously recorded tape or when the machine is working on-line. Normally the direct signals are presented to the demodulators and a general search programme used for the signal phasing. When an event is detected, the approximate azimuth can be determined from the correlator histogram output. The delayed input signals can then be selected, and the signal phasing program changed to one capable of deriving more information from the detected event. The delay enables a new program to be applied before the resumed onset of the signal of interest. The section of record on the loop can also be isolated and used for repetitive processing.

Normally, signals from the demodulators are taken to a 22-channel filter with the exception of the coded time signal which is supplied directly to the time signal delay unit (Sect. 4.5). The filters use active RC networks with feedback provided by transistor current amplifiers. A choice of five lower limit cut-off frequencies is available in the range $\frac{1}{8}$ to 2 c/s, and four upper limit, cut-off frequencies between 1 and 6 c/s. The outputs are coupled, with time constants of 12·5 seconds, into a 22-channel equalization amplifier. These couplings remove any d.c. components, to which the correlation process is very sensitive, due to drift in the input section of the analyser or in the modulators at the recording station. Low-drift operational amplifiers are used in the 22-channel amplifier. Gain is continuously variable from 0·5 to 5·0 or, alternatively, from 5·0 to 50.

3.2. Control and Test Facilities

The analogue master control unit selects, by means of the various relay units, 'normal', 'delayed' or 'array simulator' states. It can also select various test conditions which provide static and dynamic testing of the f.m. system, including measurement of dynamic range. The extensive use of relays results in short direct cables, reduces mains pick-up and interference,

leads to a very simple control unit and simplifies the f.m. testing procedure. Control of all conditions is available locally and control of the 'normal', 'delayed' and 'array simulator' states can be transferred to the control and display console.

An array simulator provided as a test facility may be connected to the 22-channel filter in place of the input channels. It consists of a resistance network fed by a 4-phase oscillator. Twenty-two outputs are available with phase angles which can be chosen between 0 deg and 355 deg, in 5 deg increments. Output amplitudes are all equal, being independent of phase. With this unit, detailed operational tests can be made on the later stages of the machine. An arrival, of chosen frequency and azimuth, can be represented for many array configurations and ratios of array size to apparent signal wavelength.

3.3. *The Mean Power Indicator*

The unit serves two purposes, namely, to aid equalization of signal or noise amplitudes, and to provide a continuous signal representing the total mean power arriving at the array.

A number of criteria may be used for equilization. When using the array to separate signal components by the process of velocity-azimuth filtering, the amplitudes of the complex signals in the individual channels should first be equalized. These amplitudes may differ due to variations in seismic coupling and differences in gain in the recording system. The former are likely to be azimuth dependent, and may also depend upon the distance of the event (and hence upon the arrival angle of the seismic wavefront to the vertical). The mean square value of the signal amplitude over the period of time of interest should be equalized, and any desired weighting of individual channels, to obtain an improved array response, applied subsequently. This procedure is difficult at low signal/noise ratios, and always requires at least two passes of the data.

The second main criterion is to obtain the maximum signal/noise ratio in the summed output for the signal onset. When the noise is random between seismometers, the maximum signal/noise ratio in the summed output is obtained when the channels are weighted in proportion to σ_s/σ_n^2, where σ_s and σ_n are the r.m.s. signal and noise voltages respectively in a given channel.[5] This is rather laborious for routine analysis, and may not be possible when the signal/noise ratio is low. Furthermore, it can only be achieved by replaying the event at least twice. A compromise can be achieved by equalizing the mean square value of the noise prior to the signal arrival in each channel, assuming the noise to be stationary. This method prevents any particularly noisy channel from degrading the output, and is the one proposed for normal operation of

S.A.D.A., since it can be applied on-line. The method of equalizing signal amplitudes will be used when carrying out velocity-azimuth filtering on specific events of interest.

The mean power indicator enables either of these methods to be applied. There are two modes of operation. In the first mode of operation, the voltage waveform in each channel is squared and then integrated within fixed time limits separated by 30, 15, 7·5 or 3·7 seconds. A meter reads the sum of the mean signal and noise powers in each channel within the fixed time bracket chosen. When equalizing the noise powers of the individual channels, a section of record is used on which no signals or spurious pulses can be observed. The time bracket will normally be set to the maximum, i.e. 30 seconds. For equalizing the amplitudes of the channels during a signal of interest, the signal must first be replayed to determine its onset time, and the duration over which equalization is required. The time bracket will then be switched to correspond to this duration, and the signal replayed again, observing the coded time signal on the display. Integration will be initiated manually immediately prior to the event.

In the second mode of operation, the voltage waveform in each channel is squared and integrated continuously with an exponential decay. The time constant of this is set to 30, 15, 7·5 or 3·7 seconds by the same control as that used for selecting the time bracket in the other mode. At any given time, each integrator output is proportional to the time-weighted mean power of the preceding signal and noise in the associated channel. An operational amplifier is used to sum the outputs of the integrators and thus produce a total mean power output which is available for display as a function of time. The feed-back resistor of the summing amplifier can be replaced by a square-law diode function generator. The signal provided for display is then the square root of the total mean power. The summing resistors are changed automatically when the time constant is selected, in such a way that the amplitude of the total mean power signal is independent of the time constant, being dependent only upon the signal and noise content within the exponential window.

3.4. *Dynamic Range*

The dynamic range of the input tape system is dependent upon bandwidth and band centre frequency. A common condition of use will be with a band of 1 c/s and 2 c/s and this yields an average dynamic range of 64 dB with a spread of ±3 dB in the individual channels. Thus, for the band 1 to 2 c/s, the mean error due to noise will be about 1/2000 of full-scale p-p signal and approximately equal to the quantization error of the 10-bit word analogue to digital converter
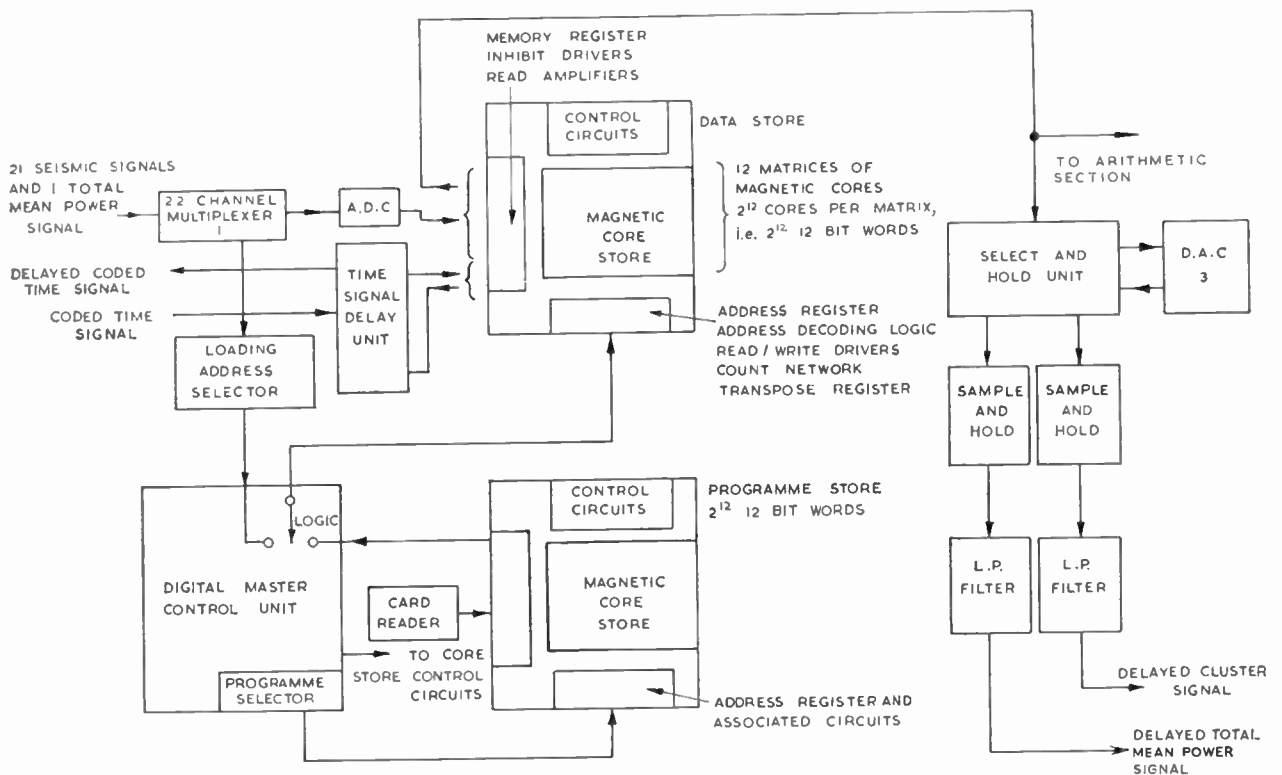
Fig. 5. Schematic diagram of the phasing section.

It can be seen that the oldest sample of each channel has been moved into the block of the next lower numbered channel. The store is now ready for the loading phase of the next sequence, in which the migrant data will be replaced by the newest samples, thus returning the pattern to that of Fig. 4(a).

Durations of the load, read-out and regression phases are 2·114, 2·654 and 32·768 ms respectively; a total of 37·536 ms. Thus, approximately 12 ms of each 50 ms sampling period is waiting time which could be used to allow slower arithmetic. However, if the regression time could be halved, then a twice real time rate machine would be possible with minimum modification. This would involve the use of a data store with half the number of addresses and double the word length. Two samples would be stored at each address, and the one required would be selected by output gates. The program store would not be affected by such a modification.

4.3.2. The program store

A schematic diagram of the phasing section is given in Fig. 5. It will be seen from this figure that the address register of the data store obtains its input from the loading address selector, during the loading phase, or from the program store during the read-out phase. The two stores are identical. Program words represent addresses in the data store, so that 12 bits are needed to define any one of the 2^{12} addresses. One program consists of 441 words, and nine such programs can be stored. Any of these can be selected instantaneously. If a program is required which is not in the store, it can be loaded by feeding the appropriate stack of seven cards, from a library of programs, into the card reader. The new program would then replace one of those already stored. The program which is to be discarded can be selected at will. Any number of the stored programs can be replaced in this way.

4.4. The Digital Master Control Unit

The digital master control unit produces the control levels and pulses which conduct the two core store systems through the complex sequences of operation which have been previously described. Also the unit synchronizes the operation of the a.d.c. and the associated multiplexer, the digital to analogue converters (d.a.c.'s) and demultiplexers, the digital part of the arithmetic section of the machine and other units. In addition, it provides the logical circuits to switch the input connections to the address register of the data store, as described in Section 4.3.2. It provides the control facilities required for program selection and to enable the program store to receive data from the card reader. Finally it enables the whole

phasing section of the machine to be subjected to a variety of functional tests.

Two separate timing systems are used. A 440 c/s oscillator drives a timing chain which controls the remultiplexing and time base triggering associated with the production of a histogram display. The high frequency timing waveforms, required to control the core store systems and the digital arithmetic, are derived from a pulse loop oscillator. No low-frequency control waveforms are derived from the pulse loop. It operates with a single resettable cycle-counting and event-timing network which is used for all three phases of the core store sequence. Each sequence of operation of the loop system is initiated by a pulse from the low-frequency timing chain. Hence the method is economic and simple relative to the control functions which are required.

Diode logic is used, with inverters or current amplifiers where necessary. This leads to low cost, and it is technically desirable because the ability to use multi-input gates results in simplification.

Control of the unit can be either local or from the control and display console. The time signal delay circuits are housed in the digital master control unit and are discussed in the next section.

4.5. *The Time Signal Delay Unit*

Because the time signal has only two amplitudes, one of which is zero, it is not applied to the data store via the a.d.c., but is gated directly into the memory register by the 'MR transfer' pulse. A sample of the time signal is entered into the store with each multiplexer channel sample. Thus each of the 22 blocks of data has corresponding samples of the coded time waveform. Read-out is always from the samples in channel 11 block, because this is near the centre of the 2·016 ms time-bracket in which the samples are gated into the memory register. The simplest system would be to use a single matrix of the store and to reconstitute the delayed waveform by the method shown in Fig. 6(a).

However, the shortest pulses of the time code have a duration of only 100 ms and this is subject to a tolerance of several microseconds. Samples of the waveform are taken in less than 1 μs; there is no synchronization between the recorded time scale and the sampling period. Thus the 50 ms sampling period can result in an uncertainty of 50 ms in the time of both front and back edges of the reformed code pulses, and of ± 50 ms in their duration. This unacceptable situation is illustrated in Fig. 6(b). The use of two matrices instead of one makes possible a technique which effectively doubles the sampling rate. This halves the magnitude of the uncertainties introduced into the time signal by its passage through the data

store. Figure 6(c) is a simplified block diagram which illustrates this technique. The logic ensures that the setting of the bistable circuit is caused by whichever of the delayed signals first indicates the presence of a time code mark. Similarly, the resetting of the bistable circuit is caused by the first signal to respond to the termination of the time mark. It will be seen that, in addition to the delay obtained from the core store, there is now an additional delay of 50 ms. A method of compensating for this would be to read the time waveform samples out of an address one count greater than the centre address, i.e. 50 ms early. However, all outputs from the machine which have been in digital form will experience a delay of 133 ms in the low-pass interpolation filters referred to in Section 5.2.1. Compensation for 100 ms of this time is effected by taking time-signal samples from one count less than the centre address, i.e. 50 ms late. The residual time difference, together with delays in the band-pass filters of the analogue input section, are compensated before the time signal is applied to the data store. After being reformed, the coded time signal is available for display.

4.6. *Select and Hold Unit*

The select and hold unit accepts the output of the memory register of the data store at the correct times, given in Section 4.3.1, to enable it to store samples of the total mean power signal in a separate register.
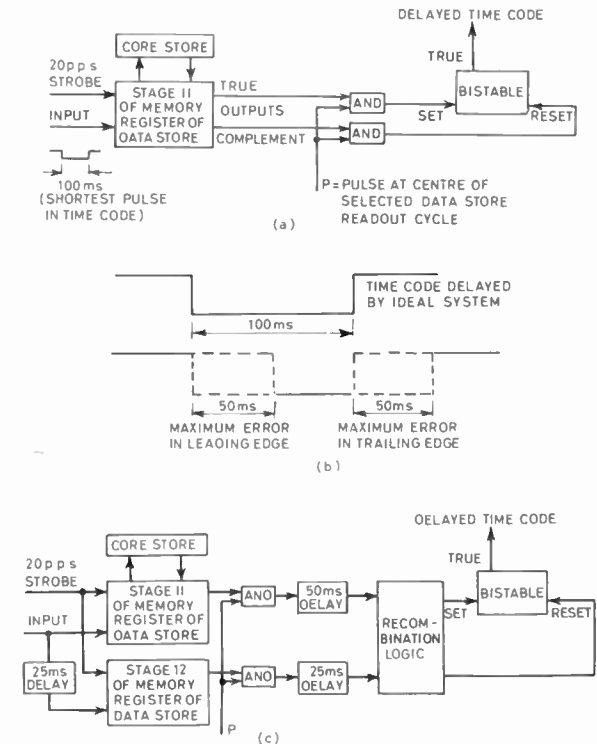

Fig. 6. Delay of the coded time signal.

register is the multiplier for the next multiplication. Total sum and partial sum 2 accumulators, and the partial sum 1 register are now reset. It is the clearing of the latter which enters its contents into the multiplicand register.

It will be seen from Fig. 7 that only 11+1 of the 13+1 bits, available for use as multiplier, are passed through the range gates; this also applies to the multiplicand. Hence, there are three possible partial sum ranges, and these can all be selected. They represent 160%, 80% and 40% of the maximum possible partial sum, and are selected simultaneously with the 80%, 40% and 20% total sum ranges.

The multiplication is carried out by a succession of additions; either the multiplicand, or a word consisting of all '0's is added into the product accumulator via the control gates. After each addition, the contents of this accumulator, and of the lower product register, are shifted one stage towards the least significant end. The control gates are operated by the digit stored in the least significant register stage. This digit is initially the least significant bit of the multiplier; after 11 shifts it has become the corresponding sign bit. For the 12th addition the function of the control gates is altered. If the sign digit is a '0', then there is no effect; it it is a '1', i.e. the multiplier is a negative number, then the two's complement of the multiplicand is added into the product accumulator. At the end of the multiplication, the sign bit and the 10 next most significant bits of the product are contained in the product accumulator. The 11 least significant bits are in the lower product register. The most significant 9+1 bits from the product could be taken to DAC2 and converted to analogue samples. Apart from the sign digit, which would be taken from the most significant stage, the input to DAC2 would be taken from the fourth most significant stage downwards. Full scale output from the converter would then represent 128%, 32% and 8% of the maximum possible product, for the three range gate settings available. To provide a wider range of sensitivity, the digit inputs to DAC2, with the exception of the sign digit, are taken from the least significant two stages of the product accumulator, and the most significant seven stages of the lower product register. The digits can be shifted between zero and nine times, each shift decreasing the sensitivity by a factor of 2. The product ranges given above are obtained when eight shifts are provided. Four binary orders of sensitivity are excluded, but these have no value, those provided being in practice more than sufficient.

5.1.4. Digital to analogue conversion

The sum and product outputs from the digital arithmetic each consist of 9+1 parallel bits in two's complement form. Inversion of the most significant, i.e. sign, bit relative to the others, effectively changes all output samples to pure binary numbers. All digital words now represent positive numbers, but are relative to a datum of maximum negative amplitude. They are converted to analogue form using unipolar 10-bit parallel digital to analogue converters DAC1 and DAC2. A similar arrangement is used in the conversion of the total mean power signal by DAC3 (Fig. 5). The converters use positive-true logic, and the outputs are 0 V to +10 V full scale. Analogue samples are produced each 126 μs during a read-out phase, and are maintained at the converter output for most of this period. These analogue output samples are in time division multiplex. Outputs from DAC1 and DAC2 are each demultiplexed to provide 20 series of pulses representing the various phased sums and products. The demultiplexers use the same techniques as the multiplexer described in Section 4.2; they are effectively multiplexers with the summing amplifier and shunt gates removed.

5.2. The Analogue Arithmetic

5.2.1. 'Sample and hold' circuits and low-pass filters

Figure 7 shows that the samples of sums and products are passed into 'sample and hold' circuits and thence to low-pass filters. In all, 40 such channels are needed. The input pulses to each 'sample and hold' circuit have a duration of about 120 μs and occur at intervals of 50 ms. Charge-storage circuits stretch the duration of the pulses by a factor of about 400. The storage capacitors are discharged to below the zero voltage datum, at the start of each input sample, by pulse discharge circuits. These are triggered by outputs from the appropriate shift register stages of the associated demultiplexers. The pulse-stretched waveforms are then applied to low-pass filters. These have two stages, each of which uses a simple operational amplifier in a frequency-dependent network. The fixed frequency response of each two-stage filter is flat to 3 c/s, 3 dB down at 6 c/s, and more than 20 dB at 10 c/s, i.e. half the sampling frequency. The phase response is almost linear in the pass band and the delay is 108 ms. Insertion loss is zero, and drift is less than 45 μV/deg C. The aperture effect of the 'sample and hold' circuits reduces the overall cut-off frequency from 6 c/s to 5·6 c/s, and causes the response to fall measureably from about 1 c/s. The attendant extra delay is 25 ms, making a total of 133 ms. Regulated current is fed into the summing junction of the second filter stage, such that the output is −5 V when the input of the preceding 'sample and hold' circuit is at earth potential. A bipolar output results, with full scale ±5 V. Continuous sum and unsmoothed product waveforms are fed from the filters to the console. The unsmoothed product voltages are also taken to the analogue integrators.

5.2.2. Analogue integrators

Operational amplifiers with appropriate feedback elements are employed. Normally exponential-window operation is used. Four time constants are available, i.e. 1·5, 3·7, 7·5 and 15 seconds. These can be selected by relays which change the input and feedback resistors, the feedback capacitor remaining constant.

For certain applications, such as the study of seismic noise in arrays, the feedback resistors are switched out, to provide integration without decay, over chosen time intervals. This condition requires low offset voltage and therefore chopper stabilized amplifiers are used. Simpler d.c. amplifiers would have been adequate for the exponential-window integration.

5.2.3. Multiple cross-correlation function

The 20 cross-correlation integrals are also supplied to a 22-channel multiplexer, the first and 22nd inputs to which are at earth potential. A histogram is generated each time the multiplexer scans its 22 gates. One scan is made each second, and is completed in 50 ms. Zero level is defined at each side of the histogram by the earthed channels, and each of the other levels represents the cross-correlation integral produced when the signal delays correspond to a different azimuth-velocity combination. Thus the histogram is a multiple cross-correlation-function. When displayed, it provides a means for instant appraisal of the direction and apparent velocity of an arrival. This appraisal will in turn indicate which programme could be substituted to extract further information from the same input signals when replayed from the delay loop.

If required, the output from multiplexer 2 can be square-rooted by the use of an operational amplifier with a feedback circuit consisting of a square law diode function generator. The resulting non-linear display makes use of the full dynamic range of DAC2.

6. Control and Display

The main output of S.A.D.A. is in the form of various continuous time series recorded on light-sensitive paper by a 25-trace ultra-violet recorder. Another output consists of a histogram of the multiple cross-correlation function, which is displayed on a cathode ray tube at intervals of one second. These outputs are presented at a console together with essential controls for all sections of the analyser. The controls are grouped for analogue input, phasing and arithmetic sections.

Each of the 25 galvonometers of the recorder can be driven by any one of 86 signals. These signals include 21 seismic channels, 20 velocity-filtered sums, 20 unsmoothed products, 20 cross-correlation integrals, the delayed or undelayed total mean power, and the delayed or undelayed coded time signal.

7. The On-Line Correlator

7.1. *The Correlator System*

The outline of the process has been given in Section 1. Two continuous waveforms, which represent the directly-summed outputs of two groups of seismometers, are cross-correlated with zero relative time shift to produce a cross-correlation integral. The two partial sums are also added together to form a total sum signal. When the cross-correlation integral exceeds a pre-determined level, an external trigger circuit causes a heat-pen record to be produced. The duration of the record can be pre-set between 30 seconds and five minutes. If a high correlation level is maintained, however, the record continues until the former falls below the trigger threshold. Typically, the record would include the cross-correlation integral, the two partial sums and a binary-coded time signal, the latter requiring approximately 90 seconds' recording time to ensure an unbroken code sequence. The correlator can also be used to edit magnetic tape records.

The method of operation will be described with reference to Fig. 8, which shows the schematic diagram of the correlator, and indicates the external equipment required. Two groups of four undelayed input channels are selected from sockets of the input selection panel and fed to the summing networks via an external switching unit. This gives direct connection until the trigger circuit operates, and then selects delayed versions of the channel waveforms, so that the previous few seconds of signal are repeated. The signals continue with the new time reference for a predetermined period, after which a reverse time shift occurs. Undelayed signals are those which are fed to the f.m. modulators of the main recording systems, and corresponding delayed signals are available at the demodulators. The delay is the travel time of the tape between record and replay heads and is approximately 18 seconds. Alternatively, the two partial sums could be obtained by summing the outputs from a large cluster of seismometers, the two summations being performed externally.

The signals are now passed through a.c. couplings, with 12·5 second time constants, to the summing junctions of variable-gain operational amplifiers A1 and A2. Any d.c. components due to drift in the amplifiers of the recording system or in the f.m. demodulators are thus blocked. The outputs of A1 and A2 are applied to F1 and F2, which are active variable band-pass filters. These have attenuation slopes of 30 dB per octave and insertion losses of 6 dB. Signals and narrowband noise at the outputs of the filters are given fixed amplification in amplifiers A3 and A4. The outputs of these amplifiers drive automatic gain control (a.g.c.) circuits which control the gains of A1 and A2. Only two filters are required

with this configuration due to the preceding summations. The filters remove the wideband noise at a sufficiently early stage to prevent it overloading either the filters themselves or amplifiers A3 and A4. To this end it is necessary to use the a.g.c. amplifiers before the filters so that the mean noise levels at the latter are held constant. The required post-filter gain is proportional to the amplitude ratio of wideband to narrowband noise, the usual band-pass being 1–2 c/s, since this gives best discrimination for teleseismic P waves.

The function of the a.g.c. is to ensure that the detection capability is always the best permitted by the prevailing narrowband noise. The a.g.c. also makes the best use of the limited dynamic ranges of the multiplier and the pen recorder. Gain control is operated by noise peaks which exceed a pre-set absolute threshold. This is a better criterion than the r.m.s. voltage, since it is the correlated noise peaks which are most liable to cause spurious trigger operation. The selected control method gives a rate of noise trips which is less affected by changes in amplitude distribution. To cater for day-to-day variations in mean noise level, a minimum control range of 10 : 1 is required. A wider control range is useful to render the gain settings between seismometers and correlator less critical. In the present unit, changes of 20 : 1 in mean peak input amplitude cause output variations of approximately 20%. The time constant of gain change resulting from a step in the mean input level depends somewhat upon the content of the signal, but is approximately seven minutes and five minutes for decreases and increases in signal respectively. These rates of gain change are more than adequate to deal with the variations in mean noise level which are experienced, and yet sufficiently slow to avoid unacceptable changes in gain in the first minute of the signal, which is of greatest interest.

The two partial sums are added by amplifier A7, which has a gain of 0·5 relative to each input. Thus, for partial sums of equal amplitude and identical waveform, A3, A4 and A7 all reach the upper limits of their linear dynamic range at the same time. Limiting signal amplitudes are approximately five times the mean peak value of the narrow band noise. They result in the multiplier also reaching its upper limit.

The quarter-square method is used for the multiplier. Therefore both phases of the two partial sums are needed and the necessary inversions are provided by A5 and A6. One pair of inputs is reversed relative to the other so that coherent inputs provide positive output polarity.

A differentiator of 10-minute time constant is inserted between the output of the multiplier and the integrator. Thus the d.c. component due to stationary coherent noise is removed, and slow changes in noise characteristics do not affect the threshold sensitivity of the succeeding trigger stage.

The product signal from the differentiator is integrated with a time-constant of six seconds by A9 and its associated network, to give the cross-correlation integral. This time constant is a compromise between the requirements of detecting signals of short and long duration. When there is high coherence between the two signals for a long time, a correspondingly long time constant can be used to advantage, since it results in a signal to noise improvement in the correlator output. However, some signals have a duration of only one or two cycles at a relatively high level, and for these the use of a long time constant is liable to worsen the signal to noise ratio. Another factor governing the choice of a relatively short time constant is that the structure of the correlator waveform is of interest for diagnostic purposes, and much of the signal detail is obscured if too long a time constant is used.

After further amplification, and inversion by A10, the integrator output, which is then positive for coherent partial sums, is applied to the trigger unit. When a trip occurs, the trigger unit resets the integrator to zero volts. The displayed correlation integral of the triggering event will thus be less distorted by stored charge. As three time-constants elapse between trigger operation and the appearance of the start of the event, distortion would only be significant if a high-triggering threshold were used.

7.2. Practical Details

The correlator uses plug-in units, the front panels of which form a patching area. This provides a degree of flexibility which has proved useful in the experimental application. The unit is for 19-inch rack mounting and occupies 12¼ inches of panel height.

Chopper-stabilized operational amplifiers are used. Each of the a.g.c. amplifiers employs a thermistor in a T-network in lieu of the usual feedback resistor. The thermistor has an associated heater which is energized by the output of the corresponding a.g.c. circuit. Signal current in the thermistor is too small, even under maximum gain conditions when the resistance is minimum, to have significant heating effect. Basically the a.g.c. circuit is a diode pump followed by an impedance convertor which drives the heating element. Provision is made to reduce greatly the effect of large positive voltage pulses at the inputs of the a.g.c. circuits. These large voltages can be presented by tape drop-outs when triggered recordings are being made, or by the first few cycles of large amplitude events. Overload protection networks form part of the feedback circuits of A1, A2, A3, A4 and
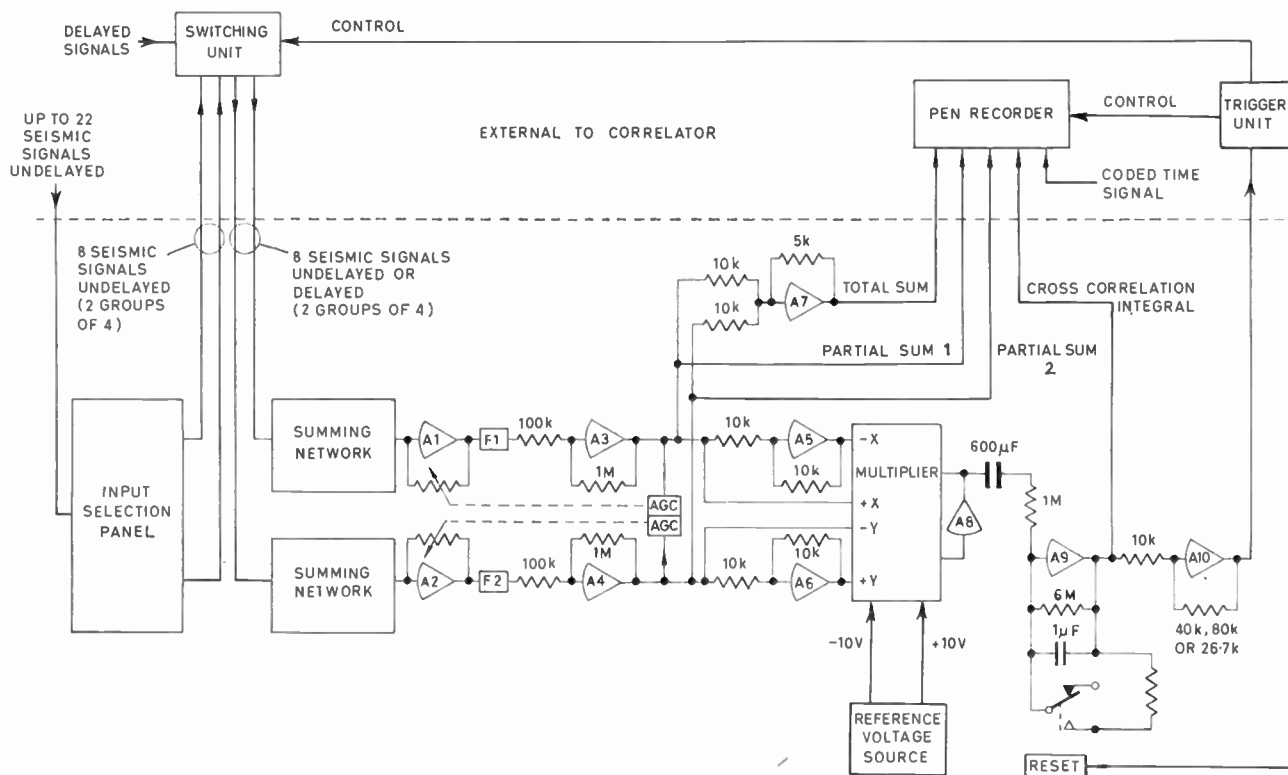
Fig. 8. Schematic diagram of the seismic correlator.

A10 and are ineffective until the outputs of these amplifiers reach either the positive or negative nominal limits. Then the overload circuits operate so that the gains of the amplifiers to those portions of signals in excess of full scale are reduced drastically, thus preventing saturation and blocking.

7.3. Results Obtained with the Correlator

At one site, a correlator has operated 24 hours per day for over two years, and the associated triggered pen recorder has provided regular edited records of high quality. Each partial sum has been derived from four selected elements of a cross-array. A limited amount of time-consuming comparison has shown that the triggering efficiency under these conditions is comparable to the 'picking' ability of a skilled man. The latter used a low-speed trace which presented the continuously-recorded sum of the same eight seismometer outputs restricted to the same frequency band as in the correlator. This method cannot give records of comparable quality without incurring the use of an excessive amount of recording paper; furthermore, the detection of low-level events by visual means is tedious and time-consuming. This study showed that the correlator rejected many unwanted signals from local events (distances less than 100 km), due to their small wavelengths. The triggered display allows

relatively high recording speeds to be used, resulting in improved record quality and timing accuracy. Better determination of optimum trigger level setting, and development of special clusters of seismometers for use with the correlator, can be expected to improve performance. False triggering is unavoidable since the correlator is required to operate at low signal to noise ratios, and the proportion of noise to 'event' trips must increase as sensitivity is increased. However, development of the correlators, and associated clusters, is aimed at reducing this ratio to a minimum.

Figure 9 shows a four-trace record which was produced when the correlator was triggered by the P wave from a distant deep focus earthquake. The two upper traces are the two partial sums, and the third trace is the cross-correlation integral. This has a simple form, typical of explosions and deep focus earthquakes at similar distances. It has not been complicated by the transmission path because the distance (approximately 7700 km) lies within the limits discussed in the introduction. The bottom trace shows the binary coded time signal from which the onset time of the P wave at the recording station can be determined. Future records will have more traces and provide additional information, including total sum signals at fixed gain with two ranges of sensitivity.
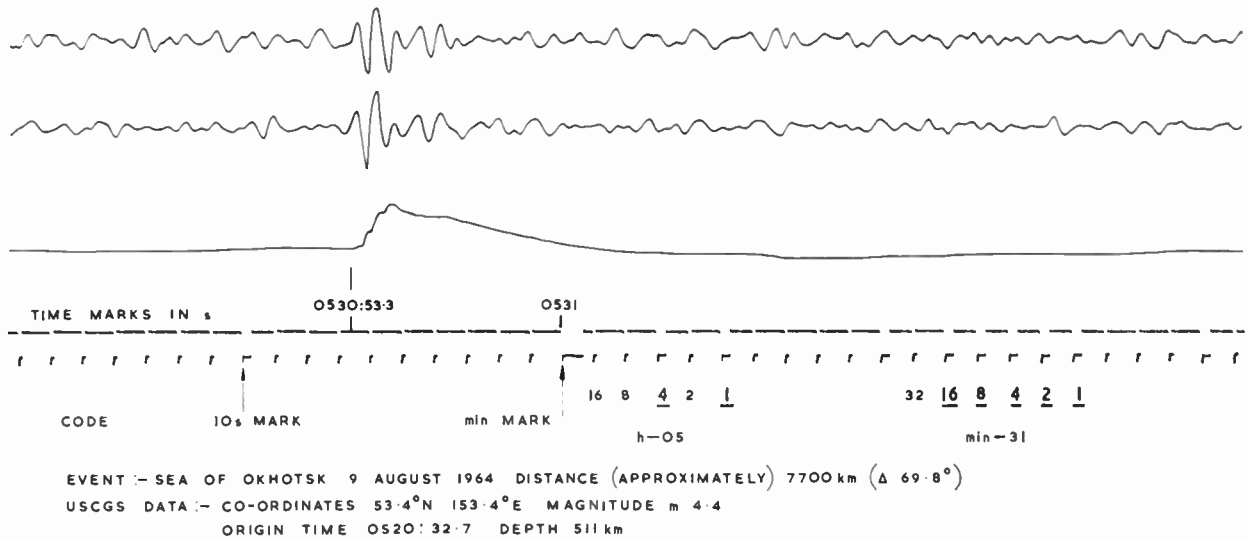
Fig. 9. A record of an event detected by the correlator.

8. Conclusions

S.A.D.A. should be capable of a standard of analysis equal to that obtained at present with the much slower combination of electro-mechanical phasing equipment and analogue computer. Also, it will be more flexible, being able to search for maximum correlation for any set of combinations of velocity and azimuth within the maximum phasing delay limits of the machine, namely 9·2 seconds.

The analyser has the new ability to present, simultaneously, phased total sums, correlation integrals, and other functions, corresponding to many different combinations of velocity and azimuth, all aligned to a common time scale. The histogram display provides a new, concentrated presentation of the processed seismic information, from which the azimuth or velocity of a signal can be immediately observed.

The present machine is a prototype research tool. After experience has been gained, it is likely that an 'engineered' version could be devised with some simplifications and with greater standardization.

Many possibilities exist for future development. In the limit, an increase in speed by a factor of about 30 is possible, but at increased cost and greatly increased difficulty. Doubling the speed, however, would be very reasonable technically, and would involve relatively small increase in cost. Other possibilities include an increase in the number of phasing conditions, and some degree of automatic program selection.

This project provides a good example of the effectiveness and economy possible from specialized data processing equipment when sufficient analysis work of a particular type has to be undertaken.

The simple on-line cross-correlator has been shown experimentally to be effective. Apart from its use in selecting events from noise for further processing, it provides useful, high quality, immediately available, visual records. It can also be used in the preparation of automatically edited magnetic tapes, and in the automatic recording of event parameters such as onset times.

9. Acknowledgments

10. References

1. F. E. Whiteway, 'The recording and analysis of seismic body waves using linear cross arrays', *The Radio and Electronic Engineer*, 29, No. 1, pp. 33–46, January 1965.

2. C. G. Keen, J. Montgomery, W. M. H. Mowat, J. E. Mullard and D. C. Platt, 'British seismometer array recording systems', *The Radio and Electronic Engineer*, 30, No. 5, pp. 297–306, November 1965.

3. J. R. Truscott, 'Approaches to Seismological Array Processing', Paper read at I.E.R.E. Symposium on 'Modern Techniques for Recording and Processing Seismic Signals', May 1964.

4. H. I. S. Thirlaway, 'Earthquake or explosion?', *New Scientist*, 18, No. 338, p. 311, 9th May 1963.

5. J. W. Birtill, and F. E. Whiteway, 'The application of phased arrays to the analysis of seismic body waves', *Phil. Trans. Royal Soc.*, A. 258, pp. 421–93, 1965.

The Application of Microelectronics to Naval Equipment

By

F. M. FOLEY, B.A., M.Sc.†

Originally presented at a Joint I.E.R.E.—I.E.E. Southern Sections' Symposium on 'Applications of Microelectronics' held at the University of Southampton from 21st to 23rd September 1965.

Summary: The paper first discusses the design criteria for Naval electronic equipment and how far they are satisfied by microelectronics. Equipments for which microelectronics is being considered or is in use are briefly described. Finally some comments are made on the choice of a particular microelectronic technique.

1. Design Criteria

The concept of any new equipment requirement is generally based on a specific functional requirement and the details of this form the basic specification. Given this functional requirement specification, the equipment can now be designed in terms of a number of possible engineering techniques, and a particular technique is chosen so that various subsidiary requirements such as reliability, maintainability, size and weight can be met. For shipborne equipments these basic requirements, broadly in order of importance, can be summarized as follows:

   (a) Reliability.

   (b) Ease of maintainability.

   (c) Standardization.

   (d) Low cost.

   (e) Small size and weight and low power consumption.

   (f) Environmental requirements.

1.1. *Reliability*

Reliability is unquestionably the most important advantage offered by microelectronics—probably in all applications—and certainly for Naval equipment. First, the need for immediate operational availability requires freedom from catastrophic failures. Further, for manpower reasons it is necessary to minimize the number of repairs and therefore to achieve a long normal component life. Taking account of the very large numbers of equipments now essential in any fighting ship it is necessary to aim for a reliability expressed very broadly as a failure rate not worse than about 0·1% circuit-unit failures per 1000 hours. Figures at least an order better than this are very desirable.

---

† Admiralty Surface Weapons Establishment, Portsmouth, Hants.

Today, argument is rife as to what reliability has been or will be achieved. Equipment designers at present adopt microelectronics hoping that manufacturers' predicted reliabilities will be fulfilled. There are good reasons for this hope because:

1. The basic materials and techniques, both of silicon integrated and thin film circuits, are fundamentally reliable, and a high degree of automation is used in their manufacture.

2. Each individual component is designed for its own specific function and operates therefore at optimum ratings.

It appears that very broadly the current position is that *unit* failure rates lie between 0·05% per 1000 hours which are suggested by some laboratory life tests, and about 3% per 1000 hours which has been reported from an industrial user, with the majority of recorded field results being greater than 1% per 1000 hours. These figures are quoted only to show that adequate reliability may not have really been achieved so far, and certainly far more reliability information, both from laboratory tests and from the field, are urgently needed. Despite this, microelectronics undoubtedly offers the best chance of meeting the Navy's requirements.

1.2. *Maintainability*

There are three parts to this requirement, rapid fault finding, easy unit replacement, and availability of spare working units. These must be achieved with the smallest possible number of men and with limited test and workshop facilities. Microelectronics gives advantages in all three.

(1) *Fault finding.* It is postulated that equipments will have built in 'go/no go' monitoring to check the performance of each replaceable unit. The small size of microelectronic elements simplifies the provision of adequate monitoring circuits.

(2) *Unit replacement.* Increasing complexity of monitoring sets a limit to the sub-division of an equipment into replaceable units and hence a lower limit to the amount of circuitry in a replaceable unit. The small circuit element size results in these replaceable units being small enough to handle easily.

It is intended that where economically possible, faulty units should be thrown away and that for larger more costly units they should be returned to base or factory for repair. Normally no unit repairs would be carried out at sea, thereby reducing and simplifying the work of the maintainers.

(3) *Availability of spare units.* The high reliability which allows a reduction of the number of spare units carried, and the small unit size, minimize the storage problem for adequate numbers of spares.

1.3. *Standardization*

This is apparently the most difficult of the basic requirements to meet in terms of microelectronics, and it is certainly of major importance to the Navy. Even with very high reliability, it is essential to carry spare units for every equipment fitted—if only to cover the possibility of action damage. There is a very large number of equipments fitted, involving something like 100,000 low power circuits in a typical ship. Currently these are maintained from the long established range of standard conventional components. This range is limited and the components themselves are fairly small. If now maintenance is by unit replacement, it is easy to see that if the circuit units are large and complex the chance of using them in more than one position in an equipment is remote, while if they are circuitally small then the monitoring problem to locate the faulty unit becomes impossible. The aim must clearly be to standardize units as widely as possible, in terms of an acceptably large unit of circuitry. In fact, there is obviously an optimum size of circuit unit and some work has been carried out on the optimization problem. It involves many factors, reliability, basic cost, maintenance cost, monitoring capability, storage and handling to mention a few.

1.4. *Low Cost*

It is hardly necessary to justify the need for low cost though it may not be fully appreciated how much is being spent on shipborne electronics. Each ship, other than small vessels like minesweepers, contains some millions of pounds worth of electronics. Of course low power circuitry only accounts for a proportion of this but any cost saving must be worth while.

Like reliability, the *cost* of a microelectronic equipment in production is still highly controversial. Opinions range between that which expects an equipment to cost somewhat more than it would in conventional component form, to that which estimates

that it might be as low as one-fifth that of the conventional design. So little is known about what forms of engineering design will be used, or how much the basic elements will cost when in full production, that no precise estimate is possible. The indications are however (at least in the writer's opinion) that a microelectronic equipment should not cost more than about one half that of the conventional equivalent. (This of course refers only to those parts to which microelectronics applies fully.)

1.5. *Small Size and Weight*

Ships are relatively large fighting vehicles and it may be difficult for the landsman to accept the need for small size and weight. However, space has always been difficult to find and with the need for more and more complex equipment to fight modern wars, this difficulty has become serious. Nevertheless, size is relative and it is not necessary to go to the extremes of miniaturization which are obviously essential for missile or satellite equipments. Microelectronic techniques engineered for easy maintainability allow considerable space saving as compared with conventional component equipments and this meets the needs of the Navy. There are of course other incidental space savings—because of the higher reliability fewer spares have to be carried and also fewer maintainers will be required. It may come as a surprise that a maintainer with his equipment and supporting services and necessary personal accommodation adds roughly 10 tons to the weight of the ship.

With regard to power requirements, with current microelectronic techniques the power used is comparable with that for a conventional equivalent and need not be discussed. In any case the power required for the general circuitry in a ship is only a small fraction of the power used in the motors used for aerial turning, or of the r.f. transmitted powers. A reduction in the power used in the general circuitry would be valuable, but mainly because of the resulting easing of the cabinet cooling problem.

1.6. *Environmental Requirements*

Generally ship environments are not extreme, mechanically, thermally or in humidity, though certain small units which are mounted at the mast head are subject to a very wide temperature range. The vibration frequency range is low and the amplitude small. Microelectronics offers no significant advantage over normal transistor circuitry but is certainly adequate to meet shipborne conditions.

2. Applications

Some actual applications and first of all some which are projected or which appear to be particularly important to the Navy will now be considered. (The same applications will probably be of interest to the
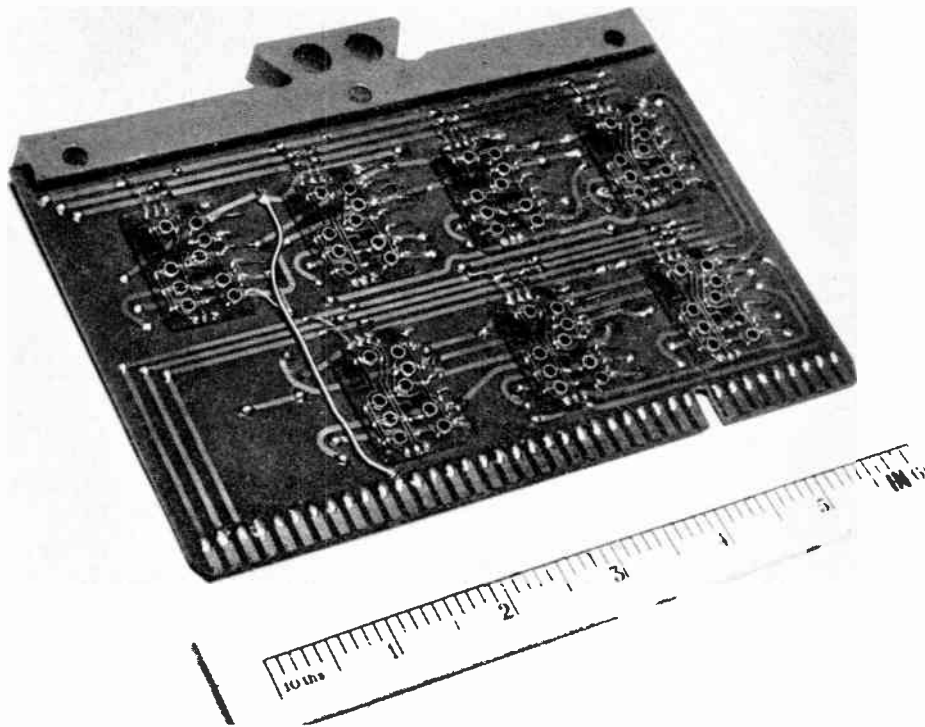
Fig. 1. Circuit board carrying 14 thin film circuits for digital monitoring unit.

other Services and to Industry also, though they might well adopt different engineering arrangements for their hardware.)

2.1. Projected Applications

It will be clear from the broad discussion of the basic design requirements for the Navy, that micro-electronic engineering should be introduced wherever it is feasible. For some applications it is becoming virtually essential.

Probably the most important of these is the computer. The computer complex to deal with the huge number of tasks involved in the daily running and operation of a fighting ship may well involve tens of thousands of circuit elements, and in ships such as submarines it is impossible to fit a conventionally engineered computer in the space available.

Then there is test equipment. It is not long since the main pulse monitor in ships weighed just 100 lb, and many items of test gear are too bulky and heavy to be truly portable in a rolling ship, particularly bearing in mind the ladders which may have to be climbed and the hatches passed through. Micro-electronics will make a big contribution here. An oscilloscope is envisaged using a very high resolution

half inch tube, all the circuitry being microelectronic. The tube would be viewed with a simple optical system which could be carried permanently in the maintainer's pocket.

Another item is the communication receiver, of which a typical ship might carry up to about fifty, covering the various frequency bands. A standard receiver design is being studied in which a receiver to any specification would be made up from a small number of standard modules, a special input amplifier being added to cover the desired frequency band.

Finally, servo systems which are used in great numbers for control of gun directors, missile mountings and radar aerials. These systems use large numbers of low power amplifiers and shaping circuits, many of which can have similar circuit design. Here reliability is of particular importance.

2.2. Applications in Hand

Two small pieces of equipment have already been in use at sea. These are not production designs but were made up in the laboratory from thin film circuit elements, some of them made in the laboratory and some by a manufacturer. These two equipments were intended as guinea pigs to give the Navy the feel of
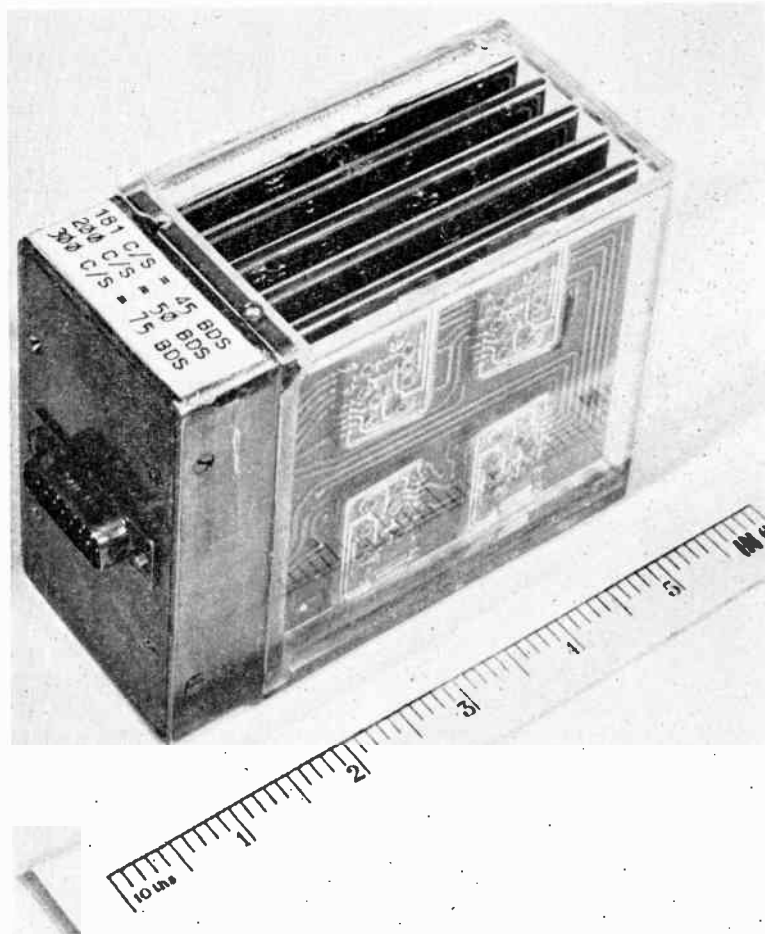
Fig. 2. Small digital simulator, using 33 film circuits.

the new technique and to give information on possible environmental difficulties. These units are:

(i) A monitoring unit for a digital transmission system. This contains about 500 thin film digital gate type circuits. There have been no failures in about 1000 hours of operational life. (See Fig. 1.)

(ii) A small digital simulator unit containing thirty-three thin film digital elements mounted on five printed boards. This portable unit has been in use since 1963, moved about between ships and establishment, without any failures. (See Fig. 2.)

Work is in hand on various other projects, some of them intended as production equipments, others mainly aimed at studying possible microelectronic engineering techniques. This is considered to be an urgent need. In the present state of the art, development of the basic circuit elements has far outstripped the engineering techniques for a complete equipment. This lack of engineering knowledge is one of the main

factors delaying a more rapid introduction of micro-electronics to the Fleet. The projects include:

(1) A communication receiver to study the design and engineering of standard modules from which any particular receiver could be made up. This is being done using evaporated circuits. It will include amplifier sections operating at 98 Mc/s and at 1·6 Mc/s.

(2) A small digital computer based on silicon integrated circuits intended as a study in the design and engineering of a microelectronic machine. It uses about 1500 elements mounted on multi-layer printed boards. It has a clock rate of 1 Mc/s. The machine, which is complete and being tested, uses techniques which would be used in a future typical large machine.

(3) A digital data link which involves some computing operations, designed to use about 1500 silicon integrated circuits. This will be the first microelectronic production equipment to reach the Fleet, probably in 1966. (See Fig. 3.)
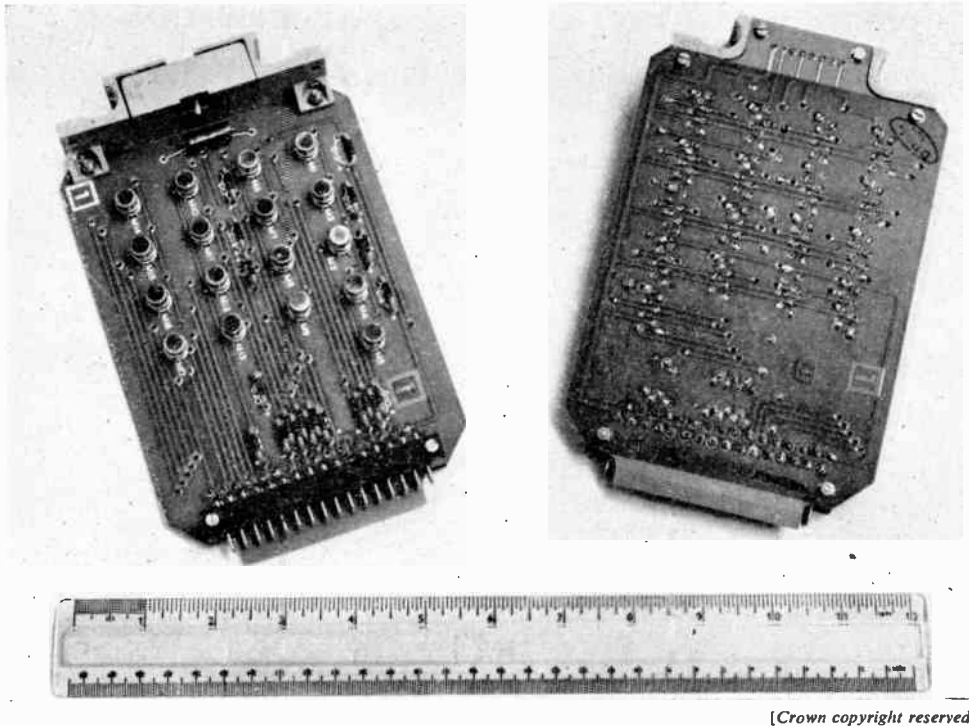
Fig. 3. Circuit board with 17 solid circuits for digital data link equipment.

(4) A digital data recorder using about 400 silicon integrated circuits. This equipment is essentially being introduced in place of a large valved equipment which has a bad reliability record. This also will probably be a production equipment.

(5) The monitoring units for the control circuitry in a major radar project. These will use thin film circuitry.

3. The Choice of Technique

There may well be some surprise at the apparently random choice of techniques for the applications referred to. The following guide lines have been evolved and should clarify the position.

1. For digital application silicon integrated circuits are used unless the speed required is outside their capability, or where only a small quantity of highly specialized elements are needed and it is economically unjustifiable to set up production of solid circuits. In each case thin film circuits, for which mask making is cheaper, are used. The present clock rate limit appears to be about 20 Mc/s.

2. For almost all analogue applications, thin film circuitry allows far greater flexibility of circuit design, much higher frequency and higher power operation. An experimental amplifier has been built which gives a useful gain at 500 Mc/s, as compared with a limit of about 120 Mc/s for the most advanced silicon linear amplifiers. Solid circuits are first choice of course where suitable elements are already available or can easily be produced.

3. It is expected that within a very few years silicon circuits will be in large production and that they will then be cheaper than film circuits. Where a choice is available, cost is likely to determine the choice of technique. At present the costs of silicon and thin film circuits are comparable.

4. From now on it is expected that hybrid circuitry either of silicon circuits mounted on passive circuit substrates, or vice versa, of passive components laid down on top of a silicon chip, will be normal practice, thus achieving the best of both worlds.

4. Conclusion

The Navy has a vital interest in microelectronics to improve its equipment reliability, thereby giving better operational availability and also easing the whole maintenance problem. It hopes for and expects lower equipment costs and gladly accepts smaller size and weight as a most valuable bonus.

The Performance of Practical Constant-Resistance Modulators in Relation to Their Use in F.D.M. Systems

By

Professor

D. G. TUCKER, D.Sc., C.Eng.
(*Member*)†

AND

G. TERREAULT, M.Sc.†

Summary: Ideally modulators with a constant input resistance produce no frequencies across their input terminals other than those impressed by the signal source. They are thus potentially important in simplifying the requirements of filters in multi-channel f.d.m. communication systems, and in the case of double-sideband signals, in eliminating filters since then the modulators can be directly paralleled. This paper discusses experiments to see how far constant-resistance modulators may approach ideal performance in practice; the results are very encouraging.

1. Introduction

The principles of modulators having an input impedance which is a constant resistance over the modulation cycle have been known for about twenty years,[1,2] and many of their properties have been studied,[3,4] but there appears to be no record of any investigation of their suitability for exploitation in multi-channel communication systems. Since this suitability depends on the smallness of effects of departures from the ideal condition, formal analysis becomes intractable. Investigation must thus be made either by numerical calculation using a computer or by direct experiment. The latter is, in this case, cheaper, quicker and more enlightening, and this paper records some results obtained this way.

2. The Problem

The modulator used initially was a normal ring modulator as shown in Fig. 1(a). When the ill-effects of the output transformer became apparent, the circuit of Fig. 1(b) was used for further investigations. The potentiometers P1 and P2 in Fig. 1(a) and P1 in Fig. 1(b) were used to provide compensation for rectifier unbalance in order to reduce the leakage of the carrier signal of angular frequency ω_p and its harmonics. This was a matter of convenience only; it is thought that this unbalance has no significant effect on the results to be discussed. In each of these circuits two rectifiers are connected in opposite polarity to the other two, as shown, so that their resistance at any point in the carrier voltage excursion may be written as $r(+V_c)$ and $r(-V_c)$ respectively, under the assumption, which we make throughout, that the signal voltage is small compared with V_c. Then, if the transformers are ideal, and the rectifiers and termination R_R are free of reactance, the input impedance at terminals 1, 1′ will be a constant resistance R_i independent of V_c if[3]

$$[r(+V_c)+r_a][r(-V_c)+r_a] = (R_R-r_a)^2 \quad \ldots\ldots(1)$$

† Department of Electronic and Electrical Engineering, University of Birmingham.

where r_a is a constant which may be positive or negative or zero. R_i is then equal to R_R-2r_a. Usually rectifiers operated over a fairly small carrier voltage excursion may be very approximately represented by the resistance/voltage relationship

$$r = a \exp(-bV_c)+r_0 \quad \ldots\ldots(2)$$

where r_0 is positive, so that $r_a = -r_0$ and is negative. Then $R_R = a-r_0$ and $R_i = R_R+2r_0 = a+r_0$.

(a) Normal ring modulator.

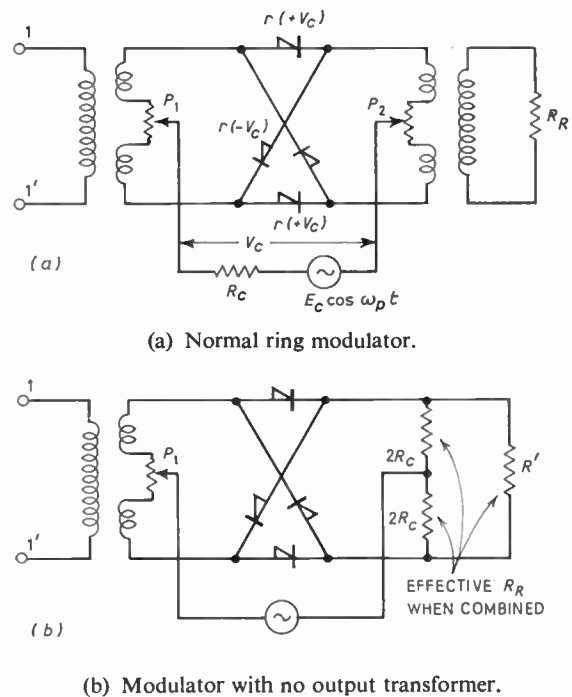(b) Modulator with no output transformer.

Fig. 1. Circuit arrangements.

In any multi-channel f.d.m. system there will be a stage when the group of channels is branched into separate channels and demodulated by a series of modulators, each with a different carrier (i.e. local) frequency as represented in Fig. 2. Although in single-

sideband systems the inputs of these modulators have to be paralleled via filters because otherwise the signals from an adjacent channel would be equally demodulated with the wanted signals, nevertheless the filters also have to prevent interchannel interference caused by even-order modulation products such as $(2\omega_{pn} \pm \omega_q)$ being produced at the paralleled terminals. For example, $(2\omega_{pn} - \omega_{q2})$ falls in the channel with carrier ω_{pn-1}; $(2\omega_{pn-1} - \omega_{q2})$ falls in the channel with carrier ω_{pn-3}; and so on. It is thus usual for the filters to be of band-pass type.

(a) Single-sideband.
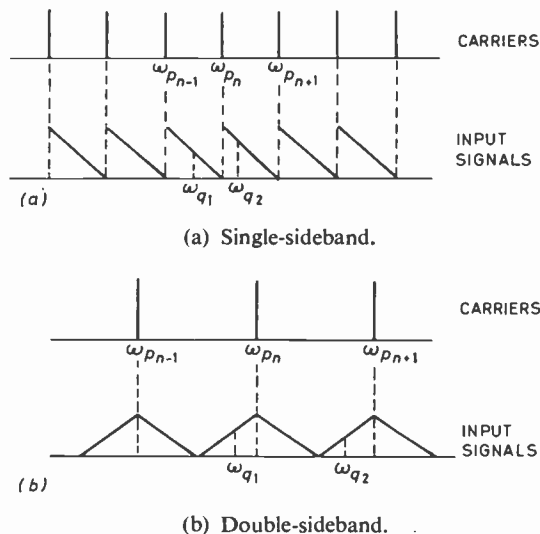

(b) Double-sideband.

Fig. 2. F.d.m. channel arrangements.

If each modulator, however, is of the constant-resistance type, no such modulation products occur at the input terminals, since the only frequencies which are present there are those imposed from the preceding part of the system; the input impedance is not time-varying and cannot therefore produce any modulation at the input terminals. The filter requirements are now merely those of separating out the unwanted sideband, and, in principle, a low- or high-pass filter could be used instead of a band-pass filter. In a double-sideband system, as used on rural carrier systems, the filters could be dispensed with altogether if the branching (or shunting) loss of $10 \log_{10} n$ dB (where n is the number of channels) can be tolerated. There is thus an economic advantage in using constant-resistance modulators, but, of course, it is necessary to ensure a constant resistance load at the output of each modulator over all significant frequencies, and not just over the audio band.

Similarly at the sending end of the system, the modulators can be made to have a constant resistance looking back into the output terminals, and the group

of channels can, as far as modulation-crosstalk effects are concerned, be paralleled without filters.

In combining groups and super-groups of channels, and in separating them out, the wanted and unwanted sidebands are well spaced in frequency and, if modulation crosstalk can be avoided by the use of constant-resistance modulators, then only relatively simple filters need to be used, and a further economic advantage is obtained.

The possible effects of other kinds of interference are discussed in Section 4.

The practical question is, of course, how closely the constant-resistance input condition can be attained in practice. Obviously rectifiers do not have exactly the law quoted in eqn. (2), nor can the terminating impedance always be a pure resistance R_R at all output-sideband frequencies. A theoretical calculation of the even-order modulation products at the input terminals of the modulator based on small departures of the rectifier law from the ideal and on various errors in the termination appears quite impossible because:

(a) functional representation of the departures would be difficult;

(b) the normal theory of constant-resistance modulators provides no analysis of modulation products;

(c) the normal method of modulator analysis in terms of periodically-varying resistances[5] requires the rectifier resistance/voltage law to be converted into a Fourier expansion of the resistance/time function, and this is, in general, not analytically possible;

(d) the equations obtained would, in general, be infinite and insoluble.

Thus an experimental investigation of the type of results which might be typical in practice was undertaken.

Point-contact diodes type OA85 (Mullards) were used, and to obtain a reasonably low value of a (see eqn. (2)), each element in the modulator comprised two diodes in parallel. All eight diodes were roughly matched to avoid excessive discrepancies in characteristics. The characteristics of one paralleled pair are shown in Fig. 3.

The transformers had twinned windings to provide a low leakage reactance for the carrier current, and were of normal design intended to give satisfactory transmission over the frequency range involved. The input transformer has no influence in the production of even-order products at the input, but the output transformer causes the effective impedance terminating the modulator to depart from the pure constant resistance R_R and so its parameters are important.
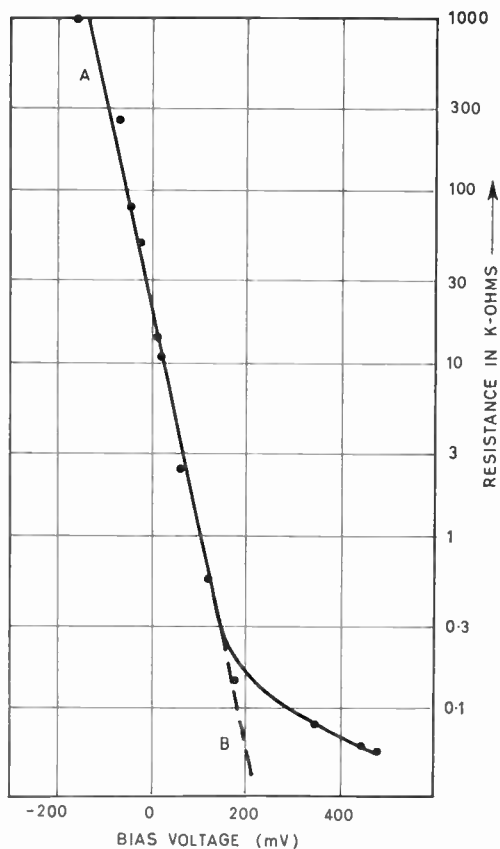
Fig. 3. Incremental resistance of a pair of diodes, (OA85) in parallel. The line AB is $r = 18\,000 \exp(-29V_c)$.

They were, at 100 kc/s,

  Inductance of primary winding (both halves in series and output winding open circuited) = 48 mH with $Q \simeq 80$.

  Capacitance of twinned primary winding = 230 pF.

  Leakage inductance, i.e. inductance of primary winding with output winding short-circuited = 0·38 mH.

The impedance ratio of the transformer was not 1 : 1, but values of R_R will be quoted as though it were.

A carrier frequency (i.e. $\omega_p/2\pi$) of 100 kc/s was chosen for all tests. The resistance R_c was 9 kΩ, and the peak value of V_c was 125 mV. The signal frequency was variable but its voltage across the input terminals 1, 1′ was maintained at −30 dBm (i.e. about 25 mV) in all tests.

3. Results

For a signal frequency of 20 kc/s, the value of R_R required to give minimum conversion loss (5·4 dB) of the output sideband frequencies, 80 and 120 kc/s, was

about 2500 Ω, and this value also gave the minimum levels of the 2nd-order products ($2\omega_p \pm \omega_q$, i.e. 180 and 220 kc/s) at the input terminals. These levels are shown in column 2 of Table 1. Changing R_R to 2000 Ω or to 3000 Ω makes the levels about 10 dB higher. The value of $R_R = 2500$ Ω was therefore chosen as that apparently corresponding most closely

Table 1

Level of even-order products relative to input signal level (dB) ($\omega_p/2\pi = 100$ kc/s). Circuit of Fig. 1(a)

Product	Signal frequency ($\omega_q/2\pi$)			
	20 kc/s	55 kc/s	90 kc/s	110 kc/s
$2\omega_p - \omega_q$	−39	−26	−9	−10
$2\omega_p + \omega_q$	−43	−36	−30	−21
$4\omega_p - \omega_q$	−35	−40	−25	−22
$4\omega_p + \omega_q$	−32	−31	−34	−24

to the constant resistance condition, although it was much lower than the value expected from the rectifier characteristics. The level of the interfering products, around 40 dB below the signal level, would be low enough for some applications. The level of the fourth-order products ($4\omega_p \pm \omega_q$) was rather higher, however, being 35 and 32 dB below the signal for 380 and 420 kc/s respectively.

It is clear from Table 1 that there is a lack of symmetry between the two sidebands of even-order modulation. When the signal frequency is increased, this discrepancy increases and the interference level rises, as shown in Table 1. This is due to the output transformer. We can see how this effect arises by considering the case of the 90 kc/s input. Here the first-order output sideband frequencies are 10 and 190 kc/s. The shunt and leakage reactances at these two frequencies are given approximately in Table 2.

Table 2

Transformer reactances

	at 10 kc/s	at 190 kc/s
Shunt reactance (ohms)	3000	− 3500
Leakage reactance (ohms)	24	455

It is clear that the shunt reactance considerably reduces the terminating impedance at 10 kc/s and 190 kc/s and gives it large and opposite phase angles at the two frequencies. The leakage reactance, which is a series reactance, has only a small effect but augments the effect of the shunt reactance. It is thus not surprising that asymmetry is introduced into the even-order interfering products at the input terminals and that their level is increased. Obviously the effect will be smaller when the signal is a lower

frequency (e.g. 20 kc/s) since the difference between the terminating impedances at the output first-order sideband frequencies is then smaller. It should be observed that although the effect of the transformer is so marked on the input-circuit interference, yet it is a quite good transformer from the point of view of transmitting the output signal. Its insertion loss does not exceed 1 dB over the whole range of output first-order sideband frequencies involved in the tests, and does not exceed 0·25 dB over the range 20–200 kc/s.

These results emphasize that the benefits of the constant resistance modulator cannot be realized unless the output transformer can be eliminated. This is especially true when the f.d.m. demodulation is considered and the lower output sideband has to extend down to the lowest audio frequencies. The transformer can be eliminated by the arrangement of Fig. 1(b). This modification was made to the experimental modulator, keeping R_c at 9 kΩ, and the tests repeated, keeping the carrier voltage across the rectifiers the same as before, namely 125 mV peak. The improvement in the results is very marked. Firstly, the value of terminating resistance R_R (i.e. R' in parallel with $4R_c$) required to give minimum even-order interference is now the expected value of about 18 kΩ, and, secondly, there is no longer any significant asymmetry between the even-order sidebands. Most important of all, the level of the interference products is now much lower than before. The figures are given in Table 3, which also shows that the results are not much affected by reducing the peak carrier voltage to only 63 mV. The effect of altering the value of R_R and of connecting a small capacitance across it is shown in Table 4. (100 pF at 190 kc/s is a reactance of about −8·5 kΩ.) The effect of any reactance in the termination comparable to the resistance is clearly very serious, and it is evidently also quite important to work near the correct value of resistance.

Table 3

Level of even-order products relative to input signal level (dB) ($\omega_p/2\pi = 100$ kc/s). Circuit of Fig. 1(b) with $R_R = 18$ kΩ. Effect of frequency and carrier voltage

Product	Carrier voltage 125 mV peak		Carrier voltage 63 mV peak	
	Signal at 20 kc/s	Signal at 90 kc/s	Signal at 20 kc/s	Signal at 90 kc/s
$2\omega_p - \omega_q$	− 57	− 58·5	− 57	− 53
$2\omega_p + \omega_q$	− 56·5	− 57	− 56·5	− 54
$4\omega_p - \omega_q$	− 72	− 63	− 61·5	− 66
$4\omega_p + \omega_q$	− 72	− 61	− 61	− 64

Table 4

As for Table 3, with carrier voltage 125 mV peak. Effect of terminating resistance R_R and capacitance

Signal frequency	Product	Terminating resistance and capacitance					
		9 kΩ	18 kΩ	36 kΩ	18 kΩ 10 pF	18 kΩ 47 pF	18 kΩ 100 pF
20 kc/s	$2\omega_p - \omega_q$	−40	−57	−46·5	−53	−29	−22
	$2\omega_p + \omega_q$	−42	−56·5	−48	−54·5	−30	−23·5
90 kc/s	$2\omega_p - \omega_q$	−37	−58·5	−41·5	−50	−25	−20
	$2\omega_p + \omega_q$	−45	−57	−49	−55	−33	−28

It should be noted that all the tests recorded used a high carrier-source resistance (R_c). When a low resistance is used, giving a constant-voltage drive, the transitions from high to low resistance (and vice versa) in the rectifiers are slower, the input resistance is less constant, and more interference is produced. In the modulator with the output transformer, the worsening of interference could be as great as 20 dB.

4. Other Causes of Interference

Once it has been decided to try to simplify filter requirements by the use of constant-resistance modulators, it is naturally necessary to consider whether there are any sources of inter-channel interference which, while previously unimportant, may now become significant.

The most important possibility of inter-channel interference is that caused by second-order modulation as already discussed above; this is relevant in almost any system since adjacent-channel interference is involved. It is, moreover, just this kind of interference which the constant-resistance modulator is intended to remove. But there are other possibilities of interference when the system has a sufficiently wide band, say approaching an octave or more. One possibility arises from odd-order modulation products occurring at the input terminals of the modulators.

In the normal conception of the ring modulator as a balanced and symmetrical circuit, with a symmetrical carrier waveform, odd-order modulation products do not occur in the input loop, nor do even-order products occur in the output.[6] But if the circuit is not well-balanced, or the carrier waveform is not symmetrical, then odd-order products occur in the input and may cause inter-channel interference. For example, if the input frequencies extend from say 40 kc/s to 100 kc/s, with local carriers also in this range, then a signal frequency of 45 kc/s can produce a first-order interference product ($\omega_p - \omega_q$) of 50 kc/s in the modulator with a local frequency around

95 kc/s; this spurious signal then falls in another channel. Similarly, a signal at 85 kc/s can produce a third-order interference product $(3\omega_p - \omega_q)$ at 95 kc/s in the modulator with a local frequency around 60 kc/s; and so on.

Now this effect has nothing to do with the constant-resistance modulator concept; it is quite separate, and is normally unimportant because the high level of even-order interference in ordinary systems necessitates input filters anyway. It becomes potentially important, however, when constant-resistance operation is to be exploited.

In the experimental modulators discussed above, these odd-order interference products proved negligible, being in all cases of lower level than the even-order products; typically they were 60–80 dB below the signal at the input terminals. In these circumstances it hardly seemed worth while to investigate their origins and dependence on the modulator elements and carrier supply.

In addition to the types of interchannel modulation crosstalk which are due to effects at the input terminals of the modulators—which the constant-resistance modulator is intended to prevent—there are other sources of interchannel interference which the use of channel-selection filters normally makes unimportant. One of these, which, like the crosstalk just mentioned above, occurs only when the system extends over at least an octave of bandwidth, is due to the fact that the modulating function of each modulator has components at the harmonics of the local carrier frequency (i.e. $n\omega_p$). Ideally only odd-order harmonics appear, but in practical single-balanced modulators even-order harmonics may be serious. In the ring modulator the even-order harmonics are easily made small, but not necessarily as low as 60 dB below the fundamental component. The third-order component will usually be between 10 and 15 dB below the fundamental component. Thus signals on a carrier frequency corresponding to these harmonics will produce an interfering demodulated output in the channel. Although there are ways of reducing certain harmonics in the modulating function[1]—or even of obtaining a purely sinusoidal modulating function by using, say, a Hall-effect multiplier—these involve serious problems of their own. The problem of harmonics in the modulating function leads to the conclusion that for systems covering an octave or more the use of filters is desirable, even when double-sideband working is employed, but that the use of constant-resistance modulators can permit a much simpler filter than usual to be used.

There is a further, but entirely different kind of potential source of interchannel interference when input filters are not used, due to non-linearity of response to the applied signal. This also is not a question of interfering frequencies being produced at the input, but concerns the production of output frequencies of the type $(\omega_p \pm n\omega_q)$ or $(\omega_p \pm n\omega_{q_1} \pm m\omega_{q_2})$. For example, if strong signals exist at 80 and 85 kc/s, putting $n = 2$ and $m = 1$ will give an audio output from the channel with local carrier frequency around 75 kc/s. Non-linear effects of this kind are sometimes calculable and can often be estimated,[7, 8] but can always be reduced by reducing the signal levels in the modulators.

5. Conclusions

The experimental results discussed above relate to one particular group of rectifiers and a particular set of frequencies. To determine whether channel branching in a particular frequency division multiplex communication system can be done without filters, or with cheaper filters, would require quite thorough tests under appropriate conditions. The results shown here demonstrate some of the properties of practical modulators designed to approximate to the constant-resistance condition, and in particular their great sensitivity to stray reactances such as those of an output transformer. But they also demonstrate that with proper care, interference levels may well be low enough, e.g. 60 dB below the signal level, to enable filters to be dispensed with, or at least considerably simplified, and that designers would be well advised to look further into the possibilities of this kind of modulator.

6. Acknowledgments

7. References

1. D. G. Tucker, 'Some aspects of the design of balanced rectifier modulators for precision applications', *J. Instn Elect. Engrs*, **95**, Part III, p. 161, 1948.

2. L. A. Zadeh, 'Constant-resistance networks of the linear varying-parameter type', *Proc. Inst. Radio Engrs*, **39**, p. 688, 1951.

3. D. G. Tucker, 'Constant-resistance modulators', *J. Brit. Instn Radio Engrs*, **21**, p. 491, 1961.

4. D. G. Tucker, 'Circuits with Periodically-Varying Parameters', Chapters 8 and 9 (Macdonald, London, 1964).

5. Ibid, Chapter 2; or D. G. Tucker, 'Circuits with time-varying parameters', *The Radio and Electronic Engineer*, **25**, p. 263, 1963.

6. See Ref. 4, Chapter 5.

7. V. Belevitch, 'Non-linear effects in rectifier modulators', *Wireless Engineer*, **26**, p. 177, May 1949; **27**, p. 130 and p. 164, April 1950.

8. D. G. Tucker, 'Intermodulation distortion in rectifier modulators', *Wireless Engineer*, **31**, p. 145, 1954.

Analysis of a Coupled Waveguide Circulator Using Non-Reciprocal Attenuation

By

J. HELSZAJN, M.S.E.E., C.Eng.

(*Associate Member*)†

Summary: This paper describes a coupled waveguide circulator in which the secondary waveguide is loaded with distributed non-reciprocal attenuation along the coupling length. In the forward direction of transmission, the difference in the attenuation constants between the two coupled waveguides is large and transmission takes place between the primary waveguide ports. The peak and average power capability for this direction is essentially that of the empty waveguide. In the reverse direction, the difference in the attenuation constants is essentially zero and complete transfer of power takes place between the two waveguides. The insertion loss for this direction of propagation is limited by the back-to-front ratio of the non-reciprocal loss.

1. Introduction

A four-port waveguide circulator[1,2] has been described which makes use of two coupled waveguides in which the secondary waveguide is loaded with non-reciprocal phase shift. Such a circulator is shown in Fig. 1. In the reverse direction of propagation the phase shifter is adjusted so that the phase velocities of the two coupled waveguides are the same and the coupling holes are arranged to give a zero dB coupler. Hence transmission takes place between ports 2 and 3 or ports 4 and 1. In the other direction of propagation, the phase velocities of the two coupled waveguides are not the same because of the effect of the non-reciprocal ferrite phase shifter. For a proper choice of the two phase velocities, transmission takes place between ports 1 and 2 or ports 3 and 4. The arrangement, therefore, behaves as a four-port circulator. The main advantage of this type of circulator compared to the conventional four-port differential phase shift type is the increased peak and average power capabilities for the situation where transmission is between ports 1 and 2. For this case the secondary waveguide containing the ferrimagnetic material is somewhat decoupled from the primary one, thereby minimizing such things as non-linear effects, breakdown and heating effects. Hence, under high power it is desirable to transmit between ports 1 and 2, and under low power to transmit between ports 2 and 3. The purpose of this paper is to review this type of circulator and to describe[3] a new type of circulator with enhanced peak and average power capability. This new circulator makes use of non-reciprocal attenuation. In the forward direction of propagation the difference in the attenuation constants between the two coupled waveguides is finite and transmission occurs between ports 1 and 2. In the reverse direction, the difference in the attenuation constants between the
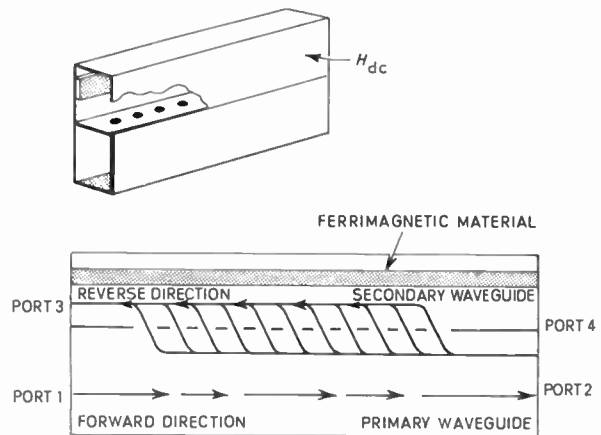
† Microwave Associates Inc., Burlington, Mass., U.S.A.

Fig. 1. Coupled waveguide with secondary loaded with ferrimagnetic material.

waveguides is essentially zero and transmission takes place between ports 2 and 3, or between 4 and 1. In the forward direction we notice that transmission between ports 3 and 4 is not possible because the secondary waveguide is in the loss state for that direction. However, port 3 is still decoupled from port 1.

2. Coupled Waveguides with Unequal Propagation Constants

The space variation of the complex wave amplitudes for a system of two coupled waveguides with uniform distributed coupling has been shown to have the following form[4]

$$\frac{dE_1}{dx} = -\Gamma_1 E_1 + jk_{21} E_2 \qquad \ldots\ldots(1)$$

$$\frac{dE_2}{dx} = jk_{12} E_1 - \Gamma_2 E_2 \qquad \ldots\ldots(2)$$

where E_1, E_2 are the complex wave amplitudes in the primary and secondary waveguides.

k_{21}, k_{12} represent the perturbed transfer effects of the coupling mechanism.

Γ_1, Γ_2 are the perturbed propagation constants in the primary and secondary waveguides, i.e.

$$\Gamma_1 = \alpha_1 + j\beta_1, \qquad \Gamma_2 = \alpha_2 + j\beta_2$$

The solutions of eqns. (1) and (2) are of the form

$$E_1 = A \exp(r_1 x) + B \exp(r_2 x) \qquad ......(3)$$

$$E_2 = C \exp(r_1 x) + D \exp(r_2 x) \qquad ......(4)$$

where

$$r_1 = -\left(\frac{\Gamma_1 + \Gamma_2}{2}\right) + jk\sqrt{\frac{(\Gamma_1 - \Gamma_2)^2}{-4k^2} + 1} \ ......(5)$$

$$r_2 = -\left(\frac{\Gamma_1 + \Gamma_2}{2}\right) - jk\sqrt{\frac{(\Gamma_1 - \Gamma_2)^2}{-4k^2} + 1} \ ......(6)$$

and for a reciprocal system, one can write

$$|k_{12}| = |k_{21}| = |k|$$

To obtain the arbitrary constants we let $E_1|_0 = 1$ and $E_2|_0 = 0$.

Making use of the above boundary conditions in eqns. (1) and (2) we also have

$$\frac{dE_1}{dx}\bigg|_0 = -\Gamma_1 \quad \text{and} \quad \frac{dE_2}{dx}\bigg|_0 = jk$$

and the four arbitrary constants in eqns. (3) and (4) are now given by:

$$A = \frac{1}{2}\left[1 - \frac{\left(\dfrac{\Gamma_1 - \Gamma_2}{2jk}\right)}{\sqrt{\dfrac{(\Gamma_1 - \Gamma_2)^2}{-4k^2} + 1}}\right] \ ......(7)$$

$$B = \frac{1}{2}\left[1 + \frac{\left(\dfrac{\Gamma_1 - \Gamma_2}{2jk}\right)}{\sqrt{\dfrac{(\Gamma_1 - \Gamma_2)^2}{-4k^2} + 1}}\right] \ ......(8)$$

$$C = \frac{\frac{1}{2}}{\sqrt{\dfrac{(\Gamma_1 - \Gamma_2)^2}{-4k^2} + 1}} \qquad ......(9)$$

$$D = \frac{-\frac{1}{2}}{\sqrt{\dfrac{(\Gamma_1 - \Gamma_2)^2}{-4k^2} + 1}} \qquad ......(10)$$

It is useful to identify $(A+C).\exp(r_1 x)$ as the fast normal mode and $(B+D).\exp(r_2 x)$ as the slow normal mode of the coupled system.
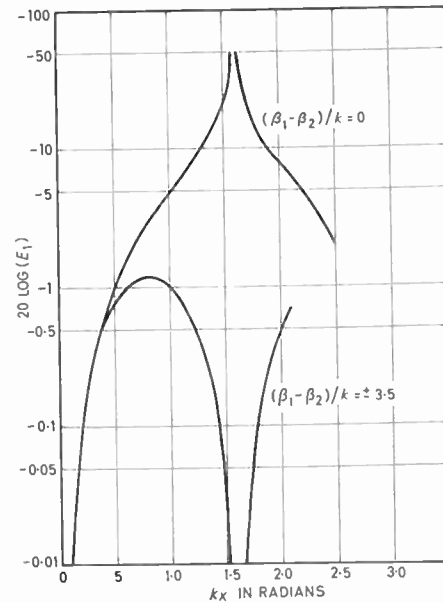

Fig. 2. Primary waveguide amplitude versus kx as a function $(\beta_1 - \beta_2)/k$ with $(\alpha_1 - \alpha_2)/k = 0$.

3. Power Handling Limitation of the Non-reciprocal Phase Shift Method of Circulation

In this section the wave amplitudes in the two waveguides for the non-reciprocal phase shift mode of circulation will be briefly examined. A circulator using this mode of operation has previously been built.[2] When the two waveguides have a fixed phase difference between them, the power division and the period is dependent on the ratio of velocity difference to coupling factor. In Figs. 2 and 3 the wave amplitudes are shown versus integrated coupling length for $(\beta_1 - \beta_2)/k = \pm 3.5$ and $(\beta_1 - \beta_2)/k = 0$ when $(\alpha_1 - \alpha_2)/k = 0$. The positive sign applies to the situation where the input wave coincides with the waveguides having the higher phase velocity. The negative sign applies when the input wave coincides with the waveguide having the lower phase velocity. For the backward direction of propagation we have $(\beta_1 - \beta_2)/k = 0$ and $kx = \pi/2$. This corresponds to transmission from port 2 to port 3. The loss for this direction is dependent on the insertion loss of the ferrite phase shifter. For the forward direction of propagation we require $(\beta_1 - \beta_2)/k = \pm 3.5$. This gives $E_1 = 1$ and $E_2 = 0$ at $kx = \pi/2$. This corresponds to transmission from ports 1 to 2. From Fig. 3, we note that the power in the secondary waveguide for $(\beta_1 - \beta_2)/k = \pm 3.5$ is periodic and that its maximum value is 6 dB below its value in the primary waveguide. This must be compared with a figure of 3 dB for a conventional differential phase shift circulator, hence insofar as non-linear effects and power breakdown are concerned, only limited increase
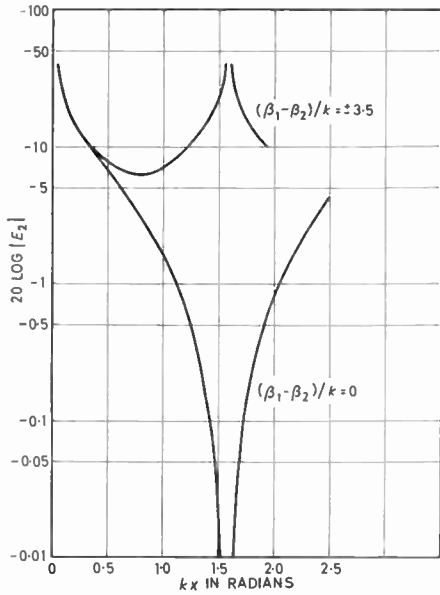
Fig. 3. Secondary waveguide amplitude versus kx as a function of $(\beta_1-\beta_2)/k$ with $(\alpha_1-\alpha_2)/k = 0$.
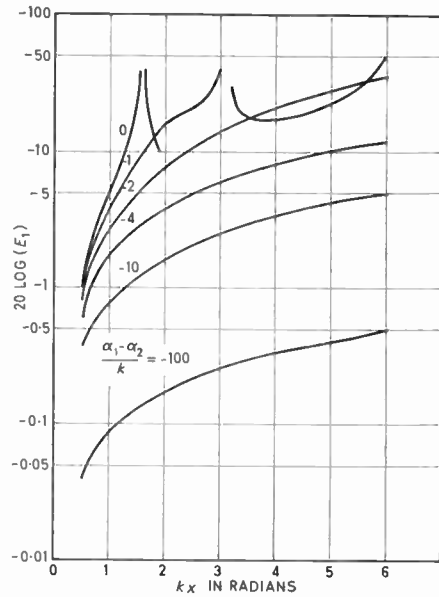

Fig. 4. Primary waveguide amplitude versus kx as a function of $(\alpha_1-\alpha_2)/k$ with $(\beta_1-\beta_2)/k = 0$.

in capability results from such an approach. This is particularly true in view of the increased length of such devices.

4. Waveguide Four-port Circulator Using Non-reciprocal Attenuation

The operation of this circulator is based on the use of non-reciprocal attenuation in the secondary waveguide instead of non-reciprocal phase shift. Non-reciprocal attenuation can be obtained with the help of distributed ferrimagnetic material biased to resonance, i.e. a distributed ferrite isolator. In the reverse direction of propagation, the ferrite material in the secondary waveguide is biased in its insertion loss condition. This gives $(\beta_1-\beta_2)/k = 0$ and $(\alpha_1-\alpha_2)/k = $ minimum. In the forward direction of propagation the ferrite material in the secondary waveguide is in its isolation condition, $(\beta_1-\beta_2)/k = 0$ and $(\alpha_1-\alpha_2)/k = $ maximum. To investigate more fully the transmission properties for these two conditions we solve eqns. (3) and (4) for $\beta_1 = \beta_2$ and $(\Gamma_1-\Gamma_2)/k = (\alpha_1-\alpha_2)/k$. We also note that $(\alpha_1-\alpha_2)/k$ is negative because the attenuation constant of the secondary waveguide is larger than that of the primary one. The wave amplitudes in the two waveguides versus integrated coupling length for parametric value of $(\alpha_1-\alpha_2)/k$ are plotted in Figs. 4 and 5. These graphs are reproduced from Miller's paper[4] with slight changes in the notation. For the reverse direction of propagation $(\alpha_1-\alpha_2)/k = $ minimum, and transmission between ports 2 and 3 occurs when $kx = \pi/2$. This is the same condition as for the non-reciprocal phase shift mode

of operation. The insertion loss in this direction can be made small by keeping $(\alpha_1-\alpha_2)/k$ small. For the forward direction of propagation, $(\alpha_1-\alpha_2)/k = $ maximum and the coupling phenomenon between the two waveguides disappears for large values of $(\alpha_1-\alpha_2)/k$. For instance, when $(\alpha_1-\alpha_2)/k = -100$, the insertion loss of the transmitted wave is less than 0·15 dB and

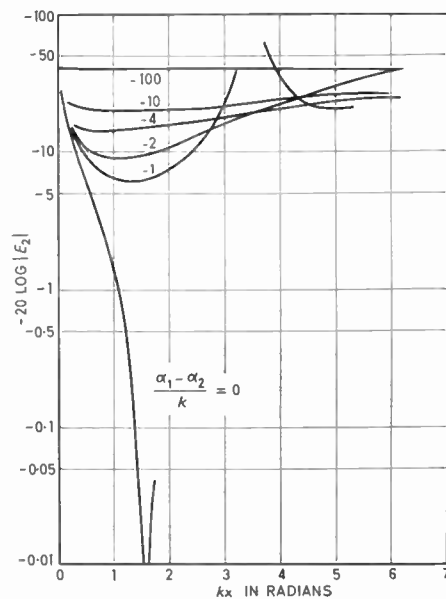**Fig. 5.** Secondary waveguide amplitude versus kx as a function of $(\alpha_1-\alpha_2)/k$ with $(\beta_1-\beta_2)/k = 0$.

the wave in the ferrite loaded secondary waveguide is decoupled by 40 dB at every point from the primary waveguide. Hence, the heat dissipation is a constant along the length of the structure for this direction of propagation. In the forward direction of propagation, the peak and average power capability for this mode of operation is therefore essentially that of the empty waveguide. This compares with a value of 6 dB for the non-reciprocal phase shift mode.

5. Practical Considerations

Since we are concerned with the design of a high average and peak power device, we first adjust the circulator in the forward direction. The insertion loss for the reverse direction of propagation will then be determined by the back-to-front ratio of the non-reciprocal loss. The latter is defined as the ratio of the reverse to forward attenuation in decibels.

The wave amplitudes in the two waveguides versus $(\alpha_1 - \alpha_2)/k$ at $kx = \pi/2$ are shown in Fig. 6. These curves determine the back-to-front ratio required when the insertion loss in each direction of transmission is specified. To obtain the overall length of the device and the non-reciprocal attenuation per unit length of the isolator we write $(\alpha_1 - \alpha_2)/k = (\alpha_1 - \alpha_2) . \frac{2x}{\pi}$ by noting that $kx = \pi/2$.

If at X-band we select a figure of 25 dB/inch for the loss of the ferrite isolator, the overall length is about 19 in for $(\alpha_1 - \alpha_2)/k = -35$. If we substitute $x = 19$ in into the equation $kx = \pi/2$ we obtain $k = 0.0825$ radians/inch. The primary waveguide can be coupled to the secondary one through a series of coupling holes in the common narrow wall. The value of k is determined by the size of the holes. The holes are normally spaced a quarter wave apart. In this example, the insertion loss in the forward direction is 0.45 dB and the secondary waveguide is decoupled by
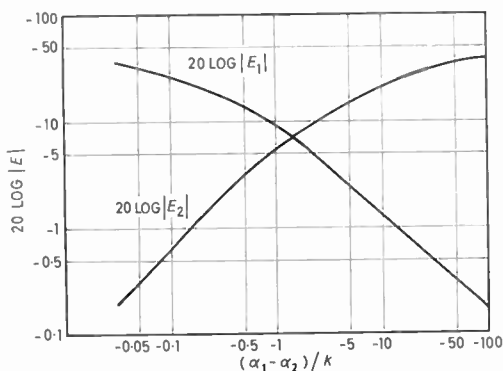

Fig. 6. Primary and secondary waveguide amplitudes at $kx = \pi/2$ as a function of $(\alpha_1 - \alpha_2)/k$ with $(\beta_1 - \beta_2)/k = 0$.
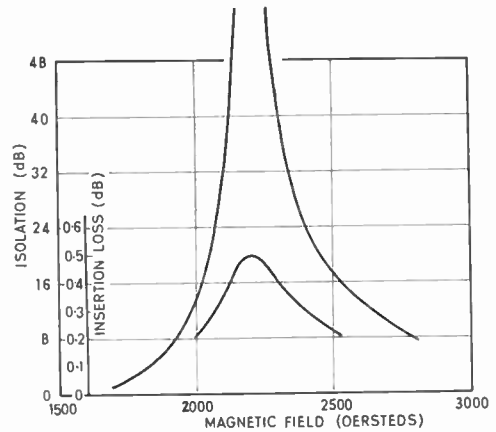

Fig. 7. Curves of isolation and insertion of practical resonance isolator.

more than 30 dB at every point from the primary waveguide. The reverse insertion loss is now determined by the back-to-front ratio of the isolator with the help of Fig. 6.

The back-to-front ratio for the ferrite resonance isolator at resonance in a uniform magnetic field is given by

$$R = \left(\frac{4\omega}{\gamma \Delta H} \right)^2 \text{ where } \omega \text{ is the frequency in Mc/s.}$$

γ is the gyromagnetic ratio in oersteds per Mc/s.
ΔH is the linewidth in oersteds.

The linewidth is defined as the width of the absorption curve at half maximum absorption. Hence the back-to-front ratio is reduced by a half on either side of the peak absorption point.

The bandwidth is primarily determined by the back-to-front ratio through the choice of linewidth. High quality resonance isolators generally utilize narrow linewidth materials which give large back-to-front ratios but also result in narrow bandwidth performance. For a typical magnesium manganese ferrite we have $R = 930$ with $\gamma = 2.8$ Oe/Mc/s, and $\Delta H = 420$ Oe. If we use a yttrium-iron garnet material we have $R = 54\,000$ with $\gamma = 2.8$ Oe/Mc/s and $\Delta H = 55$. The reverse insertion loss for these two materials is 0.30 dB and 0.05 dB. Practical devices, however, must take into account dielectric losses and the effect of ellipticity. This results in lower back-to-front ratios.

The measured insertion loss and isolation of a resonance isolator using a magnesium manganese ferrite material at X-band versus magnetic field is given in Fig. 7. The back-to-front ratio of this device is in excess of 100.

Using this value for the back-to-front ratio, the reverse insertion loss is 2.1 dB. This last figure is

322

probably objectionable when the device is to be used as a circulator.

When the circulator is used as an isolator by terminating ports 3 and 4 with matched loads, the insertion loss between ports 2 and 3 in no way limits the performance of the isolator. In this application the ferrite material in the secondary waveguide is in its insertion loss condition insofar as the reverse power due to antenna mismatch is concerned, and can be considered part of the high power load.

If the back-to-front ratio of the isolator can be increased to 200, the insertion loss in the reverse direction is reduced to about 1 dB.

If we maintain the back-to-front ratio at 200 and reduce $(\alpha_1 - \alpha_2)/k$ to -20, Fig. 6 indicates that the insertion loss in each direction is about 0·70 dB. In this example, the overall length of the structure is about 11 in and the secondary waveguide is decoupled by 27 dB at every point.

6. Conclusion

A coupled waveguide circulator has been described in which the secondary waveguide is loaded with non-reciprocal loss. For this situation, the analysis predicts that the peak power capability of the device is essentially that of the empty waveguide. The construction

of such a circulator with low insertion loss in both directions of transmission must await the development of non-reciprocal attenuators with higher back-to-front ratios than are presently available. However, the use of the device as a high-power isolator is in no way limited by the back-to-front ratio.

7. Acknowledgment

The author wishes to thank Microwave Associates, Inc. for permission to publish this paper.

8. References

1. A. G. Fox, S. E. Miller and M. T. Weiss, 'Behavior and application of ferrites in the microwave region', *Bell Syst. Tech. J.*, **34**, No. 1, pp. 5–103, January 1955.

2. L. R. Whicker, G. J. Neumann and F. E. Munyak, 'Criteria for designing high power coupled wave duplexers and isolators', *Trans. Inst. Radio Engrs. on Microwave Theory and Techniques*, MTT–10, No. 1, pp. 20–25, January 1962.

3. J. Helszajn, 'Coupled-wave description of the absorption-type ferrite modulator', *The Radio and Electronic Engineer*, **29**, No. 2, pp. 129–32, February 1965.

4. S. E. Miller, 'Coupled wave theory and waveguide applications', *Bell Syst. Tech. J.*, **33**, No. 1, pp. 661–719, May 1954.

5. P. J. B. Clarricoats, 'Microwave Ferrites', p. 112 (John Wiley, New York, 1961).

STANDARD FREQUENCY TRANSMISSIONS

(Communication from the National Physical Laboratory)

Deviations, in parts in 10^{10}, from nominal frequency for **April 1966**

April 1966	GBZ 19·6 kc/s 24-hour mean centred on 0300 U.T.	MSF 60 kc/s 1430–1530 U.T.	Droitwich 200 kc/s 24-hour mean centred on 0300 U.T.	April 1966	GBZ 19·6 kc/s 24-hour mean centred on 0300 U.T.	MSF 60 kc/s 1430–1530 U.T.	Droitwich 200 kc/s 24-hour mean centred on 0300 U.T.
1	− 298·6	− 300·8	− 1·1	16	− 300·6	− 299·8	+ 1·3
2	− 299·4	− 301·0	− 1·1	17	− 301·2	− 300·1	+ 0·9
3	− 299·5	− 301·0	− 1·6	18	− 301·0	− 300·3	+ 0·9
4	− 298·4	− 301·0	− 3·6	19	− 301·3	− 300·7	+ 1·2
5	− 298·6	− 301·4	− 3·5	20	—	—	+ 1·0
6	− 298·3	− 301·5	− 2·4	21	− 300·4	− 299·9	+ 1·1
7	− 301·7	− 299·8	− 1·3	22	− 301·7	− 298·9	+ 1·1
8	− 299·1	− 299·7	− 1·4	23	− 300·5	—	+ 0·5
9	− 299·1	− 299·5	− 1·0	24	− 300·0	—	+ 0·8
10	− 300·2	− 300·1	− 1·5	25	− 300·7	− 300·3	+ 0·4
11	− 300·5	− 299·9	—	26	− 299·6	− 299·3	+ 0·5
12	− 300·7	− 299·8	− 0·7	27	− 301·1	− 301·0	+ 0·4
13	− 301·0	− 299·9	− 0·4	28	− 300·8	—	+ 0·1
14	− 300·9	− 299·5	+ 0·6	29	− 300·9	− 301·0	+ 0·1
15	− 300·6	− 299·7	+ 0·9	30	− 301·0	− 301·6	0

Nominal frequency corresponds to a value of 9 192 631 770·0 c/s for the caesium F,m (4,0)–F,m (3,0) transition at zero field.

Note: GBR Rugby has been replaced temporarily by GBZ Criggion.

Radio Engineering Overseas . . .

The following abstracts are taken from Commonwealth, European and Asian journals received by the Institution's Library. Abstracts of papers published in American journals are not included because they are available in many other publications. Members who wish to consult any of the papers quoted should apply to the Librarian, giving full biographical details, i.e. title, author, journal and date, of the paper required. All papers are in the language of the country of origin of the journal unless otherwise stated. Translations cannot be supplied.

NOISE DISCRIMINATION IN TELEVISION CODING

Noise is inherent in any television source and will produce an increase in the channel capacity required to transmit the coded message if it is not eliminated. The approach considered in an Australian paper is to delete those signal components which are not visible under normal viewing conditions. It has been necessary, therefore, to determine what constitutes subliminal picture detail. Methods of reducing the effects of noise are then suggested and an attempt is made to determine the efficiency of these methods.

The operation and performance of an elementary type of noise discriminator which produces a modified video signal in which all changes in amplitude, smaller than a given threshold, are eliminated is described. To determine the amount of noise removed, the reduction in the number of level changes for a fixed-level, four-bit quantizer was measured. From the results it is inferred that elimination of the noise component of television signals will reduce the amount of information to be coded by less than $\frac{1}{8}$ for average and high detail pictures, and by $\frac{1}{3}$ or more for low detail pictures.

'Noise discrimination on television coding', J. O. Limb, *Proceedings of the Institution of Radio and Electronics Engineers Australia*, **27**, No. 1, pp. 10–18, January 1966.

NOISE IN DOUBLE FREQUENCY MODULATION SYSTEMS

The amount of noise power found in the base-band of double-f.m. systems when the r.f. signal is interfered with by noise, is investigated in a German paper. The starting point is a previous paper by the author covering sinusoidal interference in the case of double-f.m.

The further treatment first yields the signal/noise ratio for one channel with a 'narrow' base-band. This result is then enlarged, taking into consideration base-band pre-emphasis and psophometric weighting of a channel with a wide base-band. Actually, the signal/noise ratio may be derived in a manner simpler than the one applied here, if white noise is used, but the method of solution chosen in this paper shows which of the partial ranges of the r.f. noise spectrum contributes to the noise level in the base-band, and illustrates the magnitude of the contribution from the partial ranges. This makes it possible to calculate the signal/noise ratio for triangular r.f. noise. At the end of the paper, the effect of base-band pre-emphasis and psophometric weighting on the signal/noise ratio in one broadcast channel, and in the case of different RC pre-emphasis curves, is determined.

'Noise interference in double-f.m.', E. Metzger, *Nachrichtentechnische Zeitschrift*, **18**, No. 7, pp. 380–86, July 1965.

AERIALS IN IONIZED MEDIUM

The December 1965 issue of *L'Onde Electrique* contains the following papers which were read at a Colloquium on 'Antennes en Milieu Ionisé' organized by the Centre National d'Études Spatiales and held in Paris in June 1965:

'Introduction', E. Roubine, p. 1378.

'Radiation from an antenna in anisotropic surroundings', G. A. Deschamps, pp. 1379–85.

'Radiation and diffraction in anisotropic regions', B. Felsen, pp. 1386–92.

'Diffraction of a plane electromagnetic wave by means of an inhomogeneous plasma cylinder', P. E. Faugeras, pp. 1393–96.

'Study of calculations and measurements of the impedance of antennas in ionized surrounding', H. Weil, pp. 1397–1403.

'Impedance of a cylindrical antenna into a magneto-plasma with losses', J. P. Lafon, pp. 1404–08.

'The theory of thermal noise in the ionosphere', K. G. Budden and G. J. Daniell, pp. 1409–20.

'A theory for behaviour in the ionosphere of metallic dipole antennas of cylindrical or truncated conical form intended for the reception of very low frequency waves', G. Driancourt, pp. 1421–26.

'The design of an electric dipole antenna for v.l.f. reception within the ionosphere', L. R. O. Storey, pp. 1427–35.

'Non-reversible power and radiation resistance of antennas in anisotropic ionized gases', K. S. H. Lee and C. A. Papas, p. 1436. (Summary only.)

'The excitation of plasma resonances by a small pulsed dipole antenna', J. A. Fejer, pp. 1437–45.

'Electromagnetic wave propagation in an ionized medium surrounding a hypersonic device', J. Dorey, pp. 1446–50.

'Effects of frontal ionization on transmission during the flight of the ELDO satellite launcher', D. Cunsole and A. Gilardini, pp. 1451–58.

'Method of similitude for determination of discharge thresholds in electromagnetic systems', C. Ancona, pp. 1459–64.

'Radio frequency corona breakdown of aerials at high altitudes', I. L. Jones, pp. 1465–70.

'High frequency measurements of an antenna in the ionosphere', E. N. Bramley, pp. 1471–74.

'Low frequency measurements of dipole admittance in the ionosphere', T. R. Kaiser and J. K. E. Tunaley, pp. 1475–79.

'The effect of the ionized rocket exhaust plume on radio communication with the *Blue Streak* satellite launching vehicle', H. Williams. (Abstract only.)

'Sounding by resonance', D. Lepechinsky, pp. 1480–85.

'General conclusions', G. A. Deschamps, pp. 1486–88.

(All the papers are in French with short abstracts in English.)

L'Onde Electrique, **45**, No. 465, December 1965.